EXCITATION TRANSFER IN ORGANIC AND INORGANIC SYSTEMS

Thesis by

John Scott Winterle

In Partial Fulfillment of the Requirements
for the Degree of
Doctor of Philosophy

California Institute of Technology
Pasadena, California

1975
(Submitted August 21, 1975)

To Alison, Russell, Gladys, Mary Jo, Steve, Jackie, Norm, Jill, Atom, Ron, Wayne, Ibrahim, Vinnie, H.B.G., Larry, Connie, Frank and Susan Quina, Wendy, Jack, Cheri, and Clay Sparks Wilson.

ACKNOWLEDGEMENT

I would like to thank George Hammond for his support and inspiration without which this work would not have proceeded. My wife, Alison, has been a great help and booster and deserves a lot of credit.

While preparing this manuscript Bill and Ruth Nicholson allowed me to conveniently use their summer cottage (by the sea!) for writing. This generosity was of great benefit. I would also like to acknowledge the assistance of Dr. Dave Kliger who directed many of the LASER experiments.

Elaine Major did an excellent, dedicated typing job for which I am really grateful.

Finally, I acknowledge financial support given by the Army Office of Scientific Research and the National Science Foundation.

PART I

ABSTRACT

Iron(II) is photooxidized to iron(III) in 0.100 N sulfuric acid in the presence of the photosensitizer tris-(2,2′-bipyridine)ruthenium(II) dichloride. Control experiments show that the oxidation must be partly ascribed to a reactive oxygen species generated by interaction of molecular oxygen (dioxygen) with the excited photosensitizer because the oxidation quantum yield varies in strict proportion to the fraction of sensitizer excited states quenched by dioxygen.

The reaction was found to be dramatically pH dependent in the range studied (1 to 0). However, the oxidation quantum yield was insensitive to changes in Fe^{+2}(aq.) in the region 4×10^{-2} to 2×10^{-4} M.

In 0.100 N H_2SO_4 at 25 ± 1°C, the quantum yield for Fe^{+3} (aq.) production is 0.077 when extrapolated to 100% sensitizer quenching.

Quenching of the emissive MLCT state of $Ru(bipy)_3^{+2}$ is known to occur by two different mechanisms, energy and charge transfer. In the latter case electron transfer to dioxygen would result in superoxide anion and oxidized

sensitizer, both of which rapidly oxidize Fe^{+2} (aq.) at pH 1. That this simple mechanism is operative is ruled out by the observed pH dependence since HO_2 , O_2^- radical oxidations of iron (II) are acidity independent in the range studied.

In view of these considerations it is proposed that hydroperoxyl radicals are produced upon protonation of a transient sensitizer - dioxygen complex which otherwise decays without oxidation - reduction.

PART II

ABSTRACT

Trans, trans-2, 4-hexadiene is isomerized to its geometrical isomers when dilute benzene solutions are γ-irradiated. Because the diene receives negligible primary excitation, a solvent-to-solute excitation transfer mechanism must be invoked to explain the isomerization.

A comparison of the photochemistry and the radiation chemistry of the diene in benzene, demonstrates that the kinetic behavior of trans, trans-2,4-hexadiene under γ-irradiation is consistent with the transfer of triplet solvent electronic excitation.

The triplet yield is consistent with recent careful determinations.

Collateral photochemical experiments demonstrate that the $^1B_{2u}$ state of benzene does not efficiently isomerize trans, trans-2,4-hexadiene. Thus, the excess isomerization must be contributed by another intermediate.

By a process of elimination, an upper excited benzene singlet state is identified as the excitation donor. This choice is confirmed by an excellent concordance of the data with the model for energy transfer.

Theoretical predictions make such transfer possible, because this energy migration rate in benzene far exceeds that predicted by simple mass diffusion.

ABSTRACT OF PROPOSITIONS

Proposition I. A test of Brockelhurst's theory of recombination of radiolytically produced ion pairs is proposed.

Proposition II. Intramolecular excitation transfer between a metal and organic π system is proposed.

Proposition III. The Construction of a photoactive electrode is proposed.

Proposition IV. A test of current theories for $Co(NH_3)_5Br^{+2}$ sensitized decomposition is dilineated.

Proposition V. A new class of polarity-proximity probes are suggested for biomembrane research.

TABLE OF CONTENTS

LIST OF FIGURES

PART I

PART II

LIST OF TABLES

PART I

PART II

INTRODUCTION

What follows is a report on the characterization and interpretation of a newly discovered photoreaction between tris(2,2′-bipyridine)ruthenium(II) dichloride, $Ru(bipy)_3^{+2}$, and dioxygen to produce species capable of oxidizing $Fe(OH_2)_6^{+2}$ to $Fe(OH_2)_6^{+3}$ in acidic aqueous solution.

The possible identities of these species are suggested by the behavior shown by $Ru(bipy)_3^{+2*}$ in other chemical cases. For that reason a brief review of the spectroscopic, photodynamic, and photochemical properties of $Ru(bipy)_3^{+2}$ is in order.

Succinctly, $Ru(bipy)_3^{+2*}$ has been shown to react with suitable acceptors in two distinct ways, by charge transfer (CT), and electronic-excitation energy transfer (ET). These two pathways are illustrated below (* indicates an excited state):

$$Ru(bipy)_3^{+2*} + A \rightarrow Ru(bipy)_3^{+3} + A^- \qquad (1)$$

$$Ru(bipy)_3^{+2*} + B \rightarrow Ru(bipy)_3^{+2} + B^* \qquad (2)$$

The occurrence of reaction (1) has been confirmed by the appearance of the one-electron oxidized form of the

photosensitizer and one-electron reduced forms of acceptors following the quenching event. That reaction (2) proceeds has been established by observing sensitized emission from the acceptor or that a characteristic excited state reaction of the acceptor had occured.

Both $Ru(bipy)_3^{+2}$ and $Ru(bipy)_3^{+3}$ are kinetically inert towards ligand exchange[1]. While $Ru(bipy)_3^{+3}$ seems somewhat unstable toward unimolecular photodecomposition[2], $Ru(bipy)_3^{+2}$ is quite stable [3]. The quantum yield for $Ru(bipy)_3^{+2}$ loss following excitation at 457.9 nm is less than 10^{-5} in water and less than 10^{-4} in 0.1 N H_2SO_4[3]. A phototransient which reversibly regenerates $Ru(bipy)_3^{+2}$ in acid solution has been reported by Natarajan and Endicott[4]. The quantum yield of this species, which was hypothesized to be an intramolecular redox product, was $\sim 10^{-3}$ $N \cdot E^{-1}$. This may not, however, be a true unimolecular-decay product (vide infra). Other researchers have not reported this behavior under similar conditions[5].

The absorption and emission spectra of $Ru(bipy)_3^{+2}$ in 0.10 N H_2SO_4 at 25°C are shown in figure (1). State assignments in absorption have been made by Lytle and Hercules[6] and Paris and Brandt[7]. The intensity of the observed bands suggest that they cannot arise from metal localized d-d electronic transitions. The most intense band at 286 nm (35,000 cm^{-1}, ϵ = 79,000[8]) has been attributed to π-π^* intraligand absorption[6], while the two other

Figure 1. Absorption and uncorrected emission spectra of $Ru(bipy)_3^{+2}$ in 0.100 N H_2SO_4 at 300°K.

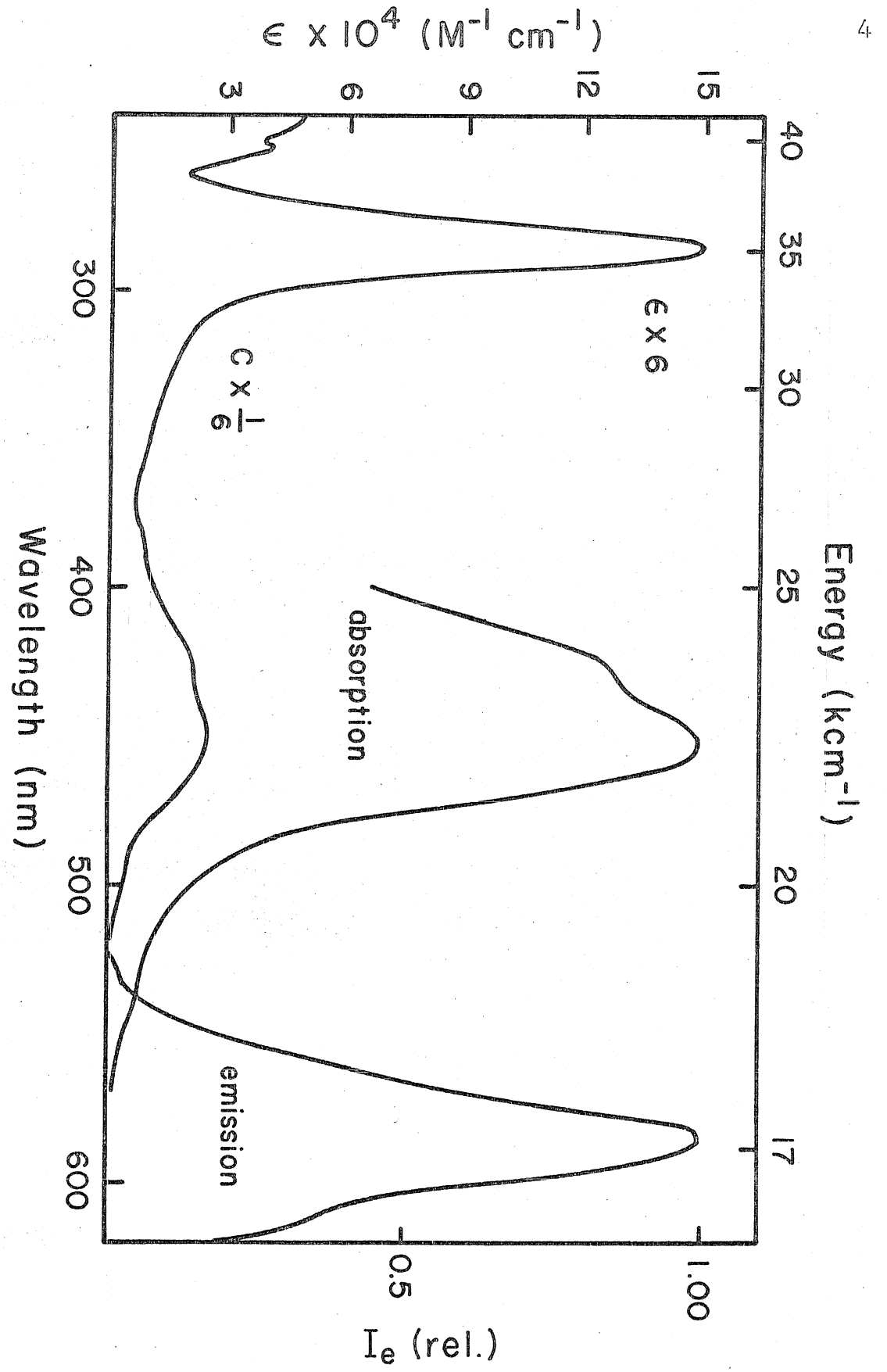
ε x 10^4 (M^-1 cm^-1)
3
6
9
12
15
40
35
30
25
20
17
Energy (kcm^-1)
300
400
500
600
Wavelength (nm)
ε x 6
c x 1/6
absorption
emission
0.5
1.00
Ie (rel.)

intense features are grossly d-π^* metal-to-ligand charge transfer (MLCT) transitions[6,7].

The polarized absorption of the intense CT band at 452 nm (22,100 cm^{-1}, $\epsilon \sim 15{,}000\ M^{-1}\ cm^{-1}$) has been examined by Palmer and Piper[9], and found to be resolvable into two differentially polarized components. The polarization ratio is 26.5 at 300°K for $Ru(bipy)_3^{+2}$ doped into an isomorphic host crystal, $Zn(bipy)_3SO_4 \cdot 7H_2O$.

In D_3 symmetry two low-lying d-π^* MLCT transitions are expected for d^6 ruthenium (II)[6]. These arise from a splitting of the metal t_{2g} orbitals into an a_1 and e set upon lowering the molecular symmetry from Oh. The $e(d) \rightarrow \pi^*$ transition is polarized pendicularly to the C_3 axis of the molecular complex, while the $a(d) \rightarrow \pi^*$ transition is parallel polarized[6]. These predictions are fulfilled by the measurements of Palmer and Piper[9].

The spectroscopic splitting factor[9] (10Dq), for the metal d orbitals has been estimated to exceed 23,000 cm^{-1}. The first spin allowed d-d transition[9] ($^1T_1 \leftarrow {}^1A_1$) in $Ru(bipy)_3^{+2}$ has been predicted to lie at 22,000 cm^{-1} (454 nm) while the lowest spin-intercombinational transition[9] ($^3T_1 \leftarrow {}^1T_1$) is placed at 20,000 cm^{-1}.

Luminescence from ruthenous bipyridine was initially observed by Paris and Brandt[7] in 1959 and correctly assigned to d-π^* charge transfer emission. This assignment was subsequently rejected by Porter and Schläfer[10] who suggested

the luminescence was metal localized d-d ($^3T_1 \rightarrow {}^1A_1$) spin forbidden emission and G. A. Crosby et al.[11] who proposed that the luminescence was derived from $^1T_1 \rightarrow {}^1A_1$ metal localized relaxation.

An abrupt re evaluation of these metal centered models was made by G. A. Crosby and D. M. Klassen[12]. It was discovered that energy of the luminescence bore no relationship to the position of various coordinating ligands in the spectrochemical series. These authors concluded that the emission was $d\text{-}\pi^* \rightarrow {}^1A_1$ in nature as originally assigned by Paris and Brandt. However, the spin multiplicity of the excited state was not established.

Both Lytle and Hercules[6] and Demas and Crosby[13] concluded that the emission was spin forbidden CT and that the anomalously short lifetime at 77°K (5.2×10^{-6}S)[14] was attributable to a large spin-orbit coupling contribution by the central metal.

Crosby and Harrigan [15,16] provided the latest and most thorough studies of $Ru(bipy)_3^{+2*}$ emission in crystalline and plastic hosts as a function of temperature (2-145°K). Dramatic increases in emission lifetime were observed below 20°K, which were adequately rationalized by assuming that emission was actually occuring from a manifold of nearly isoenergetic electronic states.

By assuming a 3 level, 5 parameter model, they were able to accurately match the experimental temperature -

lifetime behavior. Furthermore they were able to assign symmetries to their emitting states according to an electronic model for d^6 charge transfer states. Finally, the model also predicted the decrease in state lifetime observed upon immersion of an emitting sample in a 14 kG magnetic field.

This model with spin and orbital classifications is shown in figure (2). The spin designation is only formal because the large degree of spin-orbit coupling present causes the states to be substantially mixed[16]. Figure (2) will be taken as the best model for a $Ru(bipy)_3^{+2}$ excited state description in this report.

The emission spectrum in figure (1) is uncorrected for instrumental response which drops precipitously at wavelengths greater than 600 nm. It differs from published spectra[6,11] for that reason.

The emission lifetime of $Ru(bipy)_3^{+2}$ in deoxygenated solution (25°C) determined by this work (0.60×10^{-6}S)[17] agrees very closely with other measurements, as does the emission lifetime in aerated aqueous solution (0.40×10^{-6}S).[18]

The state lifetime is found to be quite temperature dependent under ambient conditions, decreasing approximately 10% for a 10°C increase in temperature near 285°K in EPA[6].

Solution emission quantum yields of ruthenous bipyridine have not been reported but the emission yield from powdered-crystalline $Ru(bipy)_3^{+2}$ is 0.003 at room temperature[19]. At

Figure 2. State diagram of $Ru(bipy)_3^{+2}$.

$Ru(bipy)_3^{+2}$

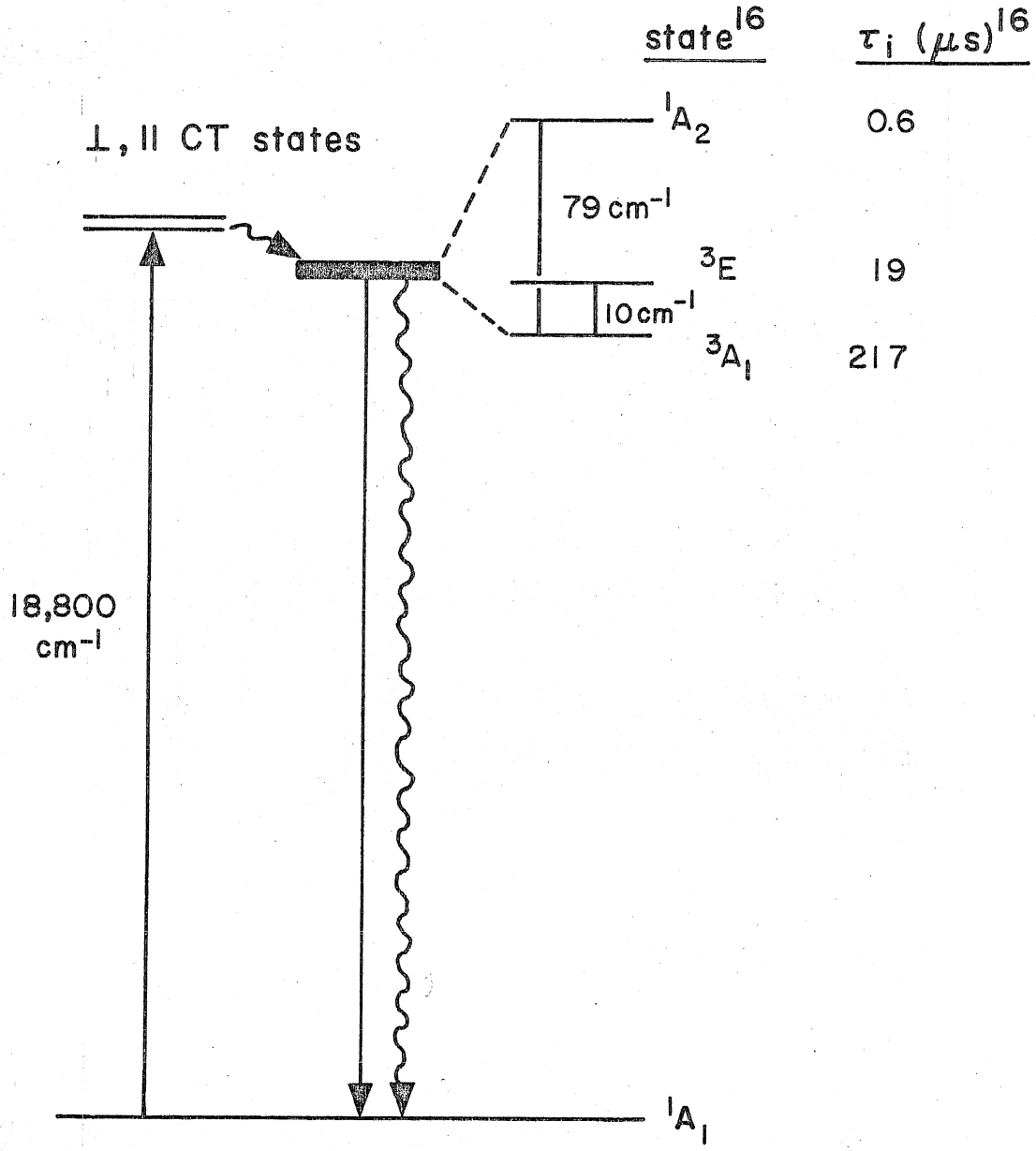
state[16]
τi (μs)[16]
⊥, ∥ CT states
1A2
0.6
79 cm-1
3E
19
10 cm-1
3A1
217
18,800 cm-1
1A1

77°K in ethanol-methanol (4:1,v/v) glass, this value is $0.376 \pm .036$[14].

The use of $Ru(bipy)_3^{+2}$ for photosensitization was first reported by J. N. Demas and A. W. Adamson in 1971[20]. The sensitized photoaquation of $PtCl_4^{-2}$ was described to proceed by electronic energy transfer from the sensitizer. The quenching was found to be dynamic, not static as revealed by the congruence of the lifetime and intensity forms of the Stern-Volmer quenching plots. $PtCl_4^{-2}$ quenched at a rate of 6.5×10^9 m^{-1} S^{-1} in aqueous solution.

Reports subsequently appeared documenting other cases of electronic energy transfer to acceptors.

N. Sabatini and V. Balzani[21] qualitatively observed sensitized ($^2E_g \rightarrow {}^4A_{2g}$) phosphorescence from hexacyanochromate in DMF. The quenching process was later placed on quantitative grounds[22].

M. S. Wrighton and J. Markham[23] studied the quenching of $Ru(bipy)_3^{+2*}$ by a series of energy-graduated organic acceptors of very low oxidizing ability. Anthracence, with a triplet energy level at 42 Kcal·mole^{-1} quenched at a diffusion controlled rate, while trans-2-styrylpyridine, trans-4-styrylpyridine, and trans-stilbene with triplet energys of 50,50 and 49 Kcal·mole^{-1}, respectively, quenched three orders of magnitude less rapidly. Cis-piperylene (E_T = 57 Kcal) showed no quenching activity whatsoever.

Clear evidence for triplet energy transfer was shown by the concomitant isomerization of the three olefin quenchers, with limiting isomerization quantum yields identical to that obtained with benzophenone sensitization.

Finally, the production of $^1\Delta g$ dioxygen by $Ru(bipy)_3^{+2*}$ energy transfer in methanol was reported by Demas, Harris, and Diemente[24]. Singlet dioxygen was identified by its characteristic olefin reactions at 0°C. Unfortunately, these authors did not report quantum efficiencies for the photo-oxidation.

The charge transfer behavior of $Ru(bipy)_3^{+2*}$ has been more extensively reported than the energy transfer pathway for acceptor excitation.

The most conclusive observations on a dynamically changing system were made by T. J. Meyer *et al.*[5] The quenching of $Ru(bipy)_3^{+2*}$ by Fe^{+3}(aq.), $Ru(NH_3)_6^{+3}$, 1,1′-dimethyl-4,4′-bipyridinium dication, and *trans*-1,2-bis(N-methyl-4-pyridyl) ethylene dication (BPE) in 1 N H_2SO_4 was followed by emission and flash spectroscopy. All of the electron acceptors quenched $Ru(bipy)_3^{+2*}$ at a near diffusion controlled rate.

Immediately after an exciting flash, $Ru(bipy)_3^{+3}$ and the one-electron reduced quenchers were found to be present in a one-to-one ratio. In all cases a rapid dark reaction ensued which quantitatively regenerated the starting reactants.

In the case of Fe^{+3}(aq.), by following the second order regeneration process $Ru(bipy)_3^{+3} + Fe^{+2}(aq.) = Fe^{+3}(aq.) + Ru(bipy)_3^{+2}$, a rate constant of 1.0×10^6 $M^{-1} \cdot S^{-1}$ was obtained, which agreed well with independent measurements by stopped flow techniques. The authors showed that $\cdot OH$ radicals were not produced by $Ru(bipy)_3^{+2*}$ decay in acid solution (although allowed thermodynamically). Hydrogen atom production by electron transfer to acidic solvent had been previously discounted[25].

The dimethylbipyridinium cation (paraquat) quenched efficiently in CH_3CN. In this instance, the lowest excited state of paraquat is at 71.5 Kcal$\cdot$mole^{-1}, so any form of electronic energy transfer is prohibited from the donor ($E_T \sim 49$ Kcal$\cdot$mole), and electron transfer must be the dominant mode of quenching.

Especially interesting in this regard was BPE. BPE with a triplet energy level at 50 Kcal$\cdot$mole^{-1} can quench by both ET and CT mechanisms. The relative extent of ET was determined by following the <u>trans</u> → <u>cis</u> isomerization of BPE which occurs as a result of ET. It was found that the CT mechanism was 100-fold more prevalent than energy transfer.

Recently, the steady-state irradiation of $Ru(bipy)_3^{+2}$ with Fe^{+2} and Fe^{+3} in deoxygenated $HClO_4$ (0.11 M ionic strength) was examined by Lin and Sutin[26]. The mechanism of ref. 5 was found consistent with their results.

In a recent communication[27] the electron transfer quenching of $Ru(bipy)_3^{+2*}$ by a series of electron deficient aromatic compounds was reported. The bimolecular quenching constant was found to vary monotonically with increasing reduction potential of the acceptor. No free ions were detected, a fact which was attributed to efficient back-oxidation in a dark reaction. The quenchers were considered to be inactive as energy transfer acceptors, an assumption which was consistent with the subsequent kinetic analysis.

A Rehm-Weller[28] plot gave an estimation of the $Ru(bipy)_3^{+3}/Ru(bipy)_3^{+2*}$ couple. The potential is -0.81 vs. the saturated calomel electrode, an astounding result in view of the ground state couple of 1.05 V. The electronic excitation of $Ru(bipy)_3^{+2}$ transforms it from a very poor reducing agent to a moderately strong reductant, a complete inversion of its ground state properties.

The static, chemical effects of electron transfer from $Ru(bipy)_3^{+2*}$ to inorganic oxidants have been studies by several authors. In the case of the decomposition of $Co(NH_3)_5X^{+2}$ ($X = F^-, Cl^-, Br^-$) there has been recent literature controversy whether quenching occurs by charge or energy transfer. However, the weight of scientific evidence is now shifting in the direction of the charge transfer mechanism[31].

The quenching and synchronous oxidation of $Ru(bipy)_3^{+2*}$ by acidopentamminecobalt(III)[3] complexes was first described

by Gafney and Adamson[25]. The reaction, which results in $Co^{+2}(aq.)$ appearance, was suggested to proceed as follows.

$$Ru(bipy)_3^{+2*} + Co(NH_3)_5X^{+2} \rightarrow Ru(bipy)_3^{+3} + Co(NH_3)_5X^{+1} \quad (3)$$

$$Co(NH_3)_5X^{+1} + 6\,H_2O \rightarrow Co^{+2}(aq.) + 5NH_3 + X^- \quad (4)$$

$$Ru(bipy)_3^{+3} + H_2O \rightarrow Ru(bipy)_3^{+2} + H_2O(ox.) \quad (5)$$

Reaction (5) was found to occur rapidly at pH 4, so that no overall oxidation of ruthenium was seen. At pH 0 ruthenic bipyridine is relatively stable toward solvent reduction. When the photoreaction was run at pH 0, a rapid build-up of $Ru(bipy)_3^{+3}$ was manifested.

The relative quenching rates of the cobalt pentammines paralleled their reduction potentials.

An alternative mechanism[29,30] was envoked by Natarajan and Endicott to explain the same results. They suggested that energy transfer from $Ru(bipy)_3^{+2*}$ produces a redox-active low lying charge transfer state. Upon unimolecular decomposition of this triplet state to Co(II) and halogen atoms the escaping fragments oxidize $Ru(bipy)_3^{+2}$:

$$Ru(bipy)_3^{+2*} + Co(NH_3)_5X^{+2} \rightarrow Co(NH_3)_5X^{+2*} + Ru(bipy)_3^{+2} \quad (6)$$

$$Co(NH_3)X^{+2*} + 6H_2O \rightarrow Co^{+2}(aq.) + 5NH_3 + X\cdot \quad (7)$$

$$X\cdot + Ru(bipy)_3^{+2} \rightarrow Ru(bipy)_3^{+3} + X^- \quad (8)$$

Positive evidence for the production of bromine atoms (in the case $X = Br^-$) was found by the flash spectroscopic observation of the dibromide radical anion in the presence of 10^{-3}M Br^- and to a smaller extent in solutions free from external bromide. Dibromide oxidized $Ru(bipy)_3^{+2}$ at a rate of 3×10^7 $M^{-1}S^{-1}$. Addition of 50% (v/v) 2-propanol decreased the initial yield of oxidized sensitizer by 50% while a 85% increase in Co(II) was noted. This result was explained by a competition reaction between $Ru(bipy)_3^{+2}$ and isopropanol for Br · .

A partial, contradictory, explanation for the effect was submitted by Navon and Sutin[31] who measured the quenching rate of $Ru(bipy)_3^{+2*}$ by $Co(NH_3)_5Br$ in 50% (v/v) 2-propanol, 0.5 M H_2SO_4 at 25°C. The rate constant decreased by 56% compared to alcohol-free solution. Hence, a lower yield of Ru(III) would be expected because of a slow down of reaction (3).

Navon and Sutin[31] showed that the photoreduction fit the Adamson CT mechanism very well, and in addition, enumerated criticisms of the ET scheme. The most compelling criticism pointed out the necessity of unit efficiency of radical production along with quantitative oxidation of

$Ru(bipy)_3^{+2}$ by these radicals for all the quenchers studied.

Finally, the electron transfer from $Ru(bipy)_3^{+2*}$ to a series of metal(III) (M = Cr, Fe, Co) oxalate complexes has been dilineated[3].

Of the three, only the redox decomposition of cobalti-oxalate was clearly mediated by charge transfer ($\Phi(CO^{+2})$ = 0.85). A sensitized racemization of d - $Cr(C_2O_4)_3^{-3}$ was observed and ascribed to ^3ET from $Ru(bipy)_3^{+2}$.

The irradiation of ferrioxalate in the presence of sensitizer gave only the amount of decomposition expected from the trivial photolysis of $Fe(C_2O_4)_3^{-3}$ alone, which resulted from incomplete light absorption by the sensitizer. Significantly, the failure to observe photoreduction, even though CT was expected in this case was proposed to arise because of rapid back-oxidation by contiguous $Ru(bipy)_3^{+3}$ immediately after quenching. In this manner, no irreversible reduction occured.

In view of the works of Wrighton and Markham[23] and Bock, Meyer, and Whitten[26], a rough guideline can be established to predict the preference of $Ru(bipy)_3^{+2*}$ to interact by electronic energy or charge transfer with a specific acceptor.

In general, diffusion controlled electronic energy transfer between donor and acceptor is expected when spin conservation rules are not violated, and the energy of the donor excited state exceeds that of the acceptor by

2 Kcal·mole at 25°C[32]. If the transfer becomes endothermic, the deficit must be compensated by thermal activation, and the rate falls off exponentially.

By this criterion, diffusion controlled energy transfer from $Ru(bipy)_3^{+2*}$ (E_T = 49[12], 51[20], 50[26] Kcal·mole^{-1}) will occur if the acceptor posseses a spin allowed excited state of energy less than 49-47 Kcal·mole^{-1} at 25°C.

Similarly outer-sphere electron transfer to an oxidant can be rapid if thermodynamically allowed. In electrochemical terms, this event is signaled if the cell potential of reaction is positive.

The cell potential of the reaction $Ru(bipy)_3^{+2*} = Ru(bipy)_3^{+3} + e^-$ is +0.81 V. vs: S.C.E. . Hence, any acceptor with a reduction potential larger than -0.81 V. is predicted to interact by charge transfer at a diffusion controlled rate if no "intrinsic barriers" exist[31].

We may now turn our attention to the present system of $Ru(bipy)_3^{+2*}$ and O_2. The reduction potential of dioxygen to superoxide anion is -0.17 V. versus the saturated calomel electrode (+ .07 V. vs: N.H.E.)[33] at 25°C. This substantially exceeds -0.81 V. so electron transfer from $Ru(bipy)_3^{+2*}$ to produce superoxide anion can be very facile. Such a transfer at pH < 4 would immediately result in the strong oxidant HO_2 , which is known to rapidly oxidize Fe^{+2} (aq.) .

Dioxygen possesses two singlet electronic excited states[34] below 47 Kcal·mole^{-1} . Since the reaction

$$^{3}Ru(bipy)_{3}^{+2*} + {}^{3}O_{2} \rightarrow Ru(bipy)_{3}^{+2} + {}^{1}O_{2} \qquad (8)$$

is spin allowed, this step is expected to be equally as fast as charge transfer.

Thus, the criteria predict a competition between ET and CT forms of acceptor activation to produce potential oxidants.

As will be seen, it is unlikely that singlet dioxygen is functionally involved as an oxidant in this system. Furthermore the mechanism cannot consist of the simple production of superoxide anion by CT from $Ru(bipy)_{3}^{+2*}$, but a slightly more complicated pathway is consistent with the experimental results.

EXPERIMENTAL AND RESULTS

The Synthesis of $Ru(bipy)_3Cl_2 \cdot 6H_2O$

$Ru(bipy)_3Cl_2$ was synthesized by the method of Burstall[1a] and also by the method of Braddock and Meyer[1b].

In the first case, 1.00 gram of $RuCl_3 \cdot 3H_2O$ and 8.39 grams of 2,2'-bipyridine were added to a 100 ml round bottom flask equipped with a 14/20 female ground glass joint and teflon stir bar. A 14/20 male ground glass joint with stem was inserted into the flask. At a right angle to the stem was a small hose connector which served as a N_2 inlet from a silicone oil bubbler. Through the center of the stem was inserted a 300°C thermometer with a tygon tubing collar for sealing.

The mixture was heated under a positive pressure of N_2 with a heat gun. The bipyridine melted at ~70°C. With continued heating the mixture turned deep red at 180°C and then a darker red-orange at 220°C. Water was seen to condense on the upper part of the inlet stem. Heating to 250°C required 30 min. The mixture was maintained at 255 ± 5°C for 3.0 hrs. under N_2.

The mixture was cooled to room temperature and removed from the flask, yielding 10.81 g of very crude product.

This mixture of bipyridine, oxidized bipyridine, and $Ru(bipy)_3Cl_2$ was placed in Soxhlet extractor and refluxed

with benzene overnight.

2 g of purified product was dissolved in H_2O. This material was filtered to remove insolubles and then poured into a 180 mm watch glass for crystallization.

The crystallization was carried out over several days yielding deep, red rhombohedral crystals as expected[1a], which correspond to $Ru(bipy)_3Cl_2 \cdot 6H_2O$. The crystals were collected with forceps and air-dried. Elemental analysis[36] for $Ru(bipy)_3Cl_2 \cdot 6H_2O$ yielded % C = 47.22 (48.1 calc.), % N = 11.40 (11.25 calc), % Cl = 10.49 (9.49 calc) and % H = 4.32 (3.52 calc).

Synthetic $Ru(bipy)_3^{+2}$ when dissolved in 0.100 N H_2SO_4 appeared identical to published spectra[6,9,11,35] and demonstrated the following extinction coefficients in the visible and uV spectrum:

ϵ(500nm) = 2074 ± 38 $M^{-1} cm^{-1}$, ϵ(453nm) = 15,210 ± 404 $M^{-1} cm^{-1}$, ϵ(436nm) = 12,085 ± 74 $M^{-1} cm^{-1}$, and ϵ(313nm) = 12,001 ± 106, for a molecular weight of 748.66 g $mole^{-1}$. The ϵ at 453 nm is within the range of other literature values[1b,35] .

A second batch of $Ru(bipy)_3Cl_2$ was prepared by a less tedious method[1b]. In a 100 ml round bottom flask with 14/20 ground glass joint, was added 0.82 g. Kodak bipyridine and 0.47 g. $RuCl_3 \cdot 3H_2O$ (3/1 molar ratio). To this mixture was further added 25 ml of dry dimethyl formamide. The solution was refluxed under N_2 for 3 hours, cooled, and poured into a

concentrated solution of tertiary butyl ammonium chloride in reagent acetone. Red-orange $Ru(bipy)_3Cl_2$ was precipitated. 530 milligrams were collected and air-dried on a fritted funnel (8.3×10^{-4} moles, 46% yield).

The UV spectrum of this material agreed with that of the previous synthesis. Further, supplementary physical data was obtained from infrared and proton magnetic resonance spectra of $Ru(bipy)_3Cl_2$. In all cases the synthetic material was found equivalent to the authentic standard material.

The 60 MHz proton magnetic resonance spectrum (D_2O) showed a nine line complex centered at $\tau = 2.16$ (470 cps) downfield from external TMS standard (1% TMS in CCl_4). The multiplet consisted of a triplet at $\tau = 2.75$, an unsymmetrical quartet at $\tau = 2.16$ and an unsymetrical doublet at $\tau = 1.56$.

The IR spectrum (4 mg. in 360 mg. KBr) revealed bands at 1305 and 1445 cm^{-1} which have been assigned to Ru — N stretching modes[6].

In solution $Ru(bipy)_3^{+2}$ demonstrated red-orange luminescence as reported[7], which matched that of the authentic substance. $Ru(bipy)_3^{+2}$ has an apparent emission maximum at 583 nm when matched with the spectral response of a S-5 photocathode. Measured luminescence lifetimes were as reported in both oxygenated and deoxygenated solution.

The Spectral Stability of Oxygenated $Ru(bipy)_3^{+2}$ Solution at 320 nm and the Effect of O_2 on Irradiated $Ru(bipy)_3^{+2}$ - Fe^{+2} mixtures.

Two experiments were formululated, one to test the spectral sensitivity of irradiated $Ru(bipy)_3^{+2}$ toward dioxygen and another to establish the importance of dioxygen for the photoreaction to proceed.

Alumina chromatographed $Ru(bipy)_3^{+2}$ (pH = 7) was added to 0.100 N H_2SO_4 to give an optical density of 1.0 at 313 nm. Samples of this solution were irradiated at 313 nm (17°C) and subsequently analyzed for spectral changes at 320 nm, the wavelength used for Fe(III) analysis (vide infra). The resultant spectral data are shown in figure (3), curve A. The light absorption rate was representative to that of all other experiments at 313 nm, 0.4×10^{-7} $E \cdot M^{-1}$.

Within experimental accuracy, there was no spectral change at 320 nm. After 104 m of irradiation more than 10 photons had been absorbed for every sensitizer molecule present with no discernible effect.

A second experiment was carried out to reveal the influence of dioxygen on the $Ru(bipy)_3^{+2}$ - Fe^{+2} mixture. A solution of Mohr's salt and recrystallized G. F. Smith ruthenous bipyridine dichloride was made up to give an O.D. of 1.4 at 313 nm. The $Fe^{+2}(aq.)$ concentration was 5.27×10^{-3} M. Four milliliters were transfered to an irradiation cell constructed by joining a square degassable absorption

Figure 3. (A) the effect of irradiation (313 nm) on aerated $Ru(bipy)_3^{+2}$ absorption compared to blank solution of 320 nm, and (B) the effect of O_2 addition to an irradiated solution of $Ru(bipy)_3^{+2}$ and Fe^{+2} (0.1 N) acid, also compared to aerated blank.

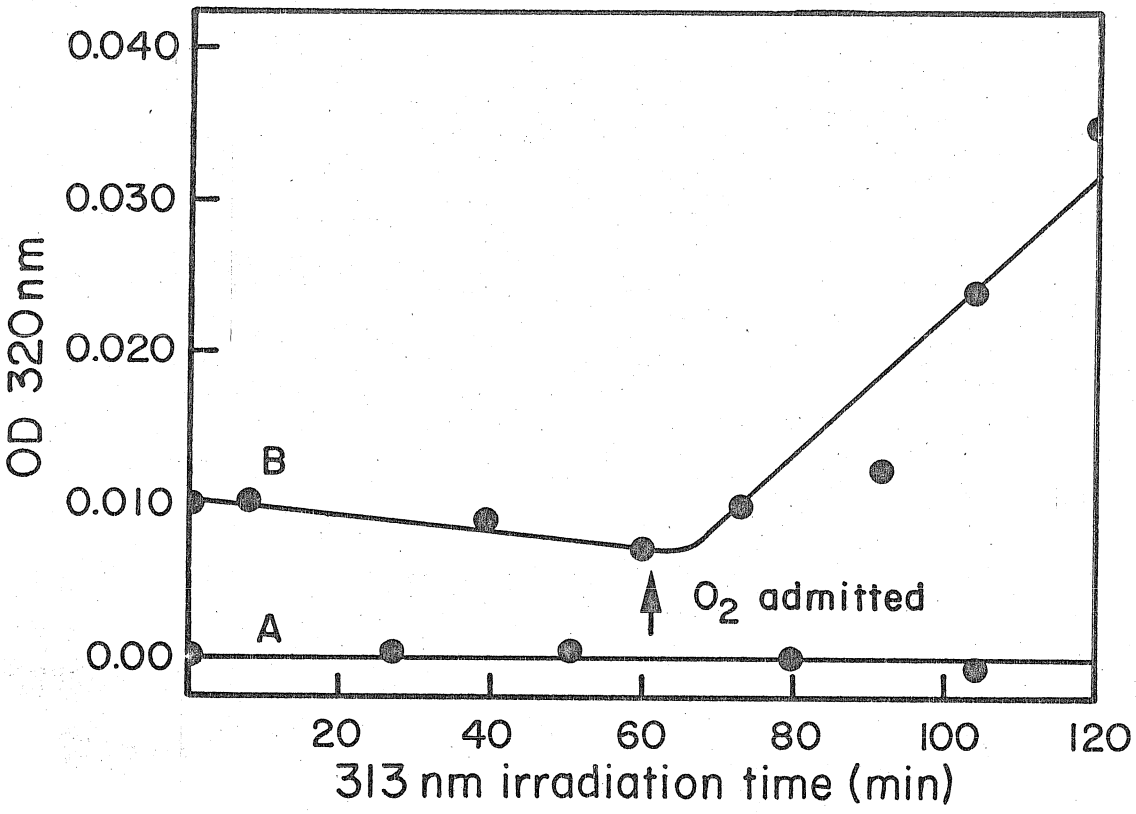
0.040
0.030
0.020
0.010
0.00
OD 320nm
B
A
O_2 admitted
20
40
60
80
100
120
313 nm irradiation time (min)

cell at a right angle to a 13 x 100 mm test tube connected to a 10/30 female ground glass joint.

The cell was designed so that the deoxygenated solution could be irradiated in the Pyrex test tube and then poured into the optical cell for absorption measurements.

The solution was degassed under high vacuum through 4 freeze-pump-thaw cycles (77°K) and sealed off the vacuum line by torch.

Six hours later, stock solution which had been left in the darkened Hitachi-Coleman cell compartment showed a +0.030 O.D. unit change at 320 nm compared to stock solution which had been stored in the dark under N_2 . This demonstrates the slow thermal oxidation of Fe^{+2}(aq.) by dioxygen, with an average O.D. change rate of 0.5×10^{-2} hr^{-1} (23 ± 2°C).

The irradiation at 313 nm was begun. At measured time increments the cell was withdrawn from the 313 nm "Merry-Go-Round", the irradiated solution poured back and forth into the absorption cell for mixing, and the O.D. measured at 320 nm . The cell was then returned to the stationary M.G.R. after pouring the solution back into the irradiation section of the ampoule.

This procedure was followed for 60 minutes. At this point the cell was carefully broken open to prevent the intrusion of glass chips into the ampoule. Air was bubbled through the solution and the irradiation was continued.

The results of this experiment are shown in figure (3), curve B. They show a slight decrease in the absorbence at 320 nm until air was admitted to the sample. This decrease is most likely caused by the thermal oxidation of the aerated optical blank during this part of the irradiation. An O.D. change of -0.003 units was observed at the end of 1 hr. This compares well with the change of -0.005 units expected from the observed average thermal oxidation rate. The photoxidation was initiated upon introducing air into the sample, which was signaled by an abrupt increase in solution absorbance due to Fe^{+3} production.

This experiment shows that the photoreaction is dioxygen mediated in some fashion and that little, if any irreversible oxidation occurs in the degassed system.

LASER Studies on the Photoprocesses of $Ru(bipy)_3^{+2}$ in 0.100 N H_2SO_4.

A pulsed N_2 megawatt Molectron UV-1000 LASER was used as an excitation source to study the luminescence decay of $Ru(bipy)_3^{+2*}$ and to search for absorbing intermediates. The LASER provides 10 ns pulses containing 10^{17} photons at 337.1 nm, so it is possible to obtain very high excitation densities on a very short time scale.

A first application of the LASER system was to measure the emission lifetime of $Ru(bipy)_3^{+2}$ in oxygenated and degassed 0.100 N H_2SO_4. This was accomplished by pulsing

samples and photographing the oscilloscopic response to the emission produced. The risetime of the oscilloscope - photomultiplier combination was less than 10 ns . Emission was collected and directed into a Bausch and Lomb grating monochromator set to 580 nm, coupled to a 50 ohm terminated 1P28 photomultiplier. A timebase calibrated Tecktronics 474 oscilloscope set to a horizontal scale of 100 ns $\cdot$ cm^{-1} was used for signal display. $Ru(bipy)_3^{+2}$ concentrations were typically 10^{-4} M .

The intensity-time data were accumulated by measuring the signal voltage change of the decay pulse from the scope baseline at 100 ns intervals. To prevent scattered light from interfering, measurements were begun 100 ns after the LASER pulse. Naperian logarithms of the data were plotted versus time and were analyzed by least squares to obtain the best fit slope (figure (4)). Also calculated was the correlation coefficient of the data, which always exceeded 0.99.

The data from six different degassed samples at 23 ± 2° in 0.100 N H_2SO_4 resulted in a solution lifetime of 0.60 ± .04 x 10^{-6} S. Data on nine different air-saturated solutions produced an average lifetime of 0.39 ± .04 x 10^{-6}S, reflecting the quenching ability of dioxygen on the emissive state.

Measurements on the ground state repopulation process of $Ru(bipy)_3^{+2*}$ were also made on a nanosecond time scale

Figure 4. Representative plots of $\log_e I$ (emission) vs: time for LASER-pulsed $Ru(bipy)_3^{+2}$ in 0.1 N acid, monitored at 583 nm.

Figure 5. Superposition of absorption spectrum of $Ru(bipy)_3^{+2*}$ and ground state depletion spectrum of $Ru(bipy)_3^{+2}$ following a 10 ns LASER pulse (R.T., 0.1 N acid).

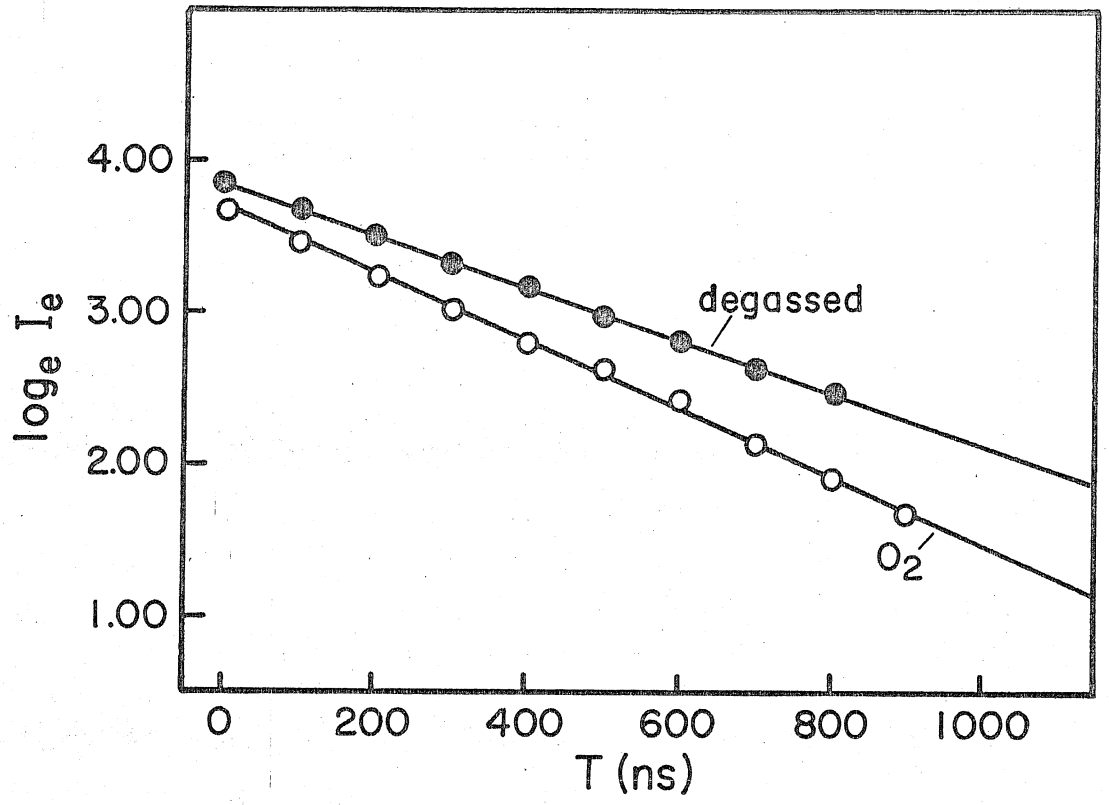
4.00
3.00
2.00
1.00
$\log_e I_e$
degassed
O_2
0
200
400
600
800
1000
T (ns)

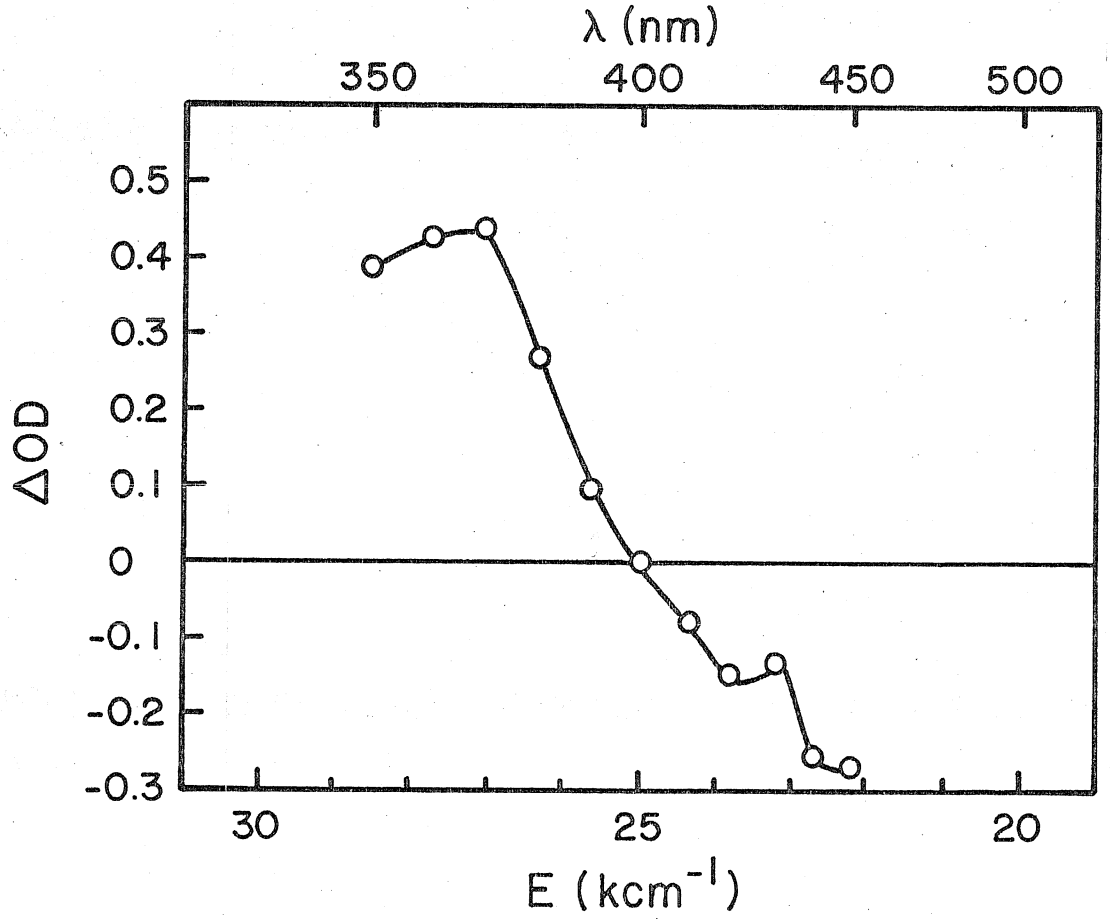
λ (nm)
350
400
450
500
0.5
0.4
0.3
0.2
0.1
0
-0.1
-0.2
-0.3
ΔOD
30
25
20
E (kcm^{-1})

while monitoring $Ru(bipy)_3^{+2}$ absorption at 453 nm (λ max). An analysing pulse was generated by triggering an H_2 thyratron-driven 5 megawatt flash lamp. A fast photodiode monitoring the lamp intensity triggered a LASER pulse when the lamp was at maximum intensity.

The flash lamp and LASER pulse were aligned to intersect inside a 1.00 cm sq. sample-containing cuvette. The active coaxial excitation volume was 0.7×10^{-4} L. After passing through the cuvette, the analysing beam impinged upon a beam director and was reflected into the photomultiplier-monochromator, which was the same unit used for fluorescence studies. The analysing pulse lasted for 10^{-6}S.

Absorption data were collected in two ways. In the first case, absorbance readings were obtained from a composite photograph of three oscilloscopic traces generated by 1) triggering the flash lamp to obtain the lamp time profile and O.D. baseline, 2) firing the LASER to correct the baseline for scattered LASER light, and 3) firing the LASER and lamp synchronously to monitor for absorbance changes produced by ground state depletion of $Ru(bipy)_3^{+2}$ and/or transient absorption.

O.D. changes were calculated from the recorded intensity data by taking the logarithm of the ratio of the $(L+F)/F$ intensities at a specific time point after correcting the $L+F$ trace for scattered light (always less than 10%). At 453 nm O.D. changes were formally negative since the light

transmission of the solution increased upon LASER flashing.

The second method gathered data with a PAR boxcar averager which was set to slowly scan its sampling aperature along the decay profile of the experiment. To prevent sample decomposition the LASER was blocked off except for 5 second intervals (10 pulses $\cdot S^{-1}$). The resultant trace, recorded on an X-Y recorder set to time scan, was very similar to the photographic recording method A except that the L + F intensity points appeared as spikes on the flash-lamp baseline. Calibration of the time scale of the instrument was accomplished by scanning a 100 ns sq. wave pulse from an external generator.

LASER pulse intensity was measured by placing a Scientech 3600 thermopile in the LASER beam. The LASER intensity was typically 0.09 joule$\cdot$flash^{-1} or 1.5×10^{17} photons$\cdot$flash^{-1}. The excitation volume was 0.7×10^{-4} L so the excitation density was 2×10^{21} photons$\cdot L^{-1}$. Since $Ru(bipy)_3^{+2}$ concentration was typically 10^{-4} M (6×10^{19} molecules$\cdot L^{-1}$) there were 30 photons for every absorbing molecule in the excitation volume.

As expected with such an overwhelming excitation ratio, there was complete ground state depletion of $Ru(bipy)_3^{+2}$. This was substantiated by observing the absorbance change as a function of LASER power, and finding that Δ O.D. at any fixed time point did not change until the LASER power was decreased to roughly one-half its original intensity.

The behavior of the system was first analysed in terms of the following kinetic model,

$$S^* \xrightarrow{K_s} S \qquad (9)$$

$$S^* \xrightarrow{K_x} X \qquad (10)$$

starting immediately after the laser pulse had terminated, and assuming that the unknown photoproduct, as well as S^*, is non absorbing at 453 nm. Under these assumptions, the time response of the optical density of the system is

$$\Delta(t) = O.D.^{\infty} - O.D.(t) = \epsilon^s \frac{K_s}{K} S^*_o \exp(-Kt) \qquad (11)$$

where ϵ^s is the molar extinction coefficient of $Ru(bipy)_3^{+2}$, K is the total decay rate constant of S^*, and S^*_o is the initial concentration of $Ru(bipy)^{+2}$ excited states. K_s is the rate constant for decay back to ground state. The inclusion of X into the scheme was necessary because the baseline changes during the course of an experiment, suggesting that a photoproduct is produced. Plots of $\log_e \Delta$ versus time should have slope -K if the analysis above is correct.

Unfortunately on the nanosecond time scale of these experiments, $O.D.^{\infty}$ was not yet attained. The O.D. of the system was still changing at the end of the analysing light pulse. A means by which $O.D.^{\infty}$ could be determined was needed.

This was solved with an empirical, iterative process by choosing $O.D.^{\infty}$ as a variable parameter. $Log_e \Delta$ versus t was plotted, using the experimental O.D. - time response of system, and arbitrary values of $O.D.^{\infty}$. This was continued until the adjusted data gave a slope which matched (±5%) the known slope K. K was determined by measuring the fluorescence lifetime of the sample immediately prior to the absorbtion measurement.

At this point of slope coincidence the variable parameter equals $O.D.^{\infty}$, if equation (12) is correct. Because $O.D.^{\infty}$, τ_s, and K are known, K_s can be calculated under conditions of complete ground state depletion with a measurement of $\Delta(t = o)$. Since $K = K_s + K_x$, K_x can also be calculated.

As can be seen from table (1), one of the assumptions used to derive equation (11) is definately incorrect. Values of Δ at $t = o$ were roughly one-tenth that expected for complete optical bleaching of the ground state absorbtion, even though 100% ground state depletion was demonstrated by reducing the LASER power without a decrease in Δ. A consistent explanation of this behavior which maintains the observed exponential return of ground state absorbtion is that $Ru(bipy)_3^{+2*}$ absorbs at 453 nm with an extinction coefficient close to that of $Ru(bipy)_3^{+2}$.

The kinetic treatment of this case requires simple

Table 1

RESULTS OF LASER FLASH EXPERIMENTS

Sample Preparation	O_2	Δ O.D. (T = 0)†	Δ O.D. (T = ∞)‡	$\frac{\Delta \text{ O.D. (T=}\infty\text{)}}{\Delta \text{ O.D. (T=0)}}$
Freshly Al_2O_3 chromatographed $Ru(bipy)_3^{+2}$	+	0.21	0.03	0.14
	0	0.22	0.05	0.23
$Ru(bipy)_3^{+2}$ aged after Al_2O_3 chromat.	+	0.22	0.07	0.32
Unpurified $Ru(bipy)_3^{+2}$	+	0.16	0.05	0.31
	0	0.14	0.06	0.43

† T = 0 was defined immediately after the LASER pulse.

‡ Calculated by iteration, see text.

modification of eq. (11) to give

$$\Delta = O.D.^{\infty} - O.D.(t) = \left(\epsilon^{s} \frac{K_s}{K} - \epsilon^{*} \right) S_o^{*} \exp(-kt) \qquad (12)$$

Where the symbols retain their previous meaning and ϵ^{*} is the extinction coefficient of $Ru(bipy)_3^{+2*}$.

That an absorbing transient was produced was verified by monitoring other wavelengths at a fixed time delay from the LASER pulse. This spectrum was not influenced by N_2 purging of the solution. A composite maximum was observed at 370 nm. A node was seen at 400 nm which indicates that ϵ^{s} and ϵ^{*} are equal at this wavelength (figure (5)). Because decay of the absorption matched the fluorescence lifetime of $Ru(bipy)_3^{+2*}$, the absorbing transient is likely $Ru(bipy)_3^{+2*}$.

Further examination of table (1) reveals that the amount of photodecomposition of $Ru(bipy)_3^{+2}$ after one LASER pulse was quenched by oxygen and was also quite sensitive to sample preparation. This suggests that decomposition occurs upon interaction of $Ru(bipy)_3^{+2*}$ with some unknown solution impurity and is not a unimolecular process. This mode of decomposition was found to be reversible between LASER pulses (0.1 S) so that a return to the original absorption baseline was observed by the time of the following flash. Natarajan and Endicott[4] have seen similar

behavior from flashed solutions of $Ru(bipy)_3^{+2}$ in acid (vide infra.).

What ever the nature of the photoproduct, it is probably not involved in producing Fe^{+2} oxidizing species. Its formation is quenched by O_2. As will be seen, oxidant formation is directly proportional to the O_2 quenching fraction.

The Quenching of $Ru(bipy)_3^{+2}$ Emission by Iron(III), Iron(II), and Dioxygen.

Since $Fe^{+2,+3}$ and O_2 were all components of the system it was necessary to know the rates of interaction of these substances with $Ru(bipy)_3^{+2*}$. Stern-Volmer plots[37] were used to determine the rate constants for sensitizer quenching. All measurements were made at room temperature, 23 ± 2°C.

Iron(III) quenching in aerated solution was investigated by observing the diminished emission from solutions of constant $Ru(bipy)_3^{+2}$ concentration but varying ferric content. The experiment was performed on a Hitachi-MPF-2A fluorimeter, exciting at 500 nm. This choice of excitation wavelength avoided the problem of competative light absorption by iron. Emission was viewed at 583 nm, the apparent maximum.

Iron solutions were prepared by dissolving known weights of $Fe(SO_4)_2NH_4 \cdot 12H_2O$ in 0.100 or 1.44 N H_2SO_4.

The Stern-Volmer plots were linear at both acidities with $R > 0.99$ and nearly identical slopes. At pH 1, $K_Q\tau$ = 1275 ± 61 M^{-1} and at pH =-0.17 (calc.), $K_Q\tau$ = 1101 ± 6 M^{-1}.

Taking $\tau = 0.39 \pm .04 \times 10^{-6}$ S gives $K_Q = 3.3 \times 10^9$ $M^{-1} S^{-1}$ at pH = 1 and $K_Q = 2.8 \times 10^9$ $M^{-1} S^{-1}$ at pH = -.17. These values compare very well with those reported by Meyer *et al.*[5] for the quenching of $Ru(bipy)_3^{+2*}$ in degassed 1.0 M perchloric acid ($K_Q = 3 \times 10^9$ $M^{-1} S^{-1}$). Balzani and Laurence[2] report a somewhat lower value of $K_Q = 1.9 \pm .2 \times 10^9$ $M^{-1} S^{-1}$ in 0.25 M $HClO_4$. This may be a reflection of the lower temperature (19 ± 2°C) employed for their experiments.

An analogous fluorescence procedure was used with iron(II). In this case a 4.09×10^{-2} M solution of Mohr's salt, $Fe(SO_4)_2(NH_4)_2 \cdot 6(H_2O)$ was prepared in 0.100 N H_2SO_4. The adventitious concentration of Fe^{+3} (aq.) in this solution was measured by the visible absorbance at 480 nm of the $Fe(SCN)_6^{-3}$ complex[38] formed by adding a known volume of NH_4SCN solution (0.100 N SA) to a known volume Fe^{+2} stock. A calibration plot established the extinction coefficient of $Fe(SCN)_6^{-3}$ to be 9,100 ± 140 $M^{-1} cm^{-1}$ at 480 nm.

By this method [Fe^{+3}(aq.)] was determined to be 1.37×10^{-4} M.

The stock solution was diluted to provide different Fe^{+2} concentrations. The resultant S-V plot of Io/I versus iron(II) concentration was reasonably linear with slope

$3.21 \pm .27\ M^{-1}$, an apparent indication that Fe^{+2}(aq.) was quenching $Ru(bipy)_3^{+2*}$ emission as reported by Laurence and Balzani[2].

However, the slope was considerably less than that obtained by ref. 2, $K_Q\tau = 6.4 \pm .7\ M^{-1}$. Furthermore, a comparison of the total quenching with that expected for the calculated quantity of Fe^{+3}(aq.) present shows that the two numbers are very nearly equal (vide infra.). The actual quenching plot and that expected by Fe^{+3} are shown in figure (6).

A Stern-Volmer plot of dioxygen quenching was prepared using a degassable fluorescence cuvette which was evacuated prior to O_2 filling. The concentration of dissolved oxygen was calculated from the Henry's Law constant and the known final pressure of O_2 [39]. For each pressure, the emission intensity of the $Ru(bipy)_3^{+2}$ containing solution was measured before and after O_2 filling. The cell was filled with O_2 by attaching the evacuated cell to the pressure regulator preset to a desired final pressure.

After opening the cuvette to the O_2 atmosphere, the cell was shaken to ensure equilibration, and finally disconnected from the regulator.

The resultant Stern-Volmer plot is shown in figure (7). The slope of the best-fit straight line is $2009 \pm 69\ M^{-1}$. Using 0.60×10^{-6} S as the lifetime of $Ru(bipy)_3^{+2*}$ in 0.100 N H_2SO_4 establishes the quenching rate constant to be

Figure 6. $Ru(bipy)_3^{+2*}$ Stern-Volmer quenching by Fe^{+2}(aq.) with small adventitious concentrations of Fe^{+3} determined by direct analysis. The lower curve is that predicted for only Fe^{+3} present (0.1 N acid, 23°C).

Figure 7. Stern-Volmer quenching by Fe^{+3} (left ordinate) and O_2 (right ordinate) in aerated 0.1 N acid.

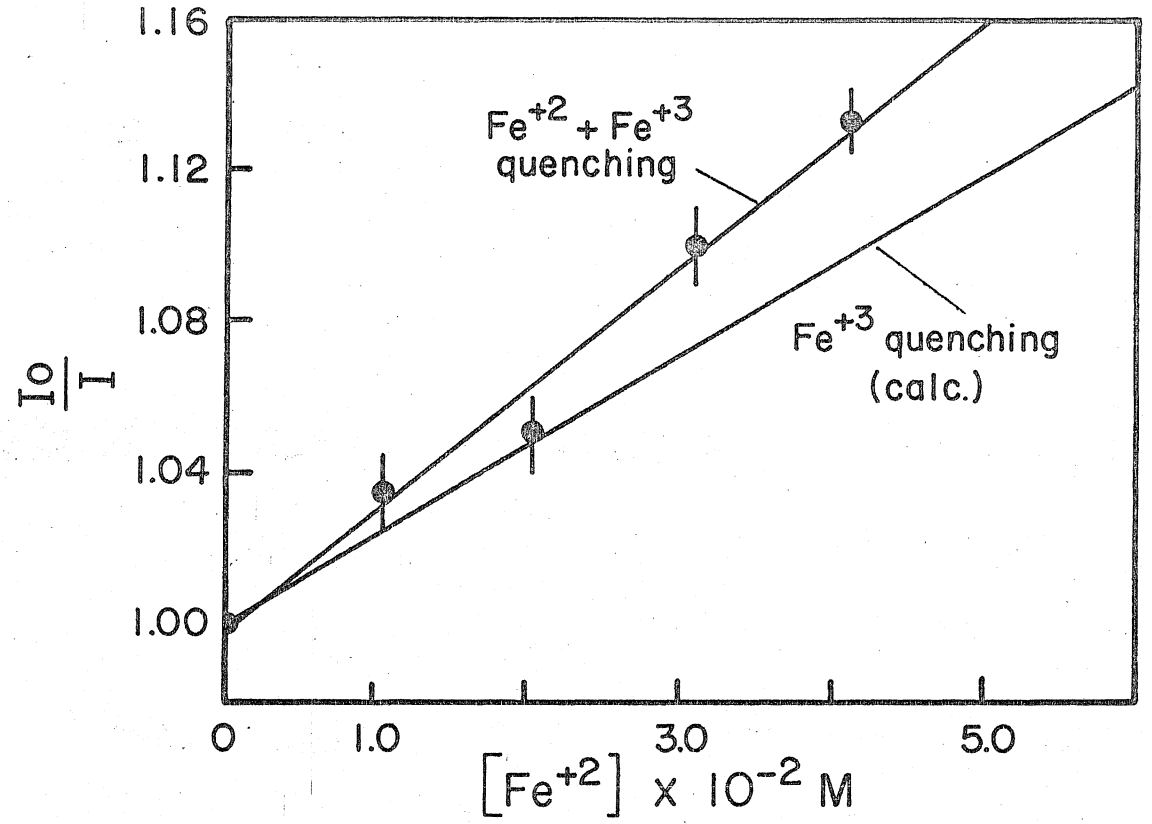
1.16
1.12
1.08
1.04
1.00
$\frac{I_0}{I}$
$Fe^{+2} + Fe^{+3}$ quenching
Fe^{+3} quenching (calc.)
0
1.0
3.0
5.0
$[Fe^{+2}] \times 10^{-2}$ M

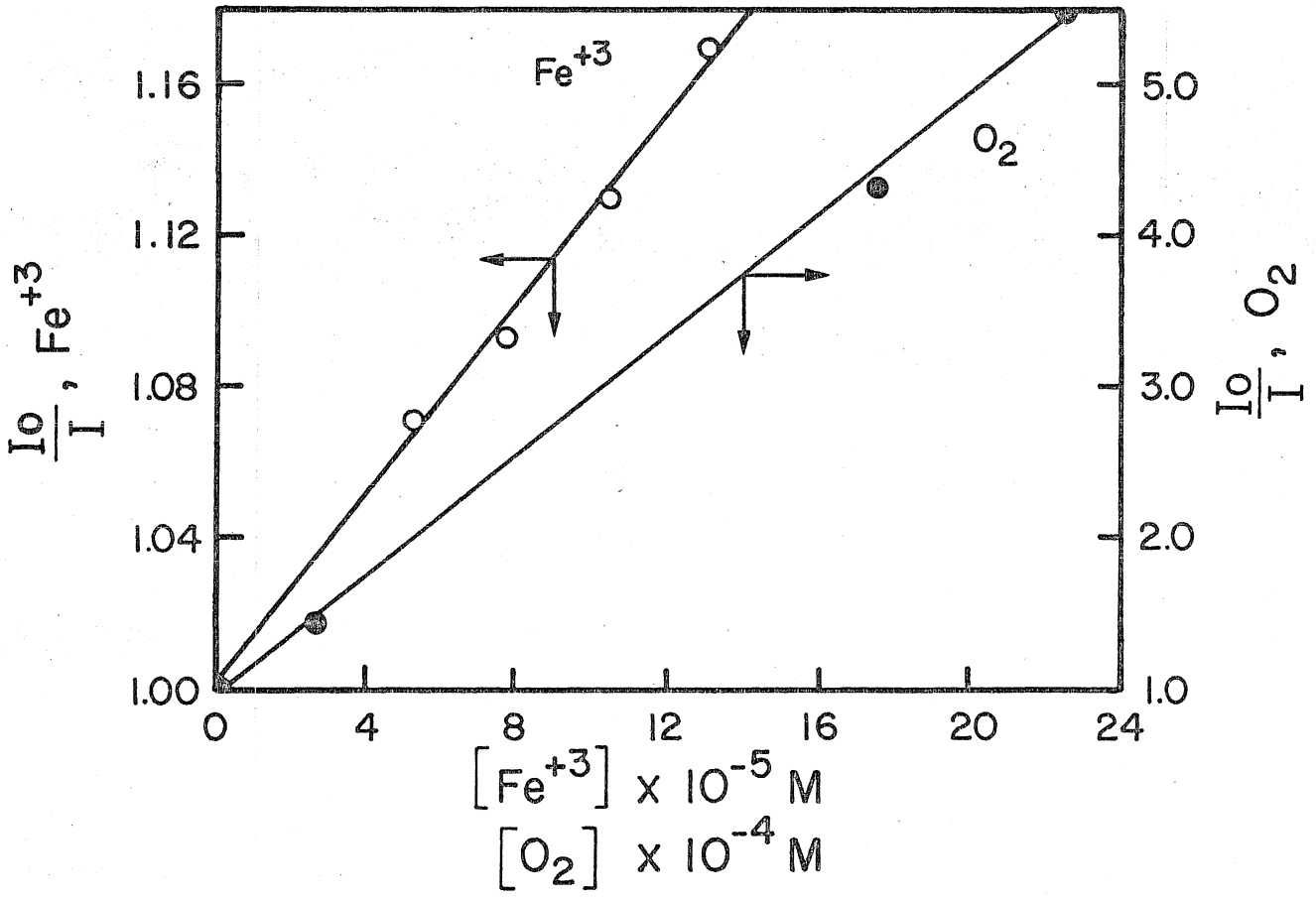
Fe^{+3}
O_2
1.16
1.12
1.08
1.04
1.00
$\frac{I_0}{I}$, Fe^{+3}
5.0
4.0
3.0
2.0
1.0
$\frac{I_0}{I}$, O_2
0
4
8
12
16
20
24
$[Fe^{+3}] \times 10^{-5}$ M
$[O_2] \times 10^{-4}$ M

$3.4 \times 10^9\ M^{-1} S^{-1}$. Other workers have measured similar values[3,24].

Oxidation Quantum Yield Measurement and the Effect of Changing Experimental Variables.

Quantum yields for Fe^{+3}(aq.) production were determined at 313 and 436 nm. Also determined were the effects of O_2 concentration, Fe^{+2} content, pH, sensitizer concentration, solution acid type, and ionic strength on the relative oxidation efficiency.

At 313 nm, oxidation quantum yields were measured in a standard Merry-Go-Round[40] apparatus using 3.00 ml sample volumes in 13 x 100 mm pyrex test tubes. Light intensities were measured by ferrioxalate actinometry ($\Phi(Fe^{+2}) = 1.21$)[41]. The irradiated solutions were maintained at 17 ± 1°C.

At 436 nm, a small rotating cell holder with precisely machined windows was used in conjunction with an external 450 w SC 679 Hanovia Hg lamp equipped with a 450 nm interference filter and a Corning 0-51 U.V. cut-off filter.

This filter combination did not completely isolate the 436 nm mercury emission line. It was found to allow a 10% light leak at 405 nm, which was measured by beaming the lamp-filter combination directly into the Hitachi-Coleman 139 monochromator. A 3 g/L solution of Rhodamine B was placed in the cell compartment of the spectometer. This solution absorbed all the incident light, giving red-shifted

fluorescence which was proportional to the incident light intensity, independent of wavelength in the range 200-600 nm[42].

Two mercury lines were thus found to be present, the major line at 436 nm and a minor line at 405 nm (10:1 ratio). Quantum yields were corrected for the differential absorption between actinometry solution and $Ru(bipy)_3^{+2}$ solution at 405 nm.

To neutralize any geometry effect on the absorbed light intensity which arose from the rotation of the cell holder in front of the fixed lamp, actinometry was performed using O.D.-matched actinometry and sample solutions. In such a case the incident light does not remain in the center of sample holder where absorption is well defined, but is refracted through smaller pathlengths. Even with large optical densities not all the light is absorbed.

If samples of different O.D. were compared, a differential absorption would occur even if 100% of the light were absorbed in the center of each sample tube.

Ferrioxalate actinometry was employed at 436 nm using $\Phi(Fe^{+2}) = 1.05$[41]. The $Fe(C_2O_4)_3^{-3}$ concentration was 0.030 M which gave an O.D. (1.00 cm) of 0.94 at 436 nm. The temperature of these measurements was 23 ± 2°C.

Qualitatively, Fe^{+3} appearance in irradiated $Ru(bipy)_3^{+2}$-Fe^{+2} solution was identified by adding NH_4SCN and noting the presence of brick red $Fe(SCN)_6^{-3}$ compared to unirradiated

blank solution[38]. Quantitatively, two different spectroscopic techniques were used for Fe^{+3} analysis.

The first, method A, directly measured the appearance of iron(III) by monitoring the absorbance change at 320 nm of irradiated solution compared to identical, unirradiated solution. The extinction coefficient of Fe^{+3} in 0.100 N H_2SO_4 was determined to be 1777 $M^{-1}cm^{-1}$. 320 nm was chosen because the absorbance of Fe^{+3} nears a maximum at this point and the sensitizer does not absorb strongly.

The second, method B, correlates the progressive diminuation of $Ru(bipy)_3^{+2}$ emission with increasing irradiation time to the production of Fe^{+3}(aq.), an excellent quencher. Of the two, method A gave the best precision, although both gave comparable accuracy. The exact procedure, and the results of method A are as follows.

A stock solution of $Ru(bipy)_3^{+2}$ was prepared by dissolving enough $Ru(bipy)_3Cl_2 \cdot 6\,H_2O$ in 0.100 N H_2SO_4 to produce a 1.00 cm. optical density of greater than 2.0 (Iabs. > 99%) at 313 nm. This solution was added to a volumetric flask containing a precisely weighed amount of $Fe(II)(SO_4)_2(NH_4)_2 \cdot 6\,H_2O$ and shaken in the dark to effect dissolution. A standard concentration of 6.3×10^{-3} M Fe^{+2}(aq.) was arbitrarily chosen for all quantum yield measurements unless otherwise noted. It was found that the oxidation quantum yield was insensitive to $[Fe^{+2}]$.

A portion of this air-saturated mixture was used as a blank for O.D. measurement. 3.00 ml aliquots of the remaining solution were pipeted into clean 13 x 100 mm pyrex culture tubes for parallel irradiation. A zero-time tube was removed and used to establish the absorption cell error arising from incomplete matching of the optical cuvettes.

Due to the large absorbance of the optical blank at 320 nm (because of the sensitizer extinction) it was necessary to use a high amplifier sensitivity to obtain apparent zero absorbance blank readings with the Hitachi-Coleman 139 spectrometer.

Tubes were irradiated in parallel for up to 70 minutes in the 313 nm M.G.R. and measured immediately for absorbance change at 320 nm. The quantum yield for Fe^{+3} production was determined by plotting the O.D. change vs. irradiation time and determining the slope of this graph by least squares analysis. It was then possible to calculate the quantum yield from this number, the extinction coefficient of Fe^{+3} at 320 nm, the sample volume, and the known light intensity. A representative plot is shown in figure (8).

An important consideration was to limit the production of Fe^{+3}(aq.) to small values because of the quenching effect of this species toward $Ru(bipy)_3^{+2*}$. Another potentially complicating factor in the course of a 313 nm irradiation was competitive absorption of the exciting light by Fe^{+3}. Oxidations were typically terminated at an iron(III)

Figure 8. A graph of iron(III) absorption vs: irradiation time at 313 nm, used to determine ΦFe^{+3} by method A.

Figure 9. Modified Stern-Volmer method showing fluorescence quenching relative to an unirradiated blank solution at 583 nm as a result of Fe^{+3} production (method B).

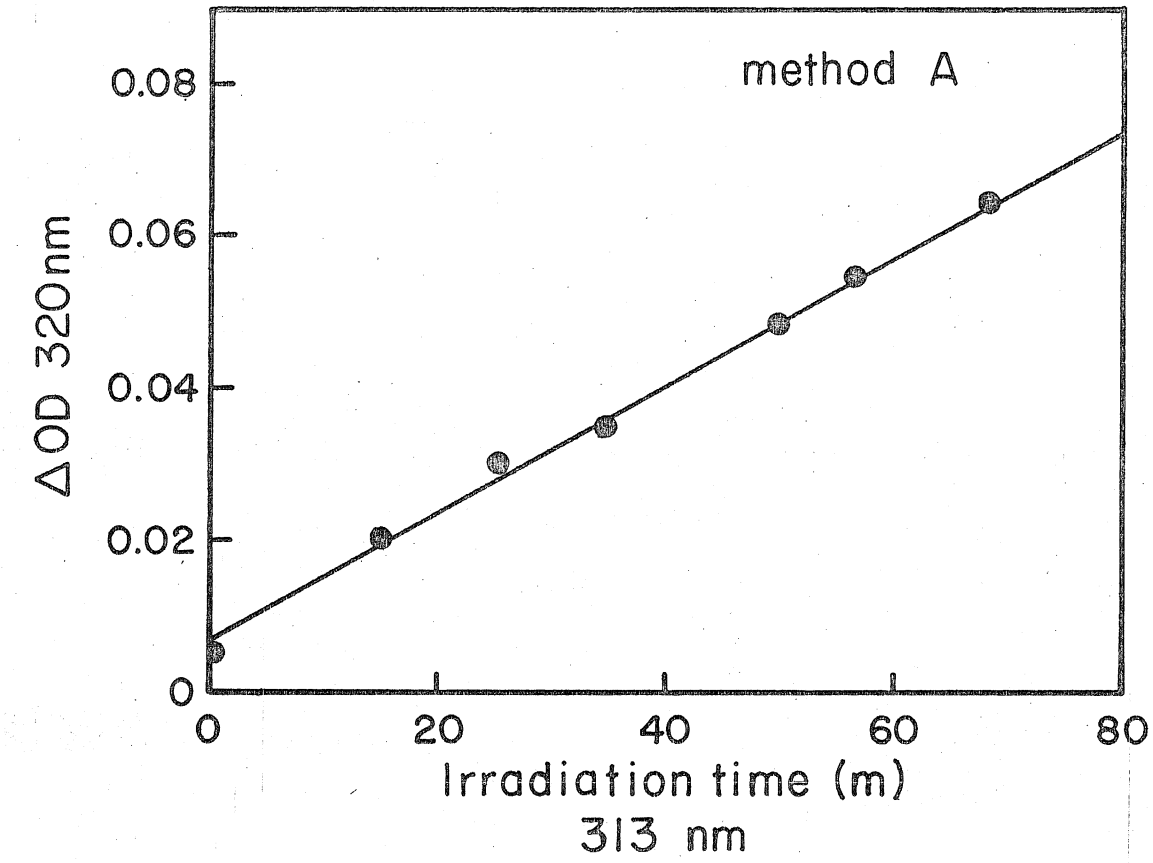
method A
0.08
0.06
0.04
0.02
0
ΔOD 320nm
0
20
40
60
80
Irradiation time (m)
313 nm

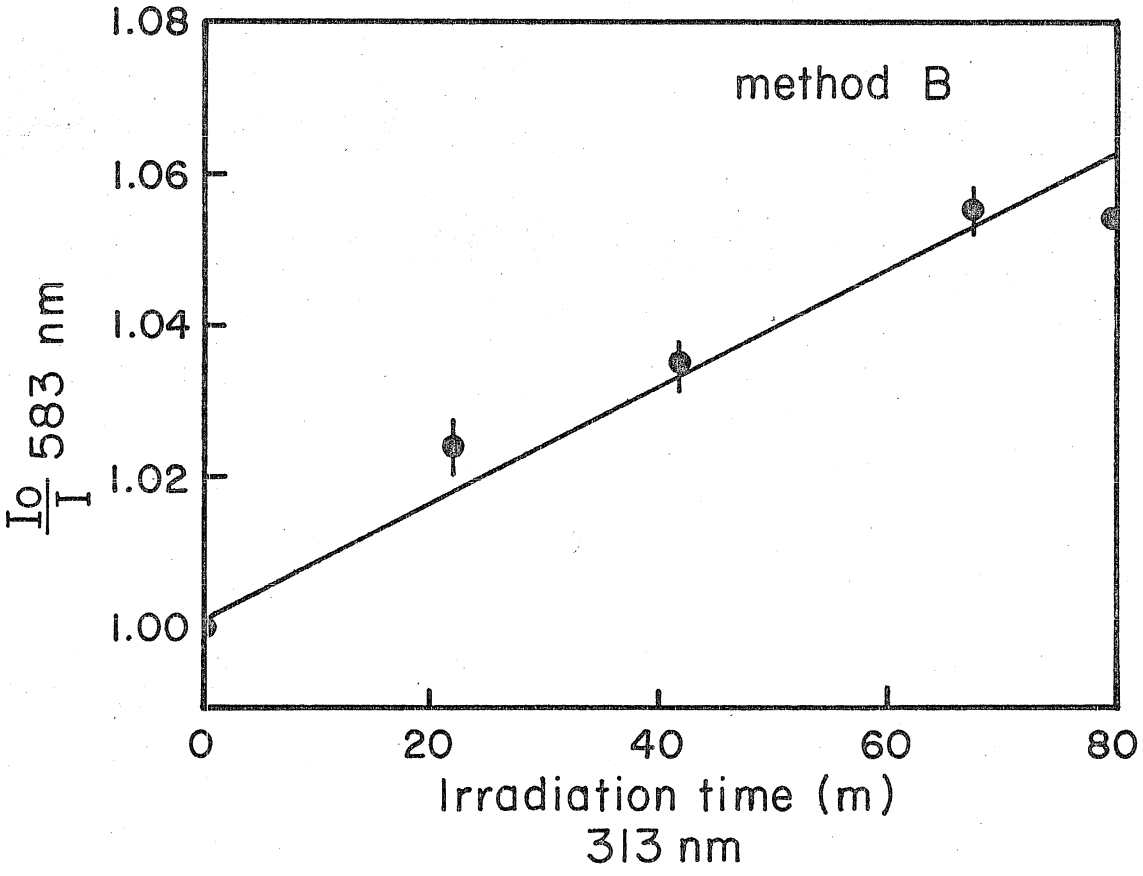
method B
1.08
1.06
1.04
1.02
1.00
Io/I 583 nm
0
20
40
60
80
Irradiation time (m)
313 nm

concentration of 5×10^{-5} M, at which there was a calculated 5% inhibition of the photoreaction. Oxidation plots were still linear at this point.

Two independent experiments at 313 nm, encompassing 11 irradiated samples, gave quantum yields of $3.39 \pm .08 \times 10^{-2}$ $N \cdot E^{-1}$ and $3.45 \pm .08 \times 10^{-2}$ $N \cdot E^{-1}$, both obtained at 17 ± 1°C. The first number was obtained from synthetic recrystallized $Ru(bipy)_3^{+2}$, while the second was derived from freshly Al_2O_3-chromatographed $Ru(bipy)_3^{+2}$.

This method was also used for irradiation at 436 nm, at a sample temperature of 23 ± 2°C. The procedure was identical to that previously mentioned except that actinometer and sample solutions had a lower, matched absorbance of 0.94 at 436 nm, thereby avoiding geometry effects on absorption in the rotating cell holder.

Again, plots of O.D.(320nm) versus irradiation time were linear with correlation coefficients > 0.99. The result of two independent runs involving nine samples gave quantum uields of $2.83 \pm .07 \times 10^{-2}$ $N \cdot E^{-1}$ and $2.8 \pm .2 \times 10^{-2}$ $N \cdot E^{-1}$ for Fe^{+3}(aq.) production. These numbers include a 5% positive correction due to the aforementioned 405 nm light leak in the lamp-filter combination.

As mentioned earlier, it was also possible by a fluorescence technique, method B. This was achieved by monitoring the progressive diminuation of $Ru(bipy)_3^{+2*}$ emission with increasing irradiation time in the presence of Fe^{+2}(aq.), a

behavior which was a direct response to Fe^{+3} quenching. In principle, the method is as accurate as method A, but in fact is not as precise. This is a consequence of the difficulty of performing accurate emission measurements on samples which differ by only a few percent in emission intensity.

The method is derived immediately from the Stern-Volmer equation in intensity form[37].

$$\frac{Io}{I} = 1 + K_{sv}[Q] \qquad (13)$$

Differentiation of (Io/I) with respect to time and rearranging gives:

$$\frac{dQ}{dt} = \frac{1}{K_{sv}} \cdot \frac{d(Io/_I)}{dt} \qquad (14)$$

Under the conditions of constant light intensity the production of Q (in this case Fe^{+3}) is constant. The derivative on the right hand side of equation (14) is the slope of a plot of $Io/_I$ versus time, from which the rate of production of Fe^{+3} can be calculated. Multiplication of (14) by the volume of the irradiated solution and division by the measured light intensity gives the quantum yield for quencher production. K_{sv} was previously determined to be $1275 \pm 60\ M^{-1}$ for Fe^{+3}.

In one experiment, a solution of 6.3×10^{-3} M Fe^{+2}(aq.) was irradiated in the presence of sufficient $Ru(bipy)_3^{+2}$ to give an O.D. > 2 at 313 nm. Four 3.00 ml aliquots were irradiated and withdrawn at roughly 20 minute intervals. Ferrioxalate actinometry was performed, which established the light intensity to be 0.517×10^{-7} $E \cdot M^{-1}$. The sample tubes were shaken after they were irradiated to provide a homogeneous solution and irradiated solutions were examined by emission spectroscopy, using a Hitachi MPF-2A fluorescence spectrometer to check for Fe^{+3} quenching.

The samples were excited at 500 nm, where Fe^{+3}(aq.) does not appreciably absorb, and emission was monitored at 583 nm. Unirradiated solution was used for a spectral blank, providing an intensity value (Io) for unquenched $Ru(bipy)_3^{+2*}$. A plot of (Io/I) versus time was reasonably linear (R = 0.97, figure (9)). The slope of this line was $0.70 \pm .08 \times 10^{-3}$ S^{-1}, which combined with the sample volume and light intensity through equation (14) gives $\Phi Fe^{+3} = 3.2 \pm .4 \times 10^{-2}$ $N \cdot E^{-1}$.

Two such experiments were also performed at 436 nm, but these experiments contained an undefined actinometry error because of the geometry problem mentioned earlier. For comparison to the other 436 nm quantum yields, the experiments gave 1.9×10^{-2} and 2.0×10^{-2} $N \cdot E^{-1}$ for the production of Fe^{+3}.

The average of the three quantum yields at 313 nm is

$3.35 \pm .13 \times 10^{-2}$ $N \cdot E^{-1}$ and the two quantum yields at 436 nm is $2.8 \pm .2 \times 10^{-2}$ $N \cdot E^{-1}$. It should be remembered these results were obtained at different temperatures in air-saturated solution. The sensitizer emission is only one-third quenched by O_2 at these concentration.

The Dependence of Φ_{ox} on Dissolved O_2 Concentration.

A solution of recrystallized G. F. Smith $Ru(bipy)_3^{+2}$ having an O.D. (313 nm) of 1.4 was prepared in 0.100 N H_2SO_4, and subsequently added to a 25 ml volumetric flask containing iron(II). The final $Fe^{+2}(aq.)$ concentration was 7.07×10^{-3} M.

A 3.00 ml aliquot of this mixture was degassed by several freeze-pump-thaw cycles under forepump vacuum at 77°K in a specially designed irradiation-absorption cell which permitted positive working pressures of O_2. The cell consisted of a high-vacuum teflon stopcock joined axially to a 13 x 100 mm pyrex test tube. At a right angle was attached a 1.00 x 1.00 cm cuvette which allowed accurate fluorescence and absorption measurements on the cell contents.

The phosphorescence intensity of the above solution was recorded before and after O_2 addition to the evacuated cell so that the fractional extent of dioxygen quenching of $Ru(bipy)_3^{+2*}$ at a specific O_2 pressure could be determined. Any long-term variations of the spectrometer sensitivity were corrected by the use of standard solution of $Ru(bipy)_3^{+2}$

to normalize the instrument sensitivity.

The evacuated cell was filled by connecting it to an O_2 cylinder which had been left flowing for a few seconds at a prescribed, regulated pressure. After the connecting tube had been flushed with O_2 , the tube was attached to the cell and the stopcock opened, pressurizing the cell. After shaking to ensure gas-liquid equilibration, the teflon stopcock was closed and irradiation of the cell was begun at a premeasured light intensity.

At measured intervals the ampoule was withdrawn from the 313 nm M.G.R. and its O.D. change at 320 nm was determined, relative to an undegassed blank solution. The cell was then returned to the stationary M.G.R. for further irradiation.

This procedure was applied at four positive oxygen pressures scanning a range of 30 to 82% emission quenching. The O_2 quenching data from this series gave an excellent Stern-Volmer plot which was described earlier in this report.

The plots of Fe(III) production were all linear with correlation coefficients > 0.99. Oxidation quantum yields were calculated from the slopes of these lines, the known sample volume, and the measured light intensities. A 4% positive correction was used to allow for the fact the solutions were not sufficiently optically dense to absorb 100% of the incident light at 313 nm .

The extent of $Ru(bipy)_3^{+2*}$ quenching was calculated by subtracting the ratio of the emission intensities with and without O_2 from unity.

$$P_Q = (1 - I_{O_2}/I) \qquad (15)$$

P_Q represents the fraction of excited states which are intercepted by dioxygen before normal decay can occur.

When the oxidation quantum yield was plotted as a function of P_Q, a linear relationship was obtained with a correlation coefficient greater than 0.99. The limiting quantum yield at 100% sensitizer quenching was 0.077 ± .005 $N \cdot E^{-1}$ (see figure (10)). At the other extreme of zero dioxygen pressure, the intercept was 0.0017, a result which is zero within experimental error.

An earlier experiment established the necessity of O_2 for the oxidation to proceed, but allowed no conclusion towards its actual mechanistic involvement. These supplementary results show that oxidant production is intimately connected with the quenching event and, for instance, does not arise from a dark reaction of dioxygen with other unknown reactive species produced by $Ru(bipy)_3^{+2*}$ in acid. In such a case a linear dependence on the number of exicted states quenched would not occur.

To investigate the lifetime of the oxidizing species produced by O_2 quenching of $Ru(bipy)_3^{+2*}$, separate volumes

Figure 10. A graph of ΦFe^{+3} versus the fraction (P_Q) of sensitizer excited states quenched by O_2 in 0.100 N acid at 26°C. Irradiation at 313 nm.

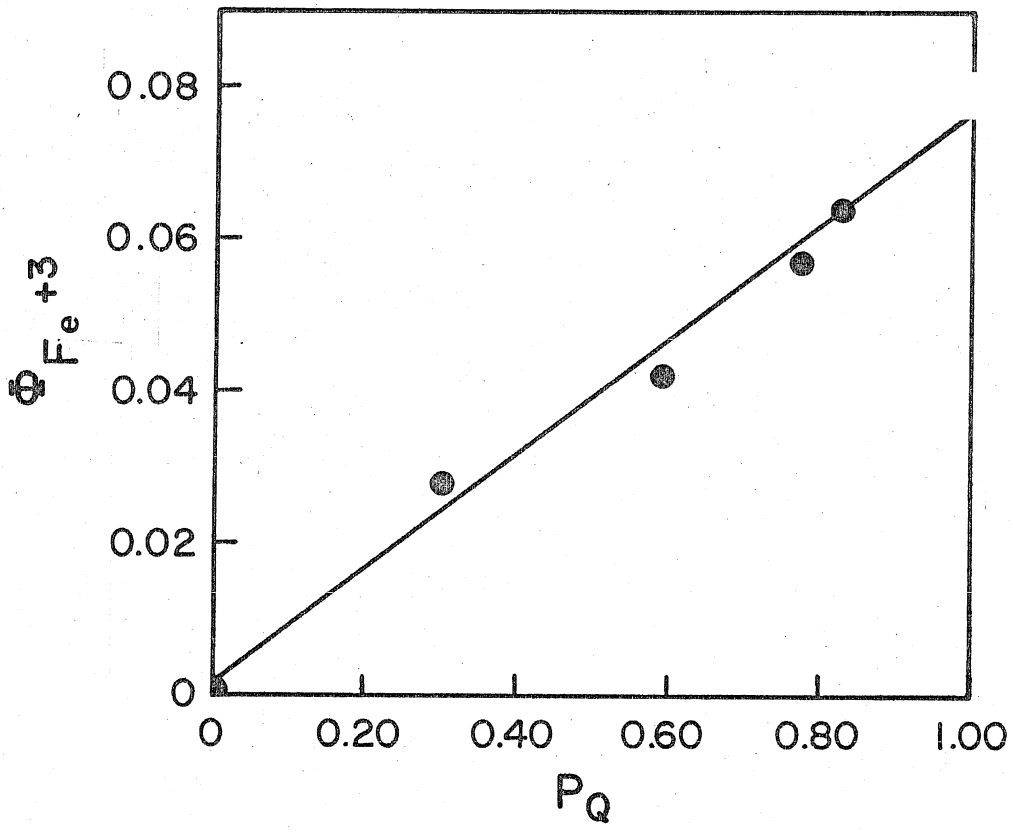
0.08
0.06
0.04
0.02
0
$\Theta_{Fe^{+3}}$
0
0.20
0.40
0.60
0.80
1.00
P_Q

of sensitizer and Fe^{+2} in 0.100 N H_2SO_4 were irradiated and then mixed. Compared to an irradiated 50/50 volume mixture of the two components as well as unirradiated blank solutions no Fe^{+3} was present even though substantial Fe^{+3} was observed in the heterogeneous tube. Since the irradiation period was 96 minutes, the lifetime of any oxidant in the system must be considerably shorter than this time.

An important conclusion is that the oxidation cannot be ascribed to the "trivial" photooxidation of Fe^{+2} which occurs when acidic solutions are irradiated at 254 nm [43] producing Fe^{+3} and H_2. There are no high-energy light leaks in these experiments. Similarly, a stable, long-lived species generated by the O_2-enhanced decay of $Ru(bipy)_3^{+2*}$ must be ruled out under these conditions.

Dependence of Fe^{+3} Production Efficiency on Iron(II) Concentration.

By comparing the slopes of oxidation plots produced by method B at different concentrations of iron(II), the relative quantum yields of oxidation were measured. In one experiment at constant sensitizer content, five different iron(II) containing series were irradiated at 436 nm. The Fe^{+2}(aq.) concentration was varied between 37.2 and 1.86 x 10^{-4} M. Within experimental error, the slopes were almost identical, but a slight inverse effect with increasing concentration was observed.

Table 2

RELATIVE DEPENDENCE OF REACTION EFFICIENCY ON $[Fe^{+2}]$.

$[Fe^{+2}] \times 10^{-4}$ M	Slope of* (Io/I) Plot	Correlation*** Coefficient	Intercept*** (T = 0)
1.86	1.16 ± .05	0.998	1.00
3.73	1.11 ± .16	0.980	1.01
7.45	1.00 ± .12	0.988	1.00
7.45	1.08 ± .06	0.996	1.01
14.90	0.96 ± .11	0.987	1.01
37.20	1.00 ± .02	0.999	1.00
40.40**	0.84 ± .04	0.997	0.997
92.10**	0.80 ± .07	0.992	0.992
182.00**	0.70 ± .03	0.997	0.998

* $\times 10^{-3}\ S^{-1}$

** Obtained at a different light intensity than 1st set.

*** Obtained from least-squares analysis of data.

This behavior was confirmed by a second experiment in which the iron(II) content was decreased from 1.82×10^{-2} M to 4.04×10^{-3} M in three steps. Again, an increase in oxidation efficiency is apparent. These data are shown in table (2).

When the three unirradiated blank tubes were compared by emission, the sensitizer emission decreased monotonically with increasing Fe^{+2} content. As seen earlier, this is due mainly to quenching by zero-time Fe^{+3}(aq.). Using the apparent S-V quenching constant obtained earlier, 3.21 M^{-1}, a 6% decrease in oxidation efficiency is predicted upon decreasing the iron(II) content from 182 to 1.86×10^{-4} M. The change seen is larger, but spurious Fe^{+3} concentrations are expected to vary depending upon solution age. It thus appears that there is no Fe^{+2} dependence (±15%) on the oxidation quantum yield in this concentration domain.

The Effect of Solution Acidity and Ionic Strength on Oxidation Efficiency.

In contrast to the effect of Fe^{+2} on the oxidation reaction, a marked pH dependence exists, which is not an ionic-strength phenomenon. To reveal the pH dependence in air-saturated solution, three sample sets of different acidity were irradiated in parallel at 436 nm at constant Fe^{+2} and sensitizer concentration (23 ± 2°C).

Solution pH was changed by adding measured volumes of concentrated H_2SO_4 to aliquotic portions of sensitizer and Fe^{+2} in 0.100 N H_2SO_4. At an iron(II) concentration of 1.9×10^{-3}M, the results of method B are shown in figure (11). A dramatic effect was encountered. From the ratio of the slopes, and known quantum yield in 0.100 N H_2SO_4, the quantum yields at higher acidities were calculated. At 0.100, 0.615, and 1.10 M hydrogen ion, quantum yields were 0.028, 0.053, and 0.065 $N \cdot E^{-1}$ respectively.

Unirradiated blank solutions showed identical emission within 3%, so the combined effects of changing oxygen solubility and changing sensitizer lifetime with acidity must be either small or counteracting. The lifetime of $Ru(bipy)_3^{+2*}$ has been reported to be unaffected by pH[44], while dioxygen solubility decreases by 12% in going from distilled water to 1 N H_2SO_4 [45] at 25°C. Similarly, a change in the quenching rate constant of Fe^{+3} does not account for changes observed in the Fe^{+3} production efficiency.

To verify an actual pH effect and not just a general ionic-strength effect, oxidations were carried out at different acidities but constant ionic strength, by adding Na_2SO_4. Method A was used, irradiating at 313 nm. Two identical solutions of $Ru(bipy)_3^{+2}$ in 0.10 and 1.0 N H_2SO_4 were prepared and enough anhydrous Na_2SO_4 was added to the first to make a 0.90 N sodium sulfate solution. The total ionic strength in both cases was 1.5 M including a 7×10^{-2}M

Figure 11. Demonstration by method B of the effect of pH change on ΦFe^{+3} at ambient temperature in aerated H_2SO_4 solution. Irradiation at 436 nm.

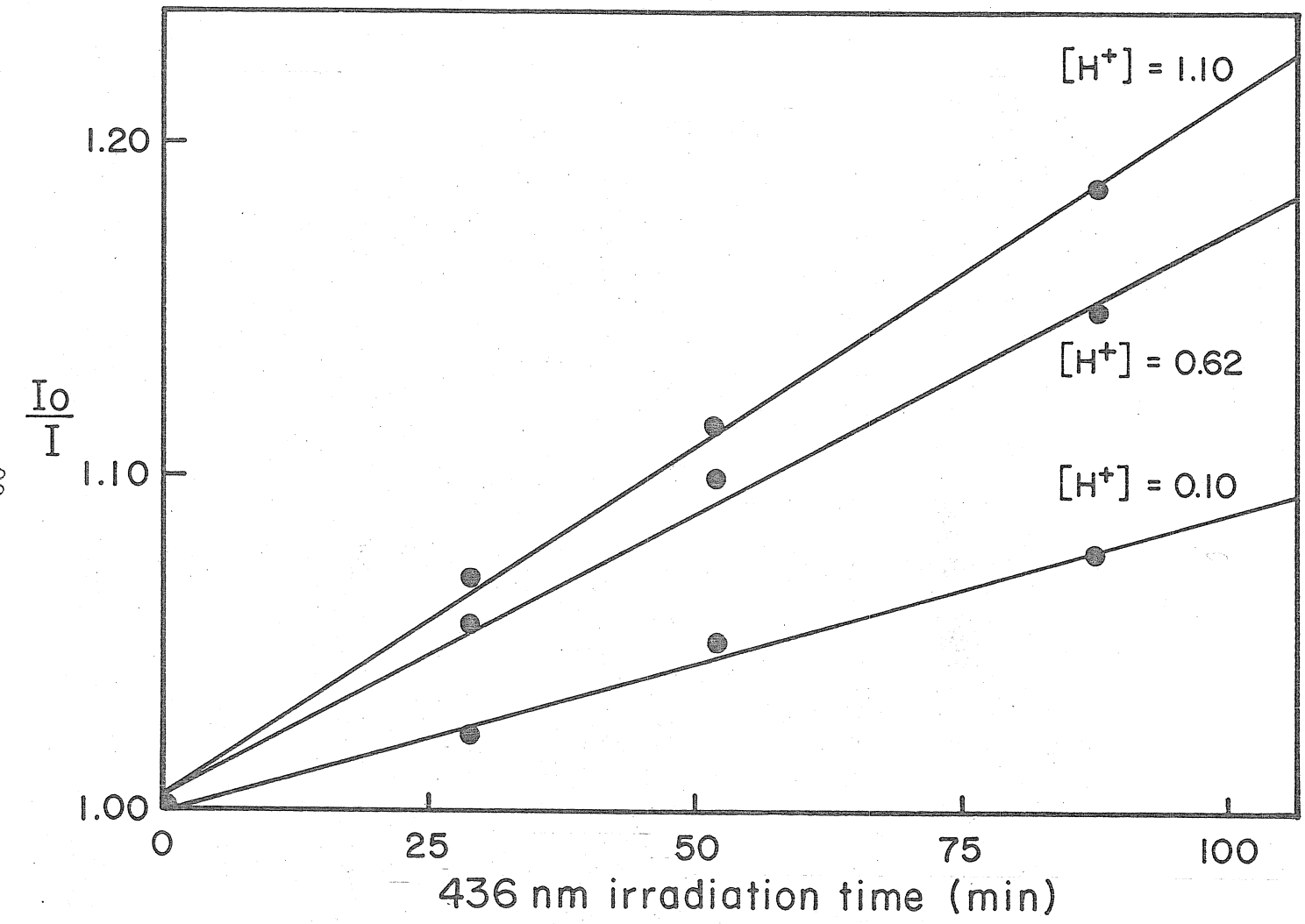
[H+] = 1.10
[H+] = 0.62
[H+] = 0.10
1.20
1.10
1.00
Io/I
0
25
50
75
100
436 nm irradiation time (min)

contribution of Fe^{+2}.

Samples of each were irradiated at the same light intensity and temperature (25 ± 1°C). Again, Fe^{+3} was found to increase 2.6 times as rapidly in the more acid solution, which is experimentally equal to the previous result in sodium sulfate-free solutions (figure (10)).

This result was confirmed by measurements in 0.09 N $HClO_4$ and H_2SO_4 at a similar iron(II) concentration. Oxidation plots by method B gave a ratio of oxidation quantum yields of 1.04 ± .09 (H_2SO_4 / $HClO_4$) also showing that the type of added acid does not influence the reaction efficiency.

Effect of Sensitizer Concentration on the Reaction Quantum Yield.

A final experiment was performed to determine if the oxidation were sensitive to sensitizer concentration. In a simple mechanism in which the reaction initiates upon quenching of $Ru(bipy)_3^{+2*}$ and proceeds with no other involvement of $Ru(bipy)_3^{+2}$, the only expected dependence is due to differential optical absorption. The reaction yield should be directly proportional to the amount of light absorbed. On the other hand, a deviation from proportionality could indicate an involvement of ground state $Ru(bipy)_3^{+2}$ or a reaction which requires bimolecular participation of intermediates generated by $Ru(bipy)_3^{+2}$ quenching.

Relative rates of iron(III) production were measured by method A in 0.100 N H_2SO_4 (Fe^{+2} = 1.4 x 10^{-3} M) at 17°C. Two different sensitizer concentrations were used, giving 1.00 cm. O.D.'s of 1.1 ± .1 and 0.305 at 313 nm, a ratio of 3.6. Corrected for the 1.10 cm path length of 13 x 100 mm sample tubes, irradiated solutions absorbed 93.7 and 53.9%, respectively, of incident light at 313 nm. The ratio is 1.47 ± .02.

Iron(III) production was found to be linear in each irradiated series, the data from both runs having a correlation coefficient > 0.99. The slope ratio was 1.55 ± .12. Dividing the absorption ratio by the quantum yield ratio gives 1.12 ± .09, a number which slightly exceeds unity within experimental error.

A likely cause for a deviation of this size is that a small reflection error occured in the sample set of lower O.D.. Some light passing through the tube (~ 50%) will reflect from the solution-glass interface and be absorbed upon its second pass through the cell. The oxidation yield is seen to be closely proportional to the light absorbance over a 4-fold sensitizer concentration range.

Measurement of the Emission Quantum Yield of $Ru(bipy)_3^{+2}$ as a Function of Exciting Wavelength in 0.100 N H_2SO_4.

The emission quantum yield of $Ru(bipy)_3^{+2}$ has been shown to be invariant with excitation wavelength in the

range 275-550 nm in alcoholic solvent[35], but not in a proton donating medium. It was decided to verify this finding in 0.100 N H_2SO_4.

The method follows that of Melhuish[42], and proceeds by determining the intensity profile of the excitation source of a fluorescence spectrometer by use of a quantum counter - a device whose emission response is wavelength independent. Under identical conditions, the fluorescence profile of the test compound is measured at constant optical density. If the ratio of the ordinates of these two curves changes, a change in the emission quantum yield of the test material with excitation wavelength is indicated.

Rhodamine B in ethylene glycol ($3g \cdot L^{-1}$) was chosen as an acceptable counter solution whose emission intensity is independent of exciting wavelength from 220 to 600 nm[42]. Wavelength calibration of the emission monochromator was accomplished by monitoring the output of a small mercury vapor lamp and recording the apparent wavelength maxima of the precisely known Hg lines. The emission monochromator was then used to standardize the excitation monochromator by monitoring the scattered light from a turbid water solution of Al_2O_3 at different excitation wavelengths.

To eliminate scattered light from the excitation beam, a Corning 375 yellow filter was placed between the emission monochromator exit slit and the photomultiplier.

For quantum counter experiments, emission was monitored at 640 nm [42], with front surface emission viewing, allowed by use of the commercial Aminco attachment [47].

$Ru(bipy)_3^{+2}$ emission was monitored at 590 nm. In this case right-angle viewing was employed, while the standard excitation conditions were maintained. Also maintained was the O.D. (0.52 ± .01) of the solution at a specific excitation wavelength. Excitation profiles were very similar to those found by Melhuish [42] using a nearly identical spectrometer and lamp.

Corrected excitation spectra were made for simply recrystallized $Ru(bipy)_3Cl_2$ and recrystallized, Al_2O_3 chromatographed (pH 10) $Ru(bipy)_3Cl_2$ in 0.100 N acid. It was found that the unchromatographed sensitizer did not have a flat excitation response and demonstrated a 10% emission exultation at 313 nm compared to 436 nm. Below 300 nm, there was a marked increase in emission of about 50%. This is the spectral region of the sharp, intense π-π^* intraligand absorbtion of $Ru(bipy)_3^{+2}$. In this region experimental error is large due to the low intensity of the exciting lamp. Furthermore, small wavelength errors between the excitation monochromator and the monochromator used to match the absorbance of the sample solutions would give large emission intensity errors. This large increase is probably due to a systematic error.

However, as shown in figure (12), the corrected excitation spectrum for the more highly purified compound is indeed flat, as expected in the absence of absorbing impurities[48]. Wavelength errors may have diminished because of the use of larger excitation slit widths for this measurement.

The Photochemical Oxidation of $Ru(bipy)_3^{+2}$ in 50% H_2SO_4.

A small amount of G.F.S. $Ru(bipy)_3^{+2}$ was dissolved in 3 ml of 50% V/V H_2SO_4 and its absorption spectrum was recorded. This solution was subsequently irradiated at 313 nm ($I = 0.8 \times 10^{-7}$ $E \cdot M^{-1}$) while bubbling air through the mixture. As the irradiation proceeded, the orange solution slowly faded, simultaneously giving a less intense green hue, characteristic of ruthenic bypyridine[1b], $Ru(bipy)_3^{+3}$.

The absorption spectrum was recorded at various times. At the end of the experiment the photooxidation was found to be almost completely reversible upon the addition of excess Fe^{+2}. The spectral results are shown in figure (13).

Control experiments showed that both oxygen and light were necessary for bleaching to occur on this time scale. Furthermore the same visual effects could be obtained by bubbling Cl_2 through the solution and adding Fe^{+2}.

A subsequent test was performed to check for the stability of $Ru(bipy)_3^{+2}$ in 0.1 N H_2SO_4 since it is known to be rapidly reduced by water at pH 4 [25] and unstable in

Figure 12. Relative emission quantum yield of Al_2O_3 - chromatographed $Ru(bipy)_3^{+2}$ in 0.100 N acid at room temperature as a function of excitation wavelength.

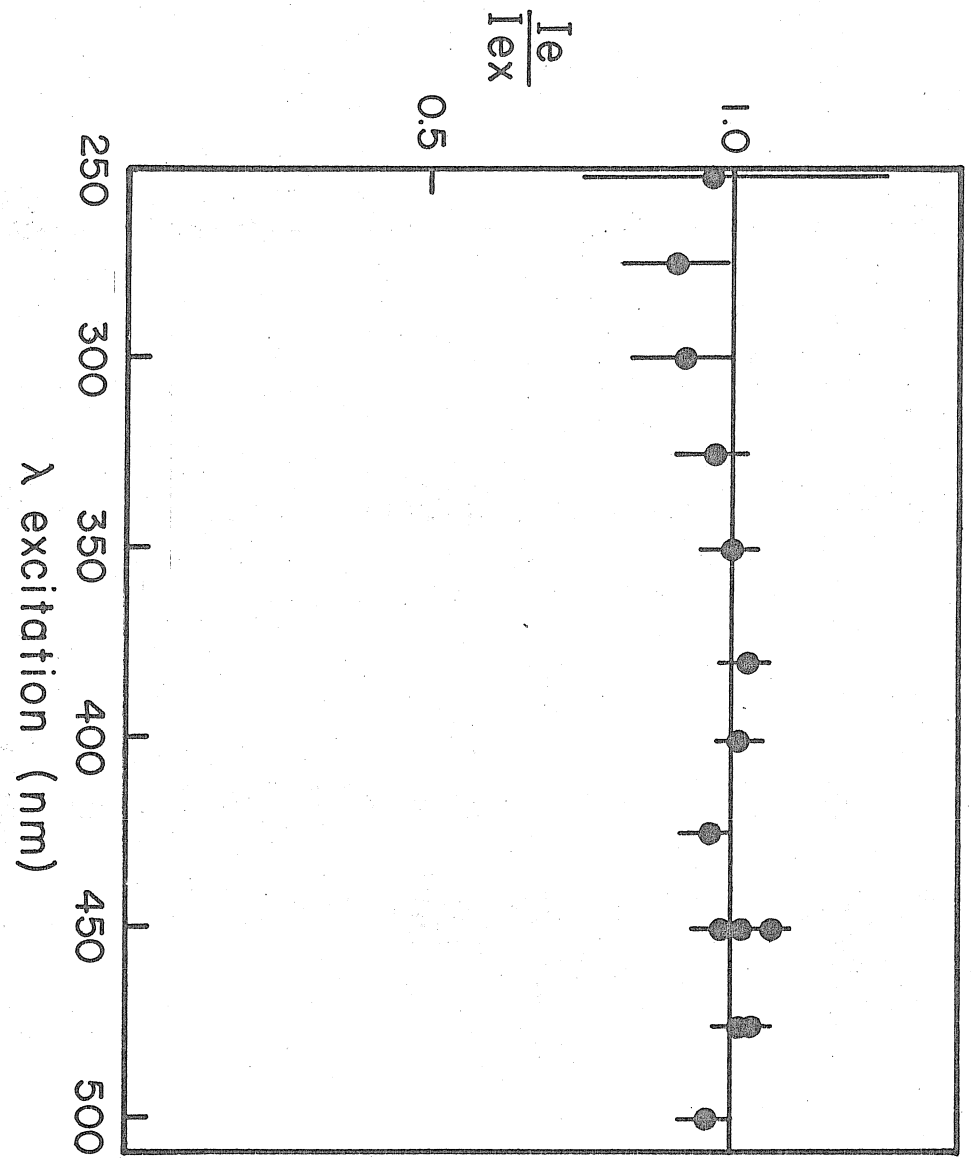
Ie/Iex
0.5
1.0
250
300
350
400
450
500
λ excitation (nm)

Figure 13. The photobleaching of aerated $Ru(bipy)_3^{+2}$ in 50 volume % H_2SO_4 at 26° in the absence of external reductants. Irradiation at 313 nm .

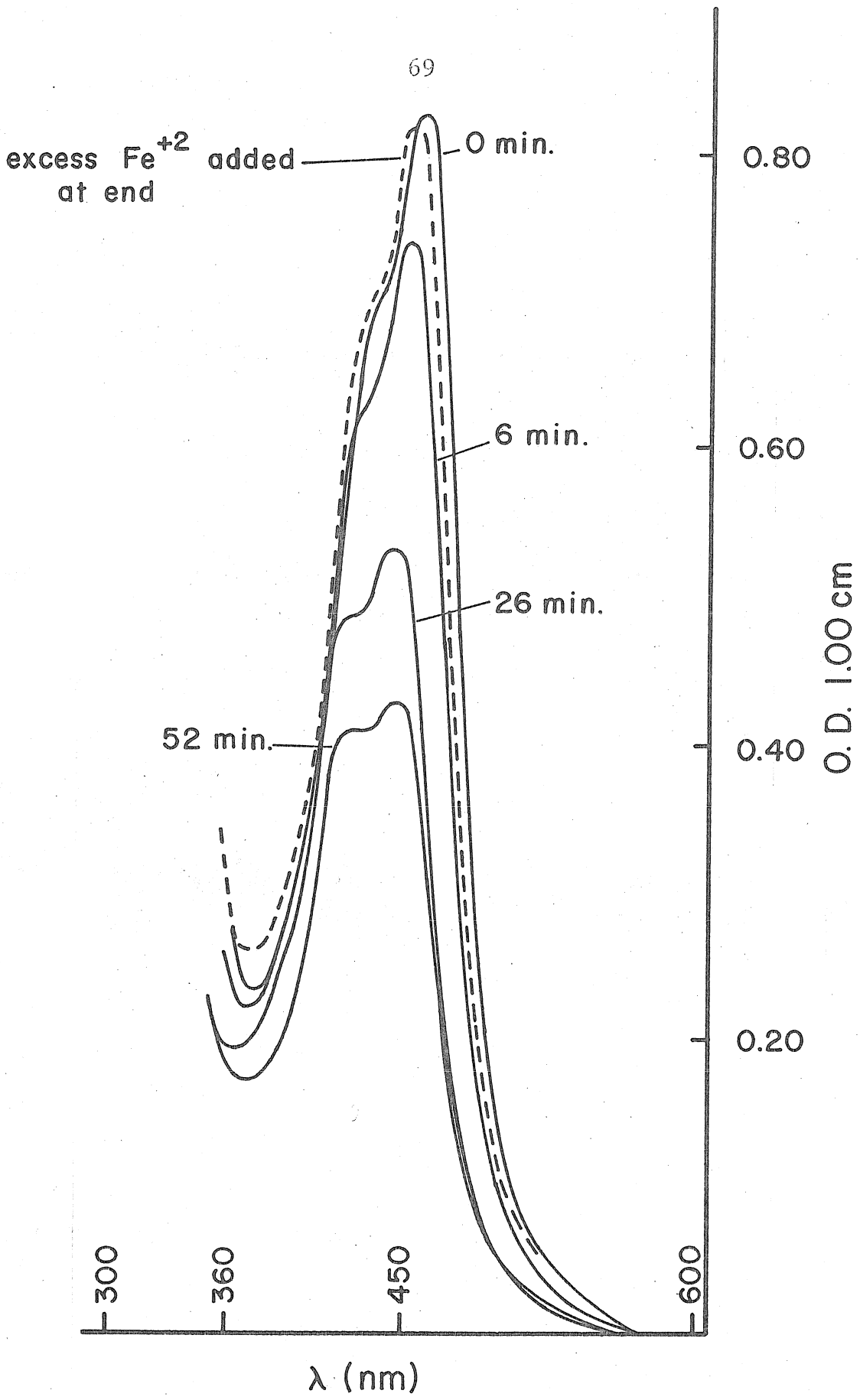
excess Fe^{+2} added at end
0 min.
6 min.
26 min.
52 min.
0.80
0.60
0.40
0.20
O.D. 1.00 cm
300
360
450
600
λ (nm)

less than 2 N sulfuric acid[49]. A solution of $Ru(bipy)_3^{+2}$ in 50% sulfuric acid was photooxidized. Of this a volume calculated to give a final acid concentration of 0.10 N was injected into vigorously stirred distilled water. On a time scale of 5 minutes no visual return to the characteristic orange color of $Ru(bipy)_3^{+2}$ was observed but could be instantaneously produced by adding a small amount of Mohr's salt.

The lifetime of $Ru(bipy)_3^{+3}$ in 0.1 N H_2SO_4 (T $\sim$30°C) is consequently greater than 5 minutes. Its lifetime in 1 N H_2SO_4 is reported to be about 1 hour at ambient temperature [3].

Search for Singlet Dioxygen: The Effect of N_1^{+2} on Reaction Efficiency.

Because of the reported efficiency of $^1\Delta g$ O_2 generation by $Ru(bipy)_3^{+2*}$ in methanol[24], it was decided to check for the participation of $^1O_2$ in the oxidation mechanism in 0.100 N H_2SO_4. Mendenhall, Suprunchuk, and Carlsson[50] have reported evidence that $NiCl_2$ catalytically quenches $^1\Delta g$ dioxygen in 2-butoxy-ethanol with an inferred rate constant of 3.1×10^8 $M^{-1}S^{-1}$ at 0°C.

It was decided to verify this finding because of the questionable method of generating singlet dioxygen by ref. 50. $Ru(bipy)_3^{+2*}$ was used to generate singlet dioxygen in methanol, and its subsequent reactions with

1,3-diphenylisobenzofuran[51] (DPBF) were monitored in the presence and absence of $NiCl_2$. $Ru(bipy)_3^{+2*}$ is an excellent choice for a photosensitizer, in contrast to other triplet sensitizers which are non-emissive. Because Ni^{+2} was found to only weakly quench $Ru(bipy)_3^{+2*}$ it is clear that an inhibition of DPBF photooxidation by Ni^{+2} must occur at some point after O_2 quenching of sensitizer, in contrast to other studies[50].

The course of DPBF photooxidation is easily followed by absorption spectroscopy at 410 nm (λ max.) because the photoproduct, 1,2-dibenzoylbenzene[51], does not absorb at 410 nm. $Ru(bipy)_3^{+2}$ absorption is quite intense at 410 nm, but by use of a matched $Ru(bipy)_3^{+2}$ blank solution, this problem is overcome. $NiCl_2$ absorption interferes slightly at 410 nm. at the concentrations used.

A stock solution of DPBF was prepared in a darkened room and diluted with methanol until its O.D. at 313 nm was 0.062 ($O.D._{410} = 0.195$). Solid $Ru(bipy)_3^{+2}$ was added until an absorbance of 1.5 was exceeded at 313 nm. Under these conditions for irradiation at 313 nm, DPBF absorbed less than 5% of the incident light so that direct involvement of $DPBF^*$ in the photoreaction is small. A 1.0×10^{-2} M solution of Ni^{+2} was created by adding $NiCl_2 \cdot 6H_2O$ to part of the solution.

The sensitizer emission from Ni^{+2} and Ni^{+2}-free solutions were compared under identical conditions, revealing

5% $Ru(bipy)_3^{+2*}$ quenching by nickel - a negligible fraction in view of the ultimately observed photooxidation efficiency change between the two solutions.

Six 3.00 ml aliquots of $NiCl_2$ containing solution were transferred by pipet to 13 x 100 mm Pyrex tubes. Similarly, Ni^{+2} - free tubes were prepared. Both series were irradiated in parallel in the 313 nm M.G.R. (17°C) for up to 51 min. and were withdrawn in comparison sets for absorption analysis at varying times.

Analysis of DPBF disappearance was accomplished by monitoring the O.D. loss at 410 nm. To improve the analytical sensitivity a $Ru(bipy)_3^{+2}$ containing reference blank was used ($A \sim 1.2$). The loss of DPBF occured much more rapidly in the Ni^{+2} - free samples. Using the reported molar extinction coefficient in DMSO ($2.82 \times 10^4 M^{-1} cm^{-1}$)[52], the initial concentration of DPBF was calculated to be less than 7×10^{-6} M.

The kinetics of photooxidation are analysed in terms of the standard triplet-sensitized $^1O_2$ - DPBF reaction mechanism[51] ($Ru(bipy)_3^{+2}$ = S, DPBF = F).

$$S + h\upsilon \rightarrow\rightarrow S^{*3} \qquad (16)$$

$$S^{*3} + O_2 \xrightarrow{K_q} {}^1O_2 + S \qquad (17)$$

$$^1O_2 + F \xrightarrow{K_r} FO_2 \quad (18)$$

$$^1O_2 \xrightarrow{K_d} O_2 \quad (19)$$

$$^1O_2 + Ni^{+2} \xrightarrow{K_n} Ni^{+2} + O_2 \quad (20)$$

$$S^{*3} \longrightarrow S + h\upsilon' \quad (21)$$

The ratio K_d/K_r has been determined for DPBF in methanol[51] to be 7.3×10^{-5}. Since K_d has also been measured [53] to be $1.4 \times 10^5\ S^{-1}$, K_r is calculated to be $2.0 \times 10^9\ M^{-1} S^{-1}$. Under these specifications of DPBF concentration and singlet dioxygen decay rate and reactivity, more than 90% of singlet dioxygen decays to ground state without reaction. A further aspect of the experiment is that the oxygen concentration exceeded by a factor of one-hundred the starting DPBF concentration, so $[O_2]$ was not appreciably altered as the reaction proceeded.

With these conditions, the loss rate of DPBF is proportional to the concentration of DPBF. Consequently, the rate equation integrates to produce an exponentially decaying concentration with time and plots of $\log_e$ [DPBF] versus time are linear. Since the loss rate is proportional to the steady-state concentration of $^1O_2$ at this low DPBF content, the relative slope of these linear oxidation plots parallels the steady-state $^1O_2$ concentration ratio between solutions.

Log_e [DPBF] versus time plots were linear in both solutions up to two-thirds consumption of DPBF. At this point the line broke, and the solution O.D. decreased less rapidly than expected. This was assumed to stem from an absorption baseline error arising either from an absorbing impurity in the DPBF solution or an actual error in the calculated zero. If a -0.030 correction was added to the raw O.D. data, the plots were linear over the whole range. In either case, the ratio of slopes ($S / S_{Ni^{+2}}$) in the linear region was 2.5 ± .5.

Because the rate of production of singlet dioxygen was the same in both solutions, a decrease in the steady-state concentration must be due to a nickel-enhanced decay rate. Solving the photostationary equation for $[^1O_2]$ gives (I = light intensity):

$$[^1O_2] = I\,(K_n[Ni^{+2}] + K_d)^{-1} \qquad (22)$$

Comparing, by the observed slope ratio, the two steady-state $^1O_2$ concentrations with 1.0×10^{-2} M $NiCl_2$ and no $NiCl_2$, K_n is calculated to be $2 \times 10^7\ M^{-1}S^{-1}$. It does appear, then, that Ni^{+2} interferes with the reactions of $^1\Delta g\ O_2$ in methanol, and 2-butoxy-ethanol. Because of this activity, the effect of Ni^{+2} on the $Ru(bipy)_3^{+2*}$ - O_2 photooxidation was investigated.

As a preliminary step, the quenching of $Ru(bipy)_3^{+2*}$ by Ni^{+2} was determined by the Stern-Volmer method[37]. The emission from solutions of constant $Ru(bipy)_3^{+2}$ content but varying $NiSO_4 \cdot 6H_2O$ content was correlated with $[Ni^{+2}]$ in 0.100 N H_2SO_4. Excitation was at 500 nm, where there was minimal Ni^{+2}(aq.) absorption. Emission was monitored at 583 nm, where, again, at the concentrations used nickel absorption was negligible.

The S-V plot was linear with $R > 0.99$, intercept 1.00 and slope $2.7 \pm .1 M^{-1}$. Taking $\tau = 0.40 \times 10^{-6}$ S gives a quenching rate constant of $6.9 \times 10^6 M^{-1} S^{-1}$. This rate is low enough at the highest concentrations used there was less than 10% "trivial" reaction quenching in the Ni^{+2} inhibition experiments.

Four independent experiments at different Ni^{+2} and sensitizer concentrations were performed. The relative inhibitory effect of Ni^{+2} was determined by comparing Fe^{+3} production in irradiated solutions differing only by the addition of Ni^{+2}. $[Fe^{+3}]$ was measured by absorbance change of the irradiated solutions at 320 nm. The results of these experiments in air saturated solution in the 313 M.G.R. at 17 ± 2°C are shown in table (3).

One anticipated effect was trivial, in that a reaction inhibition due only to sensitizer quenching was expected. The effect was calculated from the S-V equation and its magnitude is shown in the last column (β) of table (3).

Table 3

THE EFFECT OF Ni^{+2}(aq.) ON

$Ru(bipy)_3^{+2}$-O_2 PHOTOOXIDATION* OF Fe^{+2}

Set #	[SENS] x 10^{-5}M	[Ni^{+2}] x 10^{-2}M	α	β
1	1.4	0	1	1
	1.4	0.70	0.75 ± .05	0.98
	1.4	1.49	0.79 ± .05	0.96
	1.4	2.06	0.76 ± .05	0.94
	1.4	4.01	0.84 ± .05	0.90
2**	3.6	0	1	1
	3.6	0.58	1.00 ± .05	0.98
	3.6	1.04	0.95 ± .05	0.97
	3.6	1.57	0.93 ± .05	0.96
	3.6	2.01	0.88 ± .05	0.95
3***	> 5	0	1	1
		0.32	0.95 ± .05	0.99
		0.82	0.98 ± .05	0.98
		1.16	0.89 ± .05	0.97
		1.43	0.85 ± .05	0.96
4	8.6	0	1	1
		1.06	0.53 ± .05	0.97

* [Fe^{+2}] = 1.1 x 10^{-3} M .

** Inadvertantly, this concentration was not numerically recorded.

*** During this experiment, sensitizer concentration was found to change slightly.

The observed reaction inhibition is seen in the fourth column, obtained by dividing the amount of iron(III) produced in Ni^{+2}-containing solution by that produced in Ni^{+2}-free solution. Generally inhibition which exceeded the trivial effect was noted. In one case the effect was striking. However, the amount of inhibition varied erratically between experiments, and did not correlate with any other known solution variable. The largest quenching effects were seen at high and low extremes of sensitizer concentration.

The greatest inhibition was observed from $Ru(bipy)_3^{+2}$ solution which had been chromatographed on alumina at pH 10 for purification. This procedure was abandoned when the conditions were found to solubalize Al_2O_3 and, presumably, oxidizable impurities adsorbed on the column.

MATERIALS AND INSTRUMENTATION

Chemicals

The following chemicals were of Malinckrodt analytical reagent quality and used as received:

$FeSO_4 \cdot (NH_4)_2SO_4 \cdot 6H_2O$, $Fe(SO_4)_2NH_4 \cdot 12H_2O$, H_2SO_4 , $HClO_4$ (70%), NH_4SCN , $NiSO_4 \cdot 6H_2O$.

Tris-(2,2′-bipyridine)ruthenium(II) dichloride was synthesized as indicated or purchased from G. F. Smith, Inc., Columbus, Ohio.

$RuCl_3 \cdot 3H_2O$ was purchased from Venton Corp., Beverly, Mass. (stock #64103, 10+ #111673).

2,2′-Bipyridine was supplied by Eastman Organic Chemicals and used without further purification.

Rhodamine B was supplied by Allied Chemical Corp., National Aniline Division, and used as received as was Ethylene glycol (99%) from Aldrich Chemical Co. 1,3-diphenylisobenzofuran (mp 128-31°C) was also obtained from Aldrich. O_2 , obtained from Krystal Corp., Salinas, Ca. was industrial quality (> 99%).

Instrumentation

Absorbtion spectra were obtained using Cary 14 or Cary 118 scanning spectrometers. Actinometry and Fe^{+3} absorption measurements were made with Hitachi-Coleman 139 spectrometer

(wavelength calibrated).

Front surface emission spectra and S-V O_2 quenching data were gathered on an Aminco-Bowman fluorimeter while other emission measurements were taken with Hitachi MPF-2A fluorimeter. The LASER system used for lifetime and flash-spectroscopy measurements has been described in more detail elsewhere[54].

NMR and IR spectra were obtained on a Varian A56/60A and Perkin-Elmer 336 respectively.

DISCUSSION

As mentioned earlier, both theoretical and experimental results indicate that energy and charge transfer to dioxygen from $Ru(bipy)_3^{+2*}$ occur, but make no predictions to the relative involvement of these excitation pathways. Physical behavior shown by the $Ru(bipy)_3^{+2}$, Fe^{+2}, H^+ system in this study demonstrates that not only is dioxygen necessary for iron oxidation, but also that the extent of oxidation is directly proportional to the fraction of sensitizer excited states quenched by O_2. These observations are consistent with either pathway of O_2 excitation and limit the identities of the oxidants to species produced by the quenching event.

In general, oxidants are not being produced by a mechanism such as ($S^* = Ru(bipy)_3^{+2*}$) :

$$S^* + Fe^{+2}, H^+ \longrightarrow X \qquad (23)$$

$$X + O_2 \xrightarrow{K_X} XO_2 \qquad (24)$$

$$XO_2 + Fe^{+2} \xrightarrow{K_r} Fe^{+3} \times XO_2(red.) \qquad (25)$$

Sequence (23)-(25) generates an oxidant by attack of O_2 on <u>any</u> species produced by interaction of S^* with <u>any</u> component of the system except O_2 . Yields of oxidation would increase

with increasing O_2 content except for the fact that O_2 strongly quenches S^*. At high O_2 concentration the reaction must be inhibited, an occurrence which was not observed up to 82% S^* deactivation by O_2 . In any event, it is also clear that reactions of $Ru(bipy)_3^{+2*}$ with $Fe^{+2}(aq.)$ or H^+ in 0.100 N acid must be very minor in view of the independence of sensitizer excited-state lifetime on pH [44] and the low quenching activity shown by Fe^{+2}.

The choice of initial species must be limited to those which are produced by interaction of O_2 with $Ru(bipy)_3^{+2*}$. The charge-transfer nature of this event in 50% H_2SO_4 is suggested by the appearance of one-electron oxidized $Ru(bipy)_3^{+2}$ upon quenching $Ru(bipy)_3^{+2*}$ by O_2 . A provisional formulation of the mechanism in 0.100 N H_2SO_4 could be sequence (26)-(32) which is analogous to the CT quenching of $Ru(bipy)_3^{+2*}$ by iron(III)[5].

$$h\upsilon + S \longrightarrow S^* \qquad (26)$$

$$S^* + O_2 \rightleftharpoons (S \cdot O_2)^* \qquad (27)$$

$$(S \cdot O_2)^* \longrightarrow (S^+ \cdot O_2^-) \longrightarrow S^+ + O_2^- \qquad (28)$$

$$(S \cdot O_2)^* \longrightarrow {}^1S + O_2 \qquad (29)$$

$$O_2^- + H^+ \longrightarrow HO_2 \qquad (30)$$

$$S^{+} + Fe^{+2} \longrightarrow Fe^{+3} + S \qquad (31)$$

$$3H^{+} + HO\cdot_2 + 3Fe^{+2} \longrightarrow 3Fe^{+3} + 2H_2O \qquad (32)$$

Reaction (27) is completely feasable because close approach of O_2 to excited sensitizer is expected to proceed quenching[5]. Electron transfer is described by step (28), eventually resulting in kinetically free superoxide (pKa = 4.5)[55], which will be fully protonated to perhydroxyl over the entire range studied. Both $Ru(bipy)_3^{+3}$ and HO_2 are excellent oxidants of iron(II)[1b,5,56].

Sequence (26)-(32) as written produces $1e^-$ reduction of O_2 as well as $Ru(bipy)_3^{+3}$ and singlet O_2 but has several deficiencies. A primary flaw is the lack of pH dependence, since $O_2^- - HO_2\cdot$ oxidations of Fe^{+2} are not affected by $[H^+]$ in the range covered[56]. A less glaring difficulty is escape of superoxide from the solvent cage immediately following charge transfer. The separation of two oppositely charged ions is opposed by the electrostatic barrier, increasing the probability that back oxidation by $Ru(bipy)_3^{+3}$ will occur[5,57].

This reaction is thermodynamically favorable in view of the couples involved ($E^\circ(Ru^{+3}/Ru^{+2}(bipy)_3) = 1.29$ V.[28], $E^\circ(O_2/O_2^- = 0.07$ V.)[33]) and very rapid if judged by the rate of oxidation[1b,5] of Fe^{+2} by $Ru(bipy)_3^{+3}$, $K = 10^6\ M^{-1}S^{-1}$.

A final deficiency is the failure to account for $Ru(bipy)_3^{+3}$ in oxygenated, irradiated solutions of 0.100 N acid, since the +3 ion has an appreciable lifetime in this medium (in the absence of reductants).

These problems can be solved by amending the mechanism and economically changing the formalism describing the quench-complex, $(S^+ \cdot O_2^-)$ which would seem, realistically, to be a charge transfer resonance form of $(S \cdot O_2)^*$.

$$h\upsilon + S \longrightarrow S^* \tag{33}$$

$$S^* + O_2 \rightleftharpoons (S \cdot O_2)^* \tag{34}$$

$$(S \cdot O_2)^* + H^+ \longrightarrow S^+ + HO_2 \cdot \tag{35}$$

$$(S \cdot O_2)^* \longrightarrow S + {}^1O_2 \tag{36}$$

$$S^+ + HO_2 \cdot \rightleftharpoons S + O_2 + H^+ \tag{37}$$

The strong pH dependence of the reaction is now accounted for by the interception of the fleeting excited state complex of O_2 and $Ru(bipy)_3^{+2*}$ by H^+. The rate constant for reaction (35) is required to be very large since energy transfer to O_2 by reaction (36) proceeds at a rate of $3.5 \times 10^9\ M^{-1}S^{-1}$. Proton transfer rates are sufficiently fast, however, to allow (35) to occur.

Reaction (35) removes the barrier to cage escape because hydroperoxyl radical is uncharged.

Failure to observe $Ru(bipy)_3^{+3}$ in 0.100 N acid is explained by back-oxidation of kinetically free $HO_2\cdot$ by $Ru(bipy)_3^{+3}$. This is reasonable in view of the fact that $Ru(bipy)_3^{+2}$ is stable towards O_2-oxidation in 0.100 N H_2SO_4 [49] but not in 50 volume % H_2SO_4 [6,49]. That equilibrium lies to the left in 0.100 N H_2SO_4 is clearly shown by the reduction of $Fe(phen)_3^{+3}$ ($E^\circ(Fe(phen)^{+3,+2}$ = 1.14 V. [58]) by $HO_2\cdot$ [56] in this medium.

Singlet dioxygen is probably not involved as an oxidant in this system, even though an erratic inhibition of the photooxidation was produced by the singlet O_2 quencher Ni^{+2}. One reason for this belief is the lack of an $[Fe^{+2}]$ effect on ΦFe^{+3}. In general with a mechanism involving attack of $^1O_2$ on Fe^{+2}, competing with decay of $^1O_2$ to ground state,

$$^1O_2 + Fe^{+2} \xrightarrow{K_q} (Fe^{+2},O_2)^* \qquad (38)$$

$$(Fe^{+2},O_2) \longrightarrow Fe^{+3} + O_2^{\cdot-} \text{ (red)} \qquad (39)$$

$$^1O_2 \xrightarrow{K_d} O_2 \qquad (40)$$

The yield of Fe^{+3} would be related to the fraction of $^1O_2$ molecules reacting with iron to form the encounter

complex $(Fe^{+2},O_2)^*$, $F = K_q [Fe^{+2}] / (K_q[Fe^{+2}] + K_d)$. In the most favorable case K_q will be near 1.1×10^{10} $M^{-1}S^{-1}$, the calculated rate of diffusion in H_2O [59]. From the known rate of decay of $^1\Delta g$ O_2 in H_2O [53], 5×10^5 $M^{-1}S^{-1}$, F calculates to be 0.80 at the lowest Fe^{+2} concentration used. A 20% diminishment in the reaction efficiency is expected when, in fact, the efficiency of reaction is increasing slightly in this domain. Since calculations of $K_{diff.}$ are usually unreliable to the accuracy needed for this argument to apply, perhaps it is a moot point. The yields of Fe^{+3} produced by $HO_2\cdot$ oxidation are independent of $[Fe^{+2}]$ to 10^{-4} M, in agreement with the observed response of the system, however[56].

If $^1O_2$ is involved, it may be concluded that no overlap exists with thermal oxidation pathways of Fe^{+2} since a quadratic dependence on Fe^{+2} exists in sulfate media and a 1st order dependence on $[O_2]$ is observed[60,61]. Furthermore an inverse effect on $[H^+]$ is found[61].

An inner-sphere electron transfer from Fe^{+2} to $^1O_2$ can be completely discounted because the ligand exchange time of Fe^{+2}(aq.) is 10^{-6} S[62], roughly the lifetime of $^1O_2$. This would seem to limit the rate of reaction (39) to $10^6 M^{-1}S^{-1}$, a rate which is not at all consonant with the observed dependence of ΦFe^{+3} on $[Fe^{+2}]$ (vide supra). On the other hand, an outer-sphere exchange of one electron would generate a dioxygen anion which could give the proper pH behavior in

vicinity of geminate Fe^{+3}.

$$^1O_2 + Fe^{+2}(aq.) \rightleftarrows (Fe^{+2}(aq.) \cdot O_2^*) \quad (41)$$

$$(Fe^{+2}(aq.) \cdot O_2^*) \rightarrow (Fe^{+3}(aq.) \cdot O_2^-) \quad (42)$$

$$(Fe^{+3}(aq.) \cdot O_2^-) \rightarrow Fe^{+2}(aq.) + O_2 \quad (43)$$

$$(Fe^{+3}(aq.) \cdot O_2^-) + H^+ \rightarrow Fe^{+3}(aq.) + HO_2\cdot \quad (44)$$

The inverse reaction corresponding to (41) has been studied between dioxygen and the emissive doublet states of Cr(III) complexes[63],

$$Cr^{+3}X_nY_m^* + {}^3O_2 \rightarrow Cr^{+3}X_nY_m + {}^1O_2 \quad (45)$$

which also pass through an encounter complex like (41). If the ligand set XnYm contained π-electron ligands like SCN^-, acac, or ^-CN, sufficient electronic interaction ocurred to permit near diffusion controlled excitation transfer to O_2. When the ligand set consisted of only sigma-bonding "insulating" ligands such as ethylenediamine or trismethylenediamine no electronic interaction occurred and no quenching was observed.

In the present case, only sigma-bonding aquo ligands are present so an insulating effect on electronic

interactions between $^1O_2$ and $Fe(OH_2)_6^{+2}$ might be expected. Reaction (42) would then be too slow for this mechanism to be plausible. An extremely small barrier is needed to discount sequence (41)-(44) because a decrease in the overall rate constant to only $5 \times 10^9\ M^{-1}\ S^{-1}$ would produce a 50% drop in the reaction quantum yield at 2×10^{-4} M Fe^{+2}(aq.), a decrease which is completely outside the statistical error of the measuring process.

The present work determines several dynamic constants for $Ru(bipy)_3^{+2*}$ and various quenching materials including Fe^{+2}, Fe^{+3}, Ni^{+2} and O_2. Also determined were the lifetimes of $Ru(bipy)_3^{+2*}$ in aerated and degassed acid solution. In general, excellent agreement with the literature was obtained. The quenching constant of $Ru(bipy)_3^{+2*}$ by Fe^{+2} requires special comment since a value considerably lower than a previous measurement was found.

Laurence and Balzani[2] report the quenching of $Ru(bipy)_3^{+2*}$ emission by Fe(II) in 0.5 M $HClO_4$ with an observed Stern-Volmer quenching constant of $6.4 \pm .7\ M^{-1}$. This is comparable to the apparent quenching constant of $3.2 \pm .3\ M^{-1}$ obtained from this work in 0.1 N H_2SO_4, but shown to be almost equal to quenching by adventitiously present Fe^{+3}. The measured K_{sv} based upon the analytical value of Fe^{+3} present was $1528 \pm 127\ M^{-1}$ which is to be compared to $1275 \pm 61\ M^{-1}$ for Fe^{+2} - free solutions. From the known Fe^{+2}/Fe^{+3} ratio of 475, $K_Q(Fe^{+2})$ calculates to be

$1.3 \pm 1 \times 10^5$ $M^{-1}S^{-1}$, at the very most a factor of 70 less than reference 2.

Possibly an ionic strength effect has occurred upon transition from 0.15 to 1.0 M mediums because an increase in encounter rate between two dipositive ions is expected. A change of this size is not likely if compared to the quenching of $Ru(bipy)_3^{+2}$ by Fe^{+3} in 0.100 and 1.44 N H_2SO_4, or by $Cr(CN)_6^{-3}$ in 0.0 or 0.25 M KCl[64]. Reference 2 did not report an iron(III) analysis of their system, but did comment that they were prepared by reducing Fe^{+3} solutions with Zn-Hg amalgam. From this vantage point, barring an unforseen ionic strength effect, quenching was probably due to incomplete reduction of Fe^{+3} or perhaps ionic contamination by the amalgam.

The quenching constant of Ni^{+2} towards $Ru(bipy)_3^{+2*}$ may also have a contribution due to iron(III) impurity, but such quenching will be negligible if the manufacturer-stated content of 0.001% iron is correct. Unclear is the mechnaism by which Ni^{+2}(aq.) quenches ruthenium emission. One possibility is exothermic spin-allowed electronic energy transfer since $Ni(OH_2)_6^{+2}$ posseses a low lying $^1E \leftarrow {}^3A_2$ electronic transition near 15,000 cm^{-1}.

However, the observed quenching rate constant is roughly one-thousandth the expected diffusion-controlled value. This discrepancy may be due to shielding properties of the "insulating" aquation shell surrounding the nickel

nucleus as suggested by Pfeil[63]. Another factor is inhibition of close approach of the two dipositive metal centers by unfavorable electrostatic forces. Intimate overlap of donor and acceptor orbitals would be needed for excitation transfer leading to triplet-triplet annhilation as in this case[65].

A comment is necessary regarding the experimental divergence of oxidation quantum yields determined at 436 and 313 nm, 0.028 ± .002 (23 ± 2°C) and 0.034 ± .001 (17 ± 1°C) respectively. An excitation-wavelength effect is not responsible for the disagreement because the sensitizer emission quantum yield was shown to be independent of excitation wavelength in the range 250-500 nm. When the 313 nm measurement was performed at 26 ± 2°C, a decrease to 0.028 $N \cdot E^{-1}$ was observed, demonstrating that a temperature effect was responsible. Two cooperative phenomena are likely involved.

Dioxygen shows a marked drop of 21% in solubility upon changing from 15 to 25°C[45], so this effect must be important. Another change which lowers the fraction of sensitizer excited states quenched by O_2 is the decrease in sensitizer lifetime which follows an increase in temperature[6], a process which is under current study[44].

A final observation is necessary concerning the unimolecular photostability of $Ru(bipy)_3^{+2*}$ and the reported intramolecular redox photoproduct of Natarajan and Endicott[4].

This species would seem to be extremely long-lived, consisting, as proposed, of a radical anionic ligand coordinated to a +3 metal center of excellent oxidizing ability. The absorption due to this proposed species was found to decay at a rate inversly proportional to $[H^+]$. In 0.1 M acid a pseudo first order rate constant of $1.0\ S^{-1}$ was observed.

An alternative explanation which does not resort to a cumbersome intermediate is electron transfer from $Ru(bipy)_3^{+2}$ to low concentrations of iron-like metal ion impurities. According to the kinetic measurements of Bock, Meyer, and Whitten[5], as little as 5×10^{-6} M Fe^{+3} would produce the bleaching quantum yield of 10^{-3} observed by reference 4. Accordingly, solvent reduction of resultant $Ru(bipy)_3^{+3}$ parallels the pH-dependent return rate reported for the proposed intermediate.

CONCLUSION

Iron(II) is photooxidized to iron(III) in oxygen-containing acid solutions of $Ru(bipy)_3^{+2}$. From the kinetic behavior of the system it was suggested that the active dioxygen species present is $HO_2\cdot$, produced by protonation of an exciplex of $Ru(bipy)_3^{+2*}$ and dioxygen. Singlet dioxygen is expected to be present but its involvement in the reaction sequence can be virtually discounted, although non-reproducible inhibition of the photoreaction by nickel (II) was observed.

The observation of Mendenhall, Suprunchuk and Carlsson[50] that $NiCl_2$ quenches $^1\Delta g$ O_2 reactions in methanol was confirmed, although a somewhat lower quenching activity was measured.

A first measurement of the excited-state absorption spectrum of $Ru(bipy)_3^{+2*}$ was reported. The partial results of this study have been submitted for publication[66].

REFERENCES

1. (a) F. H. Burstall, J. Chem. Soc., 173 (1936)
   (b) J. N. Braddock and T. J. Meyer, J. Amer. Chem. Soc., 95(10),3158 (1973).
2. G. S. Laurence and V. Balzani, Inorg. Chem., 13, 2976 (1974).
3. J. N. Demas and A. W. Adamson, J. Amer. Chem. Soc., 95(16), 5159 (1973).
4. P. Natarajan and J. F. Endicott, J. Amer. Chem. Soc., 94, 5909 (1972).
5. C. R. Bock, T. J. Meyer, D. G. Whitten, J. Amer. Chem. Soc. 96, 4710 (1974).
6. F. E. Lytle and D. M. Hercules, J. Amer. Chem. Soc., 91(2), 253 (1969).
7. J. P. Paris and W. W. Brandt, J. Amer. Chem. Soc., 81, 5001 (1959).
8. See reference 1(b).
9. R. A. Palmer and T. S. Piper, Inorg. Chem., 5(5), 864 (1966).
10. G. B. Porter and H. L. Schläfer, Ber. Bunsenges. Physik. Chem., 68, 316 (1964).
11. G. A. Crosby, D. M. Klassen, and W. G. Perkins, J. Chem. Phys., 43(5), 1498 (1965).

12. D. M. Klassen and G. A. Crosby, J. Chem. Phys., 48(4), 1853 (1968).

13. J. N. Demas and G. A. Crosby, J. Mol. Spec., 26, 72 (1968).

14. J. N. Demas and G. A. Crosby, J. Amer. Chem. Soc., 93 (12), 2841 (1971).

15. R. W. Harrigan, G. D. Hager, and G. A. Crosby, Chem. Phys. Lett., 21(3), 487 (1973).

16. R. W. Harrigan and G. A. Crosby, J. Chem. Phys., 59(7), 3468 (1973).

17. J. F. Martin, E. J. Hart, A. W. Adamson, A. Gafney, and J. Halpern, J. Amer. Chem. Soc., 94, 9238 (1972). Also see references 3 and 31.

18. Calculated from information in reference 3, a lifetime of 0.42×10^{-6} S is observed in water. Also see reference 64.

19. M. S. Wrighton, D. S. Ginley and D. L. Morse, J. Phys. Chem., 78(22), 2229 (1974).

20. J. N. Demas and A. W. Adamson, J. Amer. Chem. Soc., 93(7), 1800 (1971).

21. N. Sabatini and V. Balzani, J. Amer. Chem. Soc., 94(12), 7587 (1972).

22. N. Sabatini, M. A. Scandola, and V. Balzani, J. Phys. Chem., 78(5), 541 (1974).

23. M. S. Wrighton and J. Markham, J. Phys. Chem., 77(26), 3042 (1973).

24. J. N. Demas, D. Diemente, and E. W. Harris, J. Amer. Chem. Soc., 95, 6864 (1973).

25. H. D. Gafney and A. W. Adamson, J. Amer. Chem. Soc., 94, 8238 (1972).

26. C. Lin and N. Sutin, J. Amer. Chem. Soc., 97(12), 3543 (1975).

27. C. R. Bock, T. J. Meyer, and D. G. Whitten, J. Amer. Chem. Soc., 97, 2909 (1975).

28. D. Rehm and A. Weller, Ber. Bunsenges. Phys. Chem., 73, 834 (1969).

29. P. Natarajan and J. F. Endicott, J. Phys. Chem., 77(7), 971 (1973).

30. P. Natarajan and J. F. Endicott, J. Phys. Chem., 77(15), 1823 (1973).

31. G. Navon and N. Sutin, Inorg. Chem., 13, 2159 (1974).

32. K. Sandros, Acta. Chem. Scand., 18, 2355 (1964).

33. P. S. Rao and E. Hayon, J. Phys. Chem., 79, 397 (1975).

34. F. A. Cotton and G. Wilkinson, "Advanced Inorganic Chemistry, Third Ed.", Interscience Publishers, New York, 1972, pp 411-412.

35. J. N. Demas and G. A. Crosby, J. Amer. Chem. Soc., 93(12), 2841 (1970).

36. Elemental analysis was performed by Micro-Tech Laboratories, Inc., Skokie, Illinois 60076.

37. N. J. Turro, "Molecular Photochemistry", W. A. Benjamin, Inc., N.Y., 1967, pp. 93-95.

38. E. B. Sandell, "Colorimetric Determination of Traces of Metals", Interscience Publishers, Inc., N. Y., 1959. pp 524-533.

39. The Henry's Law constant was calculated to be 8.68 x 10^{-5} $M \cdot psi^{-1}$ from the 25° solubility[45] of O_2 in H_2O at atmospheric pressure.

40. F. G. Moses, R. S. H. Liu, and B. M. Monroe, Mol. Photochem., 1, 245 (1969).

41. C. G. Hatchard and C. A. Parker, Proc. Roy. Soc., Ser. A., 235, 518 (1956).

42. W. H. Melhuish, J. Opt. Soc. Amer., 52(11), 1256 (1962).

43. P. L. Airey and F. S. Dainton, Proc. Roy. Soc., A291, 340 (1966).

44. J. Van Houten and R. J. Watts, J. Amer. Chem. Soc., 97(13), 3843 (1975).

45. A. Seidell, "Solubilities of Inorganic and Organic Substances", D. Van Nostrand and Co., N. Y., 1917, p. 220.

46. J. G. Calvert and J. N. Pitts, "Photochemistry", John Wiley and Sons, Inc., N. Y., 1966, pp. 5-6.

47. The front surface emission cell holder is identified by Aminco No. C73-62140.

48. J. B. Birks, "Photophysics of Aromatic Molecules", Wiley-Interscience, N. Y., 1970, p. 142.

49. A. Schilt, Anal. Chem., 35(11) 1599 (1963).

50. D. J. Carlsson, G. D. Mendenhall, T. Suprunchuk, and D. M. Wiles, J. Amer. Chem. Soc., 94(25), 8960 (1972).

51. R H. Young, K. Wehrly, and R. L. Martin, J. Amer. Chem. Soc., 93, 5774 (1971).

52. A. Zweig, G. Metzler, A. Maurer, and B. G. Roberts, J. Amer. Chem. Soc., 89(16), 4091, (1967).

53. P. B. Merkel and D. R. Kearns, J. Amer. Chem. Soc., 94, 1029 (1972).

54. E. L. Menger and D. S. Kliger, J. Amer. Chem. Soc., subnitted for publication.

55. G. Czapski and L. M. Dorfman, J. Phys. Chem., 68, 1169 (1964).

56. C. B. Amphlett, Disc. Faraday Soc., 144 (1952).

57. R. C. Jarnigan, Acc. Chem. Res., 4, 420 (1971).

58. "Handbook of Physics and Chemistry", ed. by R. C. Weast, CRC Press, Cleveland, Ohio, 53rd ed., 1972, p. D111.

59. S. Murov, "Handbook of Photochemistry", Marcel Dekker, Inc., N. Y. 1973, p. 55.

60. R. Huffman and N. Davidson, J. Amer. Chem. Soc., 78, 4836 (1956).

61. P. George, J. Chem. Soc., 4349 (1954).

62. See reference 34, p. 657.

63. A. Pfeil, J. Amer. Chem. Soc., 93(21), 5395 (1971).

64. F. Bolletta, M. Maestri, and L. Moggi, J. Phys. Chem., 77(6), 861 (1973).

65. C. A. Parker, "Photoluminescence of Solutions", Elsevier Publishing Co., Amsterdam, 1968, p. 322.

66. J. S. Winterle and G. S Hammond, J. Amer. Chem. Soc., submitted for publication.

PART II

INTRODUCTION

An abundance of experimental evidence has shown that the production of singlet and triplet solvent excited states is a major process in γ-irradiated benzene.[1] In fact, the great stability of benzene and other aromatic hydrocarbons toward ionizing radiation is attributed to the efficient production of chemically stable excited states relative to other destructive relaxation modes[2,3]. It is expected, therefore, that if a proper solute is chosen, the principal reactions of the solute will be from interactions with these abundant excited solvent states.

Pulse radiolysis[4] as well as conductivity experiments[5] have demonstrated that the yield of free ions in benzene is less than 0.1 molecule per 100 eV absorbed by the system ($G(ion) < 0.1$). Using biphenyl as a cation and anion scavenger in benzene, Cooper and Thomas[4] have shown that ionic transfer to solute is a negligible process in benzene ($G < 0.1$) and constant from 5×10^{-3} M to 0.1 M solute concentration.

The yield of solvent radicals however, is somewhat larger[6] ($G \sim 0.75$). It is therefore necessary to demonstrate that a solute reaction monitoring solvent excited states is not perturbed by interaction with these chylohexadienly-type[6,7] radicals.

The present study is concerned with the transfer of γ-ray induced solvent electronic excitation to trans, trans -2,4-hexadiene, a molecule whose excited state chemistry is well characterized. This molecule is an attractive candidate for monitoring the simultaneous transfer of singlet and triplet electronic excitation because its rate of intersystem crossing is entirely negligible, as is the case with other 1,3-dienes[8,12]. It is also a desirable choice, as will be seen, because its singlet and triplet excited state reactions can be differentiated.

There are three possible geometric isomers of the 2,4-hexadienes. They are shown below.

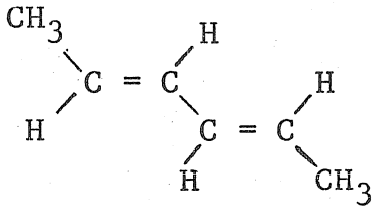

trans, trans-2,4-hexadiene

(1)

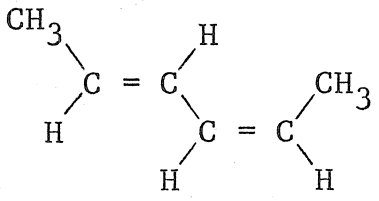

cis, trans-2,4-hexadiene

(2)

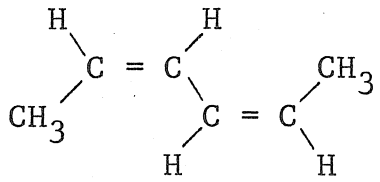

cis, cis-2,4-hexadiene

(3)

When (1) is irradiated at 254 nm in hydrocarbon solution it is geometrically isomerized in the following fashion:[8]

$$h\upsilon + \underset{\sim}{1} \rightarrow \underset{\sim}{1}^* \quad (1)$$

$$\underset{\sim}{1}^* \rightarrow \alpha\,\underset{\sim}{1} + (1-\alpha)\,\underset{\sim}{2} \quad (2)$$

$$\underset{\sim}{1}^* \rightarrow \text{cis-3,4-dimethylcyclobutene} \quad (3)$$

Further irradiation produces 3, but only after enough 2 has been built up to begin absorbing light. In a single photon process, the excited state derived from 1 does not decay to produce 3. The decay ratios α and $(1-\alpha)$ were shown to be 0.63 and 0.37 respectively[8].

Continued irradiation produces a photostationary state in which the geometric isomer content is invariant with time. This state, which is a function of the extinction coefficients of the individual isomers, has the composition[8]:

$$\underset{\sim}{1} = 0.406,\ \underset{\sim}{2} = 0.264,\ \underset{\sim}{3} = .330\ .$$

The singlet excited state of 1 undergoes an electrocyclic closure reaction, with low efficiency (Φ = 0.024) to

cis-3,4-dimethylcyclobutene. This is the expected product on the basis of the Woodward-Hoffmann rules for concerted electrocyclic closure[9].

High energy triplet photosensitization produces a different pathway for isomerization[10]. For diene concentrations less that 1 molar, the mechanism is:

$$S + h\upsilon \rightarrow\rightarrow {}^3S \quad (4)$$

$${}^3S + \underset{\sim}{1} \rightarrow {}^3D \quad (5)$$

$${}^3D \rightarrow \beta\ \underset{\sim}{1} + \pi\ \underset{\sim}{2} + (1-\beta-\pi)\ \underset{\sim}{3} \quad (6)$$

$${}^3D + \underset{\sim}{1} \rightarrow \text{dimer.} \quad (7)$$

S represents a sensitizer molecule, such a benzophenone. The intermediate ${}^3D$ actually represents a set of two rapidly equilibrating "allylmethylene" type triplet biradicals, as discussed by Saltiel et al.[11]. The effect of this rapid equilibration is to scramble the geometric configuration at the 2 and 5 carbons. An identical set of biradicals is obtained regardless of the starting isomer.

The important feature of this mechanism is the production of $\underset{\sim}{3}$ from $\underset{\sim}{1}$ in a single photon excitation. Therefore, starting from $\underset{\sim}{1}$, the appearance of $\underset{\sim}{3}$ in a single photon process is indicative of a triplet excited state diene intermediate.

A competing side reaction is the formation of diene dimers. However, this reaction is inefficient. The quantum yield is only 0.008 at 2.62 molar $\underset{\sim}{1}$[12].

The photostationary state obtained after long periods

of irradiation is quite different than that obtained by direct excitation at 254 nm . The composition is $\underset{\sim}{1}$ = .313, $\underset{\sim}{2}$ = 0.502, $\underset{\sim}{3}$ = 0.185. These numbers are also equal to the decay ratios: β = 0.313, π = 0.502, $(1-\beta-\pi)$ = 0.185[10].

To decide if energy transfer from benzene to $\underset{\sim}{1}$ is feasable, it is necessary to consider the state diagrams of these molecules. (See Table 1).

The singlet and triplet excited states of benzene are well known from a large series of spectroscopic and electron scattering experiments[13,14].

TABLE 1

THE ELECTRONIC STATES OF BENZENE AND
TRANS, TRANS-2,4-HEXADIENE, $\underset{\sim}{1}$

Molecule	State	Energy (Kcal·Mole^{-1})
Benzene	^1A_g	0
	$^3B_{1u}$	85[14]
(Benzene excimer)	($^1B_{1g}$)	99[20]
	$^3B_{1u}$	104[14]
	$^1B_{1u}$	108[14]
	$^1B_{2u}$	138[15]
	$^1B_{1u}$	156[15]
	$^1E_{1u}$	
$\underset{\sim}{1}$	^1A_g	0
	^3B_u	59.5[16],58[17]
	^3A_g	99[18]
	^1B_u	99±4[18],107[19]

The energy levels of 1,3- dienes are less well known. As a whole these molecules neither fluoresce nor phosphoresce[19] and their absorption spectra are broad structureless bands. The energy level of the lowest triplet state of 1,3-butadiene has been established by the oxygen absorption enhancement techniques of Evans[16] to be 59.5 Kcal·mole^{-1}. The introduction of terminal methyl groups has little effect on the triplet energy[16,17], so this is also the expected energy for 1.

An important paper on the electron impact spectroscopy of 1,3- butadiene by Kuppermann and Mosher[17] has recently appeared. By considering the electron impact excitation spectrum of 1,3- butadiene at different impact energies and scattering angles, the authors locate three excited states between 2 and 7 eV. The two lower states are assigned to singlet → triplet electronic transitions. In order of increasing energy, these are: 1: $^3B_u \leftarrow {}^1A_g$, onset at 2.5 eV = 58 Kcal·mole^{-1}, and 2) $^3A_g \leftarrow {}^1A_g$, onset at 4.3 eV = 99 Kcal·mole^{-1}. The highest energy state is assigned to the $^1B_u \leftarrow {}^1A_g$ transition. Its onset was ~5.3 eV = 112 Kcal·mole^{-1}.

A subsequent brief note[18] reported the e^- impact spectra of trans-1,3-pentadiene and cis, trans-2,4-hexadiene as being essentially similar to 1,3-butadiene. The main difference was in the case of 2, where the ^3A_g feature is seen as a shoulder on the allowed ^1B_u transition. These states must

therefore be almost isoenergetic.

This means that $E\left({}^1B_u\right) \sim 100 \pm 4$ Kcal·mole^{-1}. This estimate seems to be ~ 5 Kal too low, in light of the results of the present work (vide infra).

Reference to Table 1 shows that energy transfer from both the ${}^1B_{1u}$ and ${}^1E_{1u}$ states of benzene to the ${}^1B_u$ state of $\underset{\sim}{1}$ is highly exothermic. Transfer would therefore, be expected to occur at every collision. It is also clear that triplet energy transfer from the ${}^3B_{1u}$ state to the diene ${}^3B_u$ state should be very rapid, because the process is exothermic by ~ 25 Kcal·mole^{-1}.

However, the case for energy transfer from the ${}^1B_{2u}$ state of benzene to the ${}^1B_u$ state of $\underset{\sim}{1}$ is not clear cut. Because of the close energy match and the uncertainty in the energy of the ${}^1B_u$ diene state, the theoretical prediction is uncertain. Similar 1,3-dienes are known to quench benzene fluorescence without energy transfer[21].

Consider now the following reaction sequence for delivering electronic excitation to $\underset{\sim}{1}$ in γ-irradiated benzene solutions (the rate constant notation follows that of ref. 3):

$$B \rightsquigarrow B^{1,3} \tag{8}$$

$$B^1 \xrightarrow{k_{fm}} B + h\upsilon \tag{9}$$

$$B^3 \xrightarrow{k_{gt}} B \tag{10}$$

$$B^1 + \underset{\sim}{1} \xrightarrow{k_{ym}} \underset{\sim}{1}^* + B \qquad (12)$$

$$B^3 + \underset{\sim}{1} \xrightarrow{k_{yt}} D^3 + B \qquad (13)$$

$$\underset{\sim}{1}^* \xrightarrow{k_{ds}} \alpha\ \underset{\sim}{1} + (1-\alpha)\ \underset{\sim}{2} \qquad (14)$$

$$^3D \xrightarrow{k_{dt}} \beta\ \underset{\sim}{1} + \pi\ \underset{\sim}{2} + (1-\beta-\pi)\ \underset{\sim}{3} \qquad (15)$$

This mechanism explicitly assumes low conversion of $\underset{\sim}{1}$ to its isomers so that back reactions of $\underset{\sim}{3}$ and $\underset{\sim}{2}$ to $\underset{\sim}{1}$ may be neglected. Reaction (8) represents the generation of solvent excited states by γ-radiation.

Let N_i represent the number of molecules of species i. Since $\underset{\sim}{3}$ can only be produced by decay of ^3D, their numbers are related by the decay coefficient $(1-\beta-\pi)$:

$$N_{3_D} = (1-\beta-\pi)^{-1} N_{\underset{\sim}{3}} = 5.38\ N_{\underset{\sim}{3}} \qquad (16)$$

Equation (16) permits the calculation of $N_{\underset{\sim}{2}'}$, the number of molecules of cis, trans-2,4-hexadiene formed by decay of triplet diene:

$$N_{\underset{\sim}{2}'} = \pi\ N_{3_D} = \pi\ (1-\beta-\pi)^{-1}\ N_{\underset{\sim}{3}} = 2.69\ N_{\underset{\sim}{3}} \qquad (17)$$

Any excess of $\underset{\sim}{2}$ must be produced by decay of $\underset{\sim}{1}^*$ via equation (14). Representing this number by $N_{2''}$, then:

$$N_{2''} = N_2 - N_{2'} = N_2 - 2.69\ N_3 \qquad (18)$$

Finally, equation (19) allows the calculation of $N_{\underset{\sim}{1}^*}$ because $N_{\underset{\sim}{2}''}$ and $N_{\underset{\sim}{1}^*}$ are stoichiometrically related by

equation (14).

$$N_{\underset{\sim}{1}^*} = (1-\alpha)^{-1} N_{\underset{\sim}{2}''} - N_{2'} = 2.70 (N_{\underset{\sim}{2}} - 2.69 N_{\underset{\sim}{3}}) \qquad (19)$$

Equations (16) and (19) permit the calculation of the number of singlet and triplet excited states produced by energy transfer from benzene from the experimentally available quantities $N_{\underset{\sim}{2}}$ and $N_{\underset{\sim}{3}}$. By using sufficient concentration of $\underset{\sim}{1}$, all benzene excited states would be quenched before decaying through equations (9), (10), and (11). In this instance, $N_{\underset{\sim}{1}}^*$ and $N_{\underset{\sim}{3}_D}$ would be numerically equal to N_{1_B} and N_{3_B} so that the yield of solvent excited states would be determined.

As will be seen, the experimental evidence is consistent with singlet and triplet energy transfer from benzene to $\underset{\sim}{1}$, described by sequence (8) - (15) when benzene is γ-irradiated. It will be shown that transfer from the $^1B_{2u}$ state of benzene is inefficient, and cannot account for the singlet excitation observed. A convenient explanation of this result is that short-lived upper excited benzene singlet states are excitation donors. This is made possible at moderate acceptor concentrations because singlet energy transfer in benzene is not limited by mass diffusion, so that trapping can occur very quickly (vide infra).

EXPERIMENTAL

Chemicals

Aldrich 2-ethylnapthalene (n_D^{20}= 1.5991) was vacuum distilled and 2x chromatographed on alumina before use.

Baker analytical spectrophotometric grade benzene was used as received for fluorescence experiments.

Matheson, Coleman and Bell reagent grade thiophene-free benzene was used for all other samples after further purification. This involved irradiating 1.5 liters of water-saturated benzene with the full output of a 450 watt medium pressure Hanovia lamp through quartz, while bubbling chlorine through the reaction[22]. Irradiation time was 1 hour. The benzene was then dried over anhydrous magnesium sulfate and distilled. Final purification step was a distillation from lithium aluminum hydride, with collection of the middle fraction. This benzene was stored in two 500 ml round-bottom flasks equipped with drying tubes.

Trans, trans-2,4-hexadiene was obtained from Chemical Samples Company (stated chemical purity > 99%) and bulb-to-bulb distilled under vacuum immediately prior to use. G.L.C. analysis showed that the isomeric content of the diene was 99.7% trans, trans- and 0.3% cis, trans-2,4-hexadine. Cis, cis-diene was not present in measurable amounts. A second batch of $\underset{\sim}{1}$ showed a different starting composition of $\underset{\sim}{1}$ =

99.1% and $\underset{\sim}{2}$ = 0.9%, but still zero cis, cis- content.

Spectroquality Matheson, Coleman and Bell methylcyclohexane was chromatographed on alumina just before use.

Water used in making dosimetry solution was doubly distilled and was a courteous gift of Dr. Fred Anson.

Ferrous sulfate, $FeSO_4 \cdot 7H_2O$ was Baker and Adamson reagent quality (min. 99.5%). This compound was employed in making dosimetry solutions, as was sodium chloride, Mallinckrodt Analytical Reagent.

Procedures

Sample Preparation

Degassable fluorescence cuvettes equipped with 10/30 outer ground glass joints were cleaned with chromic acid cleaning solution and thoroughly rinsed with distilled water. They were then base rinsed with concentrated ammonium hydroxide, followed by distilled water washing and overnight drying at 120°C.

Benzene solutions of $\underset{\sim}{1}$ were made up by adding a known volume of $\underset{\sim}{1}$ by 100 µl syringe to 10.00 ml volumetric flask, partially filled with benzene. After addition of the freshly distilled diene, the flasks were filled to their fiducial marks. Diene concentration was calculated from the known density of $\underset{\sim}{1}$[23].

The cells were degassed by the freeze-pump-thaw technique to less than 5×10^{-5} torr, and sealed off the vacuum

line. To clean the outer optical faces of the cuvettes, they were soaked in concentrated HNO_3 overnight.

Sample tubes for γ-irradiation were made from 13 x 100 mm Pyrex test tubes connected to 10/30 ground glass joints. The ampoules were drawn about 2 inches from the end to effect easy sealing-off under vacuum. After washing with chromic acid cleaning solution and copious amounts of distilled water, sample tubes were dried in an oven at 120°C for at least 2 hours before filling.

All solutions were made up in chromic acid cleaned volumetric glassware and desired solute concentrations were arrived at by addition of appropriate volumes of solute with calibrated microliter syringes.

Solutions were transferred to ampoules via disposable pipets. Sample volumes were 1-2 ml. Samples were degassed on a vacuum line equipped with an oil diffusion pump. Degassing was accomplished through at least 4 freeze-thaw-cycles at 77°K until residual gas pressure above frozen solutions was less than 5×10^{-5} Torr. After the ampoules were cut off of the vacuum line, they were wrapped with aluminum foil for light protection.

Samples for UV isomerization experiments in benzene and 2-ethylnaphthalene were prepared in the same fashion as the samples for γ-irradiation.

γ-Irradiation of Samples

Tinfoil-wrapped sample tubes were carried from Caltech to the Jet Propulsion Laboratory where the ^{60}Co source used for irradiating samples is located. Sample tubes were placed in a 400 ml beaker and lowered into the radiation source for a precisely measured time interval. After irradiation, samples were returned to Caltech where they were stored in a refrigerator until analysis by G.L.C.

U.V. Irradiation of Samples

Samples were placed in a small motor-driven Merry-go-round with 10 cell positions. The optical slits were precisely machined to ensure that slit areas were identical. The M.G.R. was suspended in the center of an Ultra Violet Products, Inc. irradiator (Model PCQX1) equipped with one or two circular lamps.

For irradiation at 254 nm, 1amp model 50053 was used. Light intensity was $\sim 10^{-7}$ E·m^{-1}. For irradiation at 305 nm, 1amp model 50053, factory coated with an inorganic fluor to spectrally shift the low pressure mercury resonance radiation to 305 nm, was employed.

Measurement of Radiation Dose Absorbed by Samples

Dosimetry was carried out on August 24, 1970. Standard Fricke (ferrous sulfate) dosimetry was employed, as recommended by Spinks and Woods[24]. The method involves the

measurement of the production of ferric ions when an air-saturated, aqueous, acidic solution of ferrous sulfate is γ-irradiated. It is known that in such a solution 15.5 ferric ions appear when 100 electron volts of energy are absorbed from ^{60}Co γ-radiation[24]. By convention, the yield in molecules per 100 eV energy absorbed by the system is assigned the symbol G. Thus, in this case, the G value for Fe^{+3}(aq.) production is 15.5.

Dosimetry solutions were made by dissolving 400 mg of $FeSO_4 \cdot 7H_2O$, 22 ml of H_2SO_4 (analytical reagent grade), and 60 mg of NaCl in 1.000 liters of doubly distilled H_2O. Resultant solution was 0.0014 M with respect to ferrous sulfate, 0.4 M with respect to sulphuric acid, and 0.001 M with respect to sodium chloride. This solution was stored in a ground glass stoppered bottle, covered with brown paper for protection from light.

Pyrex test tubes (13 x 100 mm) were cleaned with hot fresh cleaning solution ($K_2Cr_2O_7$, H_2SO_4), and then rinsed 5 times with high purity distilled water. After drying in an oven, seven test tubes were filled with dosimetry solution. Six of these were irradiated, while one was saved for a zero-time run. The six tubes were irradiated for integral multiples of time from 1.00 to 6.00 minutes.

Optical density was measured at 305 nm versus unirradiated solution with a Beckman DU spectrophotometer. The decadic molar extinction coefficient of Fe^{+3}(aq.) is reported to be 2174 $M^{-1}cm^{-1}$ at 305 nm (23.7°C) [25]. The slope of the

resultant straight line was 0.354 ± 0.009 $min.^{-1}$ by least squares analysis (R = 0.998).

Using the above data, the dose rate into the dosimetry solution was calculated to be 3.80×10^{19} $eV \cdot gram^{-1} \cdot hr^{-1}$. On later dates, the dose rate was corrected for radioactive decay f the source by equation (20)

$$D(t) = D_o e^{-\lambda t} \qquad (20)$$

where $D_o = 3.80 \times 10^{19}$ $eV\text{-}gram^{-1}$ hr^{-1} and t = 0 was taken to be August 24, 1970. For the dose rate into other substances, use if made of the fact that the absorption of electromagnetic radiation by Compton interaction, the principal interaction of ^{60}Co gamma rays, is directly proportional to the electron density of that material[26]. Using this correction for the benzene solutions irradiated gives equation (21):

$$D(t) = 3.24 \times 10^{19} e^{-(0.131)t}\ eV\text{-}hr^{-1}ml^{-1} \qquad (21)$$

D(t) is now the dose rate into benzene at time t (t = 0 on 8-24-70). Note that this rate has also been expressed per unit volume of benzene instead of unit weight as in eq. (20).

Measurement of Benzene Fluorescence From Solutions of <u>trans</u>, <u>trans</u>-2,4-Hexadiene in Benzene.

Fluorescence measurements were made with an SPF Aminco-Bowman Spectrofluorimeter equipped with a "solid sample attachment", catalog #C73-62140. The instrument utilized a 1P28 photomultiplier tube.

To provide light of high monochromaticity for some experiments, the normal xenon high pressure lamp was replaced by a Hg resonance lamp (Spectroline Quartz Pencil Lamp, Model 11SC-1, Black Light Eastern Corp.).

In all cases, the emission slits were opened as wide as possible to provide maximum signal intensity.

Analyses

Quantitative determination of the isomeric 2,4-hexadienes was effected by gas-liquid partition chromatography on a Hewlett Packard HP 700 gas chromatograph, equipped with flame ionization detector. Nitrogen was used as carrier gas. Two columns were used for hexadiene analysis. The first (1/8" o.d. x 25' β,β'-oxidipropionitrile, 25% by weight on Chromsorb P) was destroyed by accident when overheated. The second column was identical except that it was slightly shorter (22'). Both columns gave sufficient separation of trans, trans-, cis, trans- and cis, cis-2,4-hexadiene.

Analyses were carried out near 50°C on the first column and at room temperature on the second column. Peak areas were determined by mechanical integrator (Disc Instruments,

Inc.), or by cutting and weighing Xeroxed G. L. C. traces.

RESULTS

Fluorescence Quenching of Benzene by Trans, Trans-2,4-Hexadiene.

Five matched, degassable fluorescence cuvettes were filled with benzene solutions of 1. Solutions were made up by adding appropriate volume of bulb-to-bulb distilled 1 by 100 μl syringe to 10.00 ml volumetric flasks. Deoxygenation was accomplished by 4 freeze-pump-thaw cycles until the residual system pressure over the frozen samples (77°K) was less than 5×10^{-5} Torr.

Emission was observed from the front surface of the sample cuvettes, of necessity, because of the large optical densities encountered.

Fluorescence from the $^1B_{2u}$ state of benzene is quenched by 1. The emission intensity decreased monotonically with increasing diene concentration, as shown in Figure 1.

This behavior is analyzed in terms of the Stern-Volmer equation, which has the following form:

$$\frac{I_o}{I} = 1 + K_Q \tau [Q] \qquad (22)$$

Its derivation and interpretation is described elsewhere by Turro[27]. [Q] is the quencher concentration, τ is the lifetime of the emissive state in the absence of quencher,

Figure 1. Front surface emission from neat benzene (degassed), quenched by 1 at room temperature. The marker at 320 nm indicates the wavelength at which quenching data was gathered.

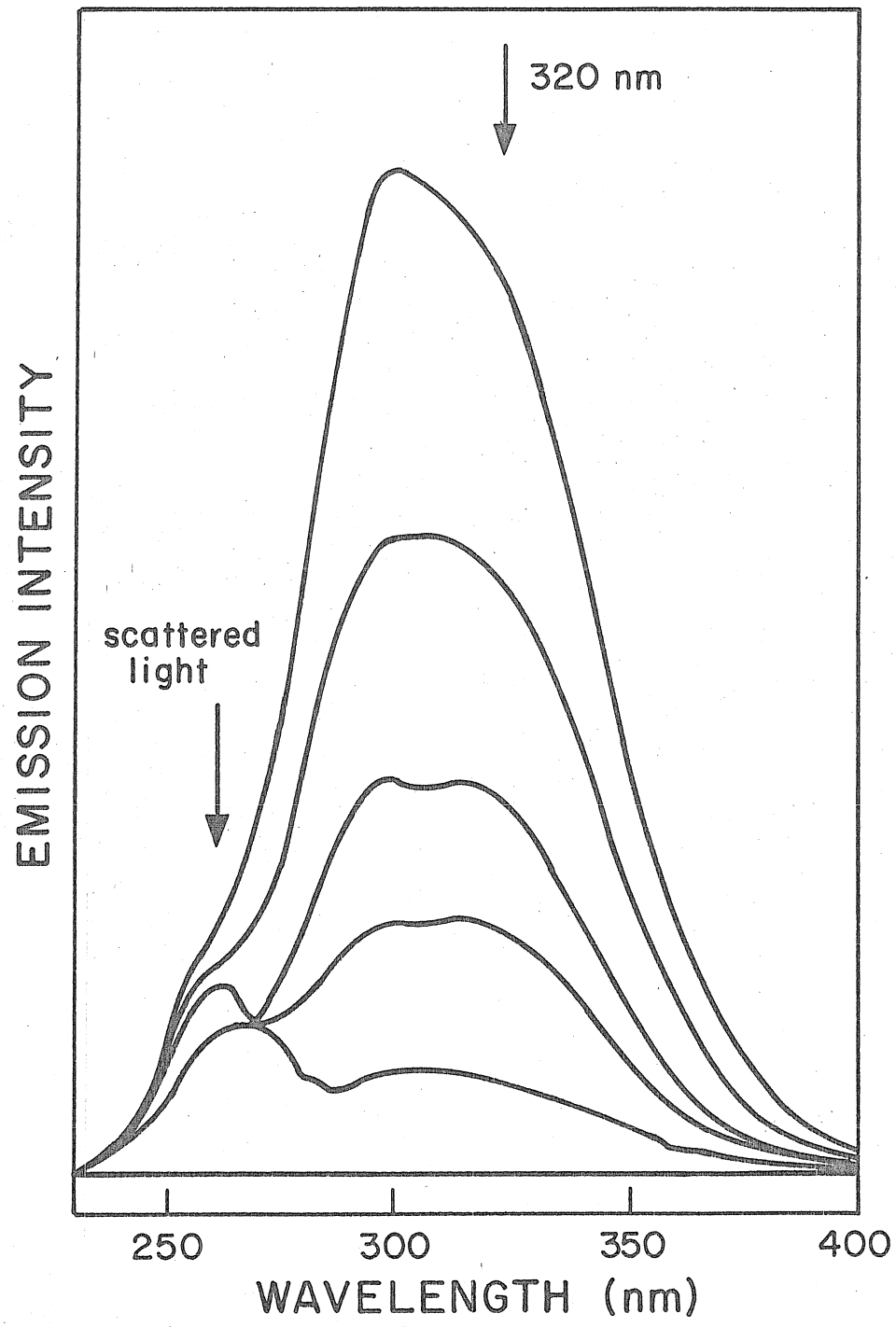
320 nm
scattered
light
EMISSION INTENSITY
250
300
350
400
WAVELENGTH (nm)

K_Q is the bimolecular rate constant for quenching, and Io/I is the ratio of emission intensities at fixed wavelength of quenched (I) and unquenched (Io) solutions.

Io/I values for broadband excitation centered at 250 nm are plotted as a function of diene concentration in Figure 2. The data fit an excellent straight line, of slope 61.8 M^{-1}, which is equal to the product $K_Q\tau$. The correlation coefficient determined by least squares analysis is 0.998.

The bandwidth of the exciting light in this experiment was approximately 20 nm . It was necessary to eliminate the possibility that a portion of the quenching could be ascribed to competitive light absorption by the diene. This effect becomes evident when the samples were excited at much shorter wavelengths. For excitation at 220 nm the slope of quenching plot increased, as is demonstrated by the upper line in Figure 2.

A supportive experiment was performed with precisely defined exciting light. A mercury resonance lamp was placed in the excitation nomochromator lamp housing and used for excitation at 253.7 nm .

At this wavelength the molar extinction coefficients of 1 and benzene[28] are 100 and 90 $M^{-1}\,cm^{-1}$ respectively. At 0.0438 M, the highest diene concentration, the optical density contribution of the 1 is 4.4. The total O.D. due to benzene (11.4 M) is 1026. Because the diene component

Figure 2. Stern-Volmer plot of benzene emission quenching by 1, monitored at 320 nm. The upper line was produced upon excitation at 220 nm, showing the effect of internal filtering by diene.

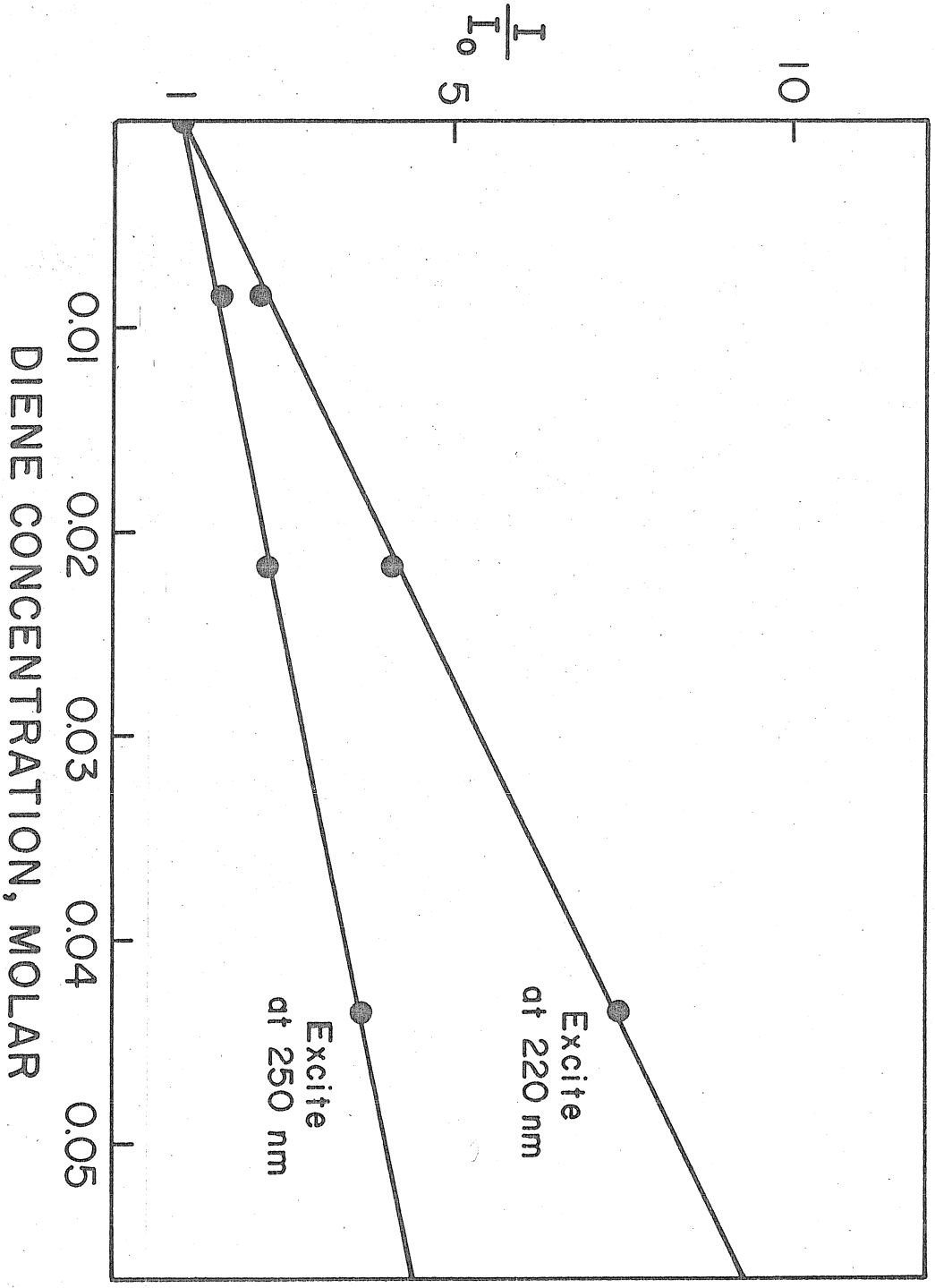
I/I₀
10
5
1
0.01
0.02
0.03
0.04
0.05
DIENE CONCENTRATION, MOLAR
Excite at 220 nm
Excite at 250 nm

is less than 0.5% of the benzene absorption internal filtering is not a problem.

The data were in excellent agreement with the first experiment, giving a slope of 61.1 M^{-1} (R = 0.9999). The combined data gave a value of 61.5 M^{-1} for the product $K_Q \tau$. The lifetime of the $^1B_{2u}$ state in liquid benzene is 26 ± 1 ns [29]. This establishes K_Q to be 2.35 ± .08 x 10^9 $M^{-1} S^{-1}$.

K_Q for this quenching interaction is large, but significantly slower than that expected for exothermic singlet energy transfer. In liquid benzene[30] this rate constant is typically 3-5 x 10^{10} $M^{-1} S^{-1}$. This result is significant because it implies that the $^1B_{2u}$ states of benzene and 1 are poorly matched for efficient energy transfer.

The 2-Ethylnaphthalene Triplet Photosensitized Isomerization of 1.

Saltiel et al.[10] report a value of 2.81 (20°C) for the relative rates of production of cis, trans- and cis, cis-2,4-hexadiene from 1, utilizing benzophonone as a triplet sensitizer. To check this crucial ratio, the experiment was redetermined using a $^3\pi$-π^* photosensitizer, 2-ethylnaphthalene.

A solution of freshly distilled 1 was made up in purified liquid 2-ethylnaphtalene to give a final concentration

of 0.050 molar.

Four 2.0 ml aliquots were degassed to better than 10^{-5} Torr. and sealed off the vacuum line.

Three of these ampoules were irradiated in parallel at 305 nm for varying lengths of time in a small "merry-go-round" apparatus.

After irradiation, these tubes, as well as the zero time tube, were analyzed by G.L.C. to determine relative isomer ratios. It was assumed that there was negligible diene disappearance.

The data are displayed in Table 2 (See Appendix I, p.165) as well as Figure 3. The production of both 2 and 3 is seen to be linear with time. The ratio of the slopes of the two lines, determined by least squares analysis, is 2.6 ± 0.3, in excellent agreement with Saltiel's results[10].

The Benzene Sensitized Photoisomerization of Trans, Trans-2,4-Hexadiene.

The fact that 1 quenches benzene fluorescence by no means implies that quenching proceeds with energy transfer to the quenchee. The effect may be catalytic as is the case with other selected 1,3-dienes,[21] or the quenching reactivity may be due to chemical reaction between excited donor and acceptor. 1,3-dienes are known to form addition products when irradiated with benzene at 254 nm[31-33].

As pointed out in the introduction, enhanced 2/3

Figure 3. The 2-ethylnaphthalene triplet sensitized isomerization of 1, irradiating at 305 nm (neat sensitizer).

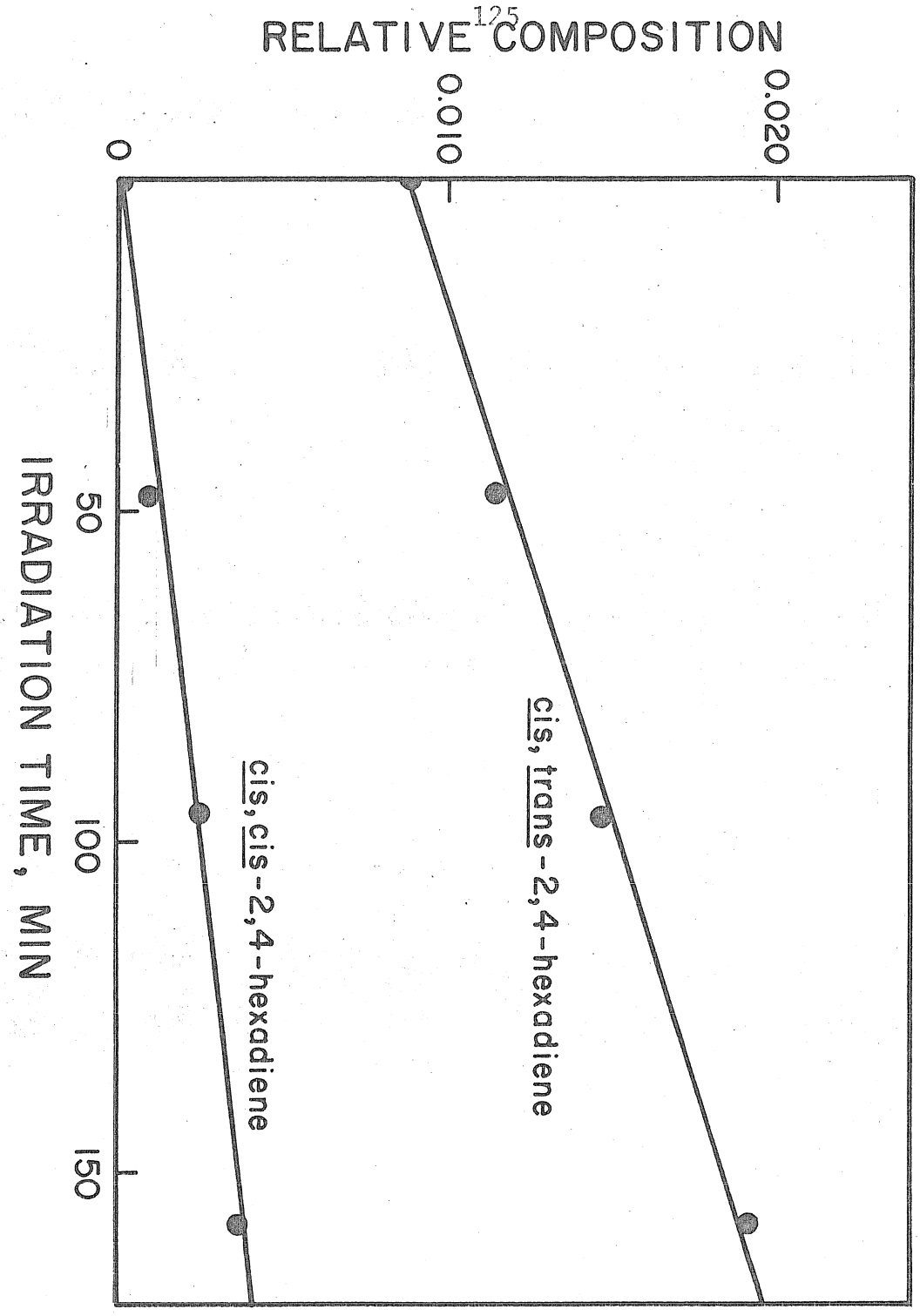
RELATIVE COMPOSITION
0
0.010
0.020
50
100
150
IRRADIATION TIME, MIN
cis, trans-2,4-hexadiene
cis, cis-2,4-hexadiene

production relative to the standard triplet derived ratio is indicative of the generation of diene singlet states. It was decided to investigate the possibility of singlet excitation transfer from benzene to 1 by looking for an exultation in the initial relative rate of production of 2 and 3.

Four aliquots of a solution of 0.050 M 1 in benzene were degassed in quartz ampoules and sealed off the vacuum line. Three of these were irradiated at 254 nm in parallel for varying lengths of time, and all four were subsequently analyzed for relative isomer content. Under such conditions, the diene absorbed a negligible fraction of the incident light.

Results are tabulated in the appendix (Table 3) and shown graphically in Figure 4. There is a marked enhancement of 2 production relative to 3, indicating that an additional excitation pathway besides triplet energy transfer is occurring through benzene sensitization. The observed ratio is 4.1 ± 0.4 which is to be compared with 2.71, the pure triplet ratio[10].

On the basis of the measured ratio, a transfer efficiency is 0.11 ± 0.03. The production of diene singlet states is inefficient, but still significant.

Gamma Irradiation of 0.1 M Solutions of trans, trans-2,4-Hexadiene in Benzene.

Figure 4. Benzene sensitized isomerization of 1, exciting at 254 nm at ambient temperature.

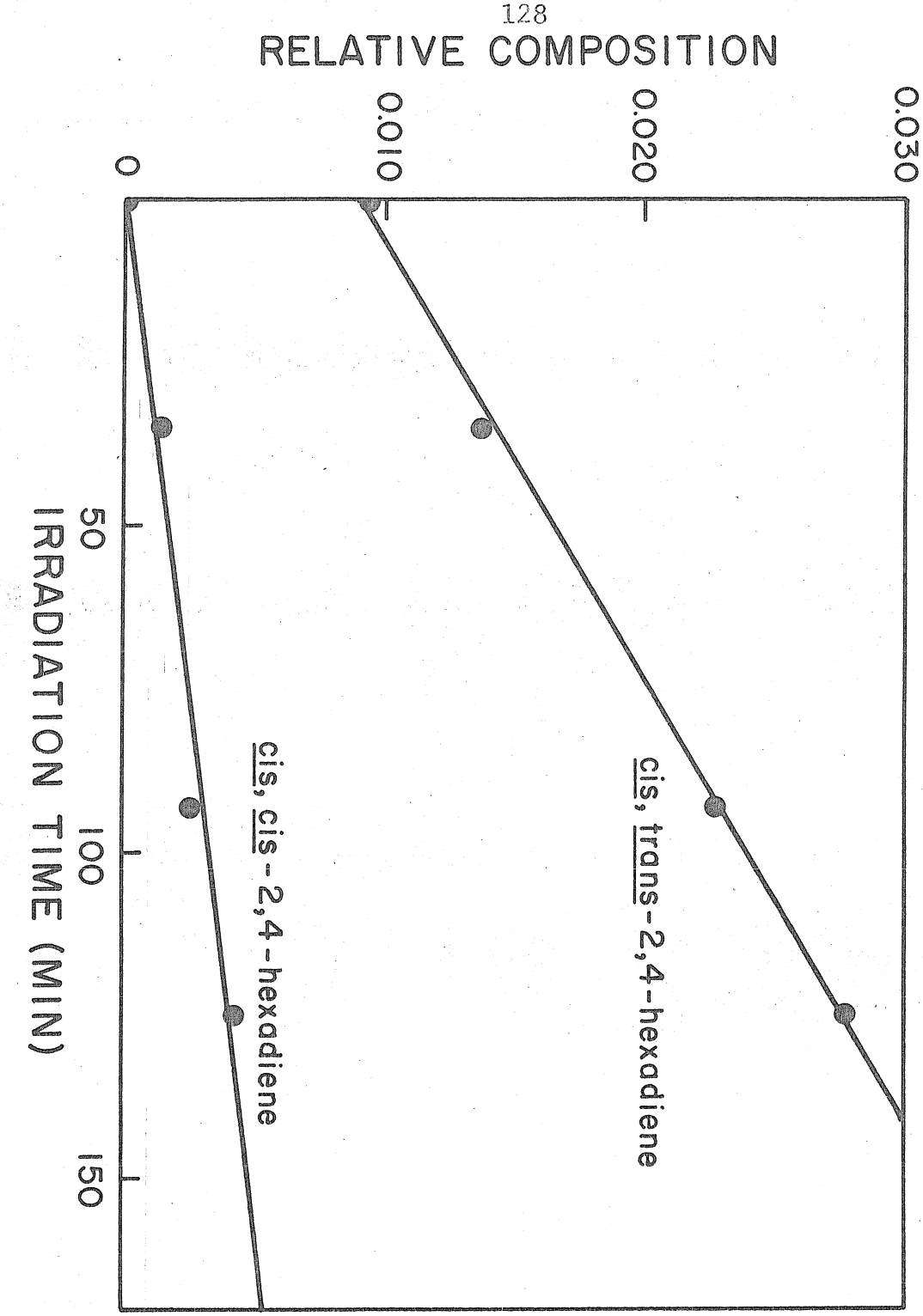
RELATIVE COMPOSITION
0
0.010
0.020
0.030
IRRADIATION TIME (MIN)
50
100
150
cis, trans-2,4-hexadiene
cis, cis-2,4-hexadiene

Two sets of four ampoules were prepared. These contained methylcyclohexane as internal standard (0.0157 M) and 0.100 M trans, trans-2,4-hexadiene in benzene. Three tubes of the first set of four were irradiated for varying times on December 15, 1970. ($D = 3.00 \times 10^{19}$ eV·ml^{-1}·hr^{-1}). One tube was saved for a zero-time tube.

This procedure was repeated on January 19, 1971, for the second set of tubes. These tubes were irradiated at a higher dose rate (4.19×10^{19} eV·ml^{-1}·hr^{-1}) as a result of being abnormally positioned inside the source. Isomer production in these tubes was corrected for higher dose rate and plotted with the first set of tubes in Figure 5.

At low conversions, cis, cis- and cis- trans- production is seen to be linear with time. A marked enhancement of 2 relative to 3 is observed as in experiment III. The dotted line shows the predicted 2 concentration if only triplet excitation were being delivered to the diene.

A dose effect, indicated by a fall off of the rate of 2 production after long irradiation times is observed. The trivial explanation is that energy transfer to 2 is now occurring because of its non-negligible concentration (~ 6%). An alternative explanation is that a radiation generated quencher is competing for the singlet excitation at this large absorbed dose ($D_A > 1.5 \times 10^{20}$ eV·ml^{-1}).

Hentz and Perkey[34] report such a dose effect on the rate of singlet excitation transfer to 3,5-cycloheptadienone

Figure 5. Solute isomerization following γ-irradiation of 0.1 M 1 in benzene at ambient temperature.

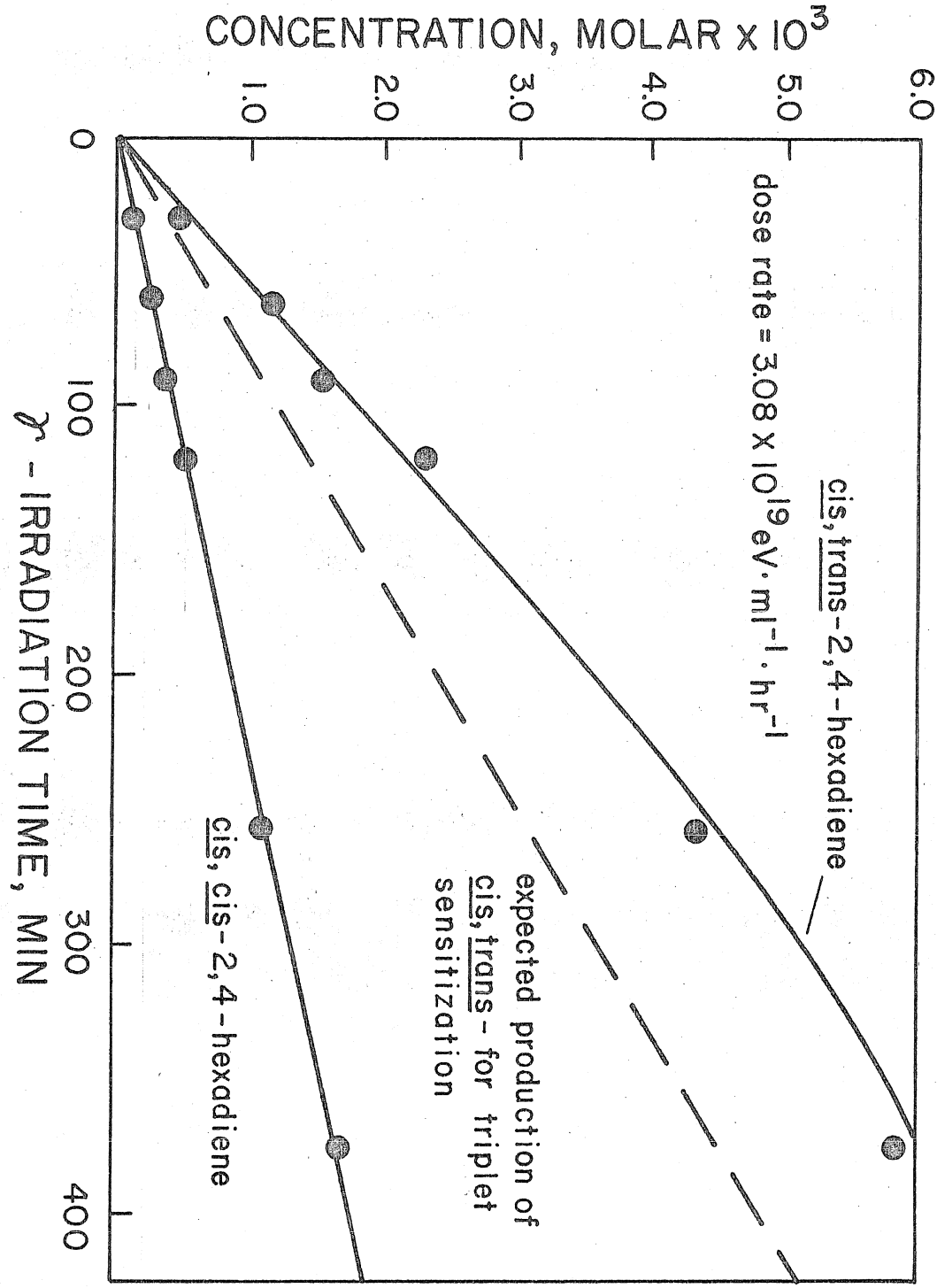
CONCENTRATION, MOLAR x 10³
6.0
5.0
4.0
3.0
2.0
1.0
0
100
200
300
400
γ - IRRADIATION TIME, MIN
cis, trans-2,4-hexadiene
dose rate = 3.08 x 10¹⁹ eV. ml⁻¹. hr⁻¹
expected production of cis, trans- for triplet sensitization
cis, cis-2,4-hexadiene

from benzene at considerably smaller absorbed dose ($D_A < 2\ 10^{19}$ eV·ml^{-1}).

Loss of total diene versus internal standard was noted. This decrease is plotted against time in Figure 6. G (- diene) is less than 1 at T = 0.

Determination of Radio-Stationary State Composition of Solutions of Trans, Trans-2,4-Hexadiene in Benzene.

Six ampoules containing 0.0157 M methylcyclohexane and 0.100 M trans, trans-2,4-hexadiene in benzene were prepared. Five of these were placed in the ^{60}Co source, while the sixth tube was retained for a zero-time sample.

Tubes were removed after varying amounts of time and analyzed to determine the amount of geometrical isomerization which had occurred. The first tube was extracted from the source after 72 hours of irradiation. The fourth tube was removed after 168 hours. Unfortunately, the experiment was terminated abruptly at this point when the remaining sample was removed by another experimenter.

At the adventitious removal of the last tube, isomer fractions were still changing, and appeared to be asymptotically approaching the photostationary state ratios obtained by high energy triplet sensitization.

At 168 hrs., the composition of the mixture was $\underset{\sim}{1}$ = 0.378, $\underset{\sim}{2}$ = 0.457, $\underset{\sim}{3}$ = 0.166. If only triplet excitation were being delivered to the diene, at infinite time these

Figure 6. Loss of total diene content following γ-irradiation of 0.1M *trans*, *trans*-2,4-hexadiene in benzene.

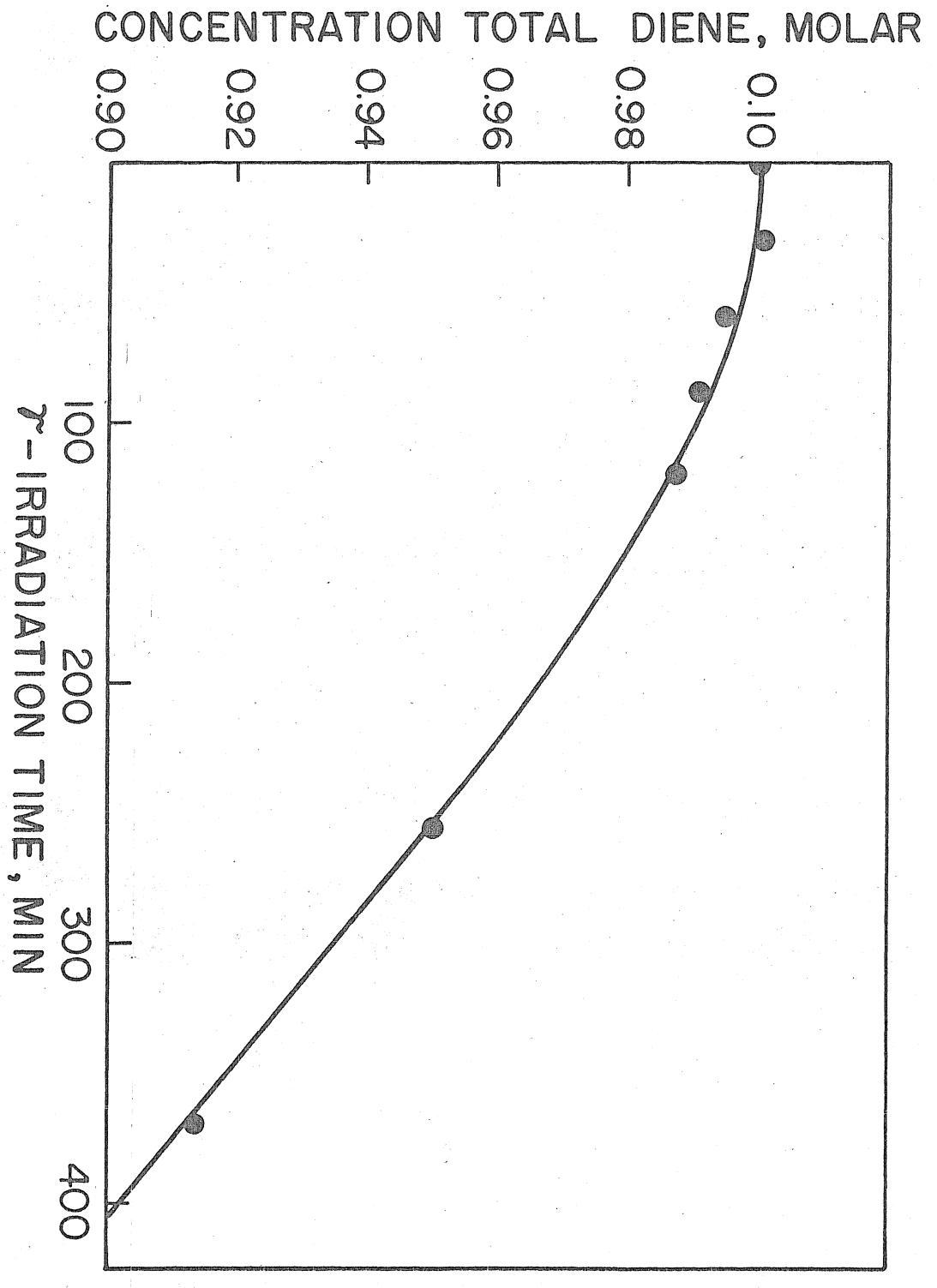
CONCENTRATION TOTAL DIENE, MOLAR
0.90
0.92
0.94
0.96
0.98
0.10
100
200
300
400
γ- IRRADIATION TIME, MIN

fractions would be $\underset{\sim}{1}$ = 0.313, $\underset{\sim}{2}$ = 0.501, $\underset{\sim}{3}$ = 0.185 (see Figure 7)[10].

It appears that after long irradiation times, singlet excitation of the dienic mixture does not substantially perturb the triplet derived stationary state. This is either coincidental or demonstrates that the excess excitation pathway is quenched after substantial irradiation. The yield of solute singlet excited states is known to decrease with increasing absorbed dose in benzene[34].

The observed ratios are clearly much different than the thermodynamic ratios[35] at 20.2 ^{oc}, which are $\underset{\sim}{1}$ = 0.655, $\underset{\sim}{2}$ = 0.307, 3 = 0.038. This result precludes an important catalytic ground state isomerization pathway involving free radials (G ~ 0.7) or other intermediates. For example,

$$R\cdot + \underset{\sim}{1} = X = R\cdot + \underset{\sim}{1} + \underset{\sim}{2} + \underset{\sim}{3} \qquad (23)$$

reaction (22) could only be expected to move the mixture towards thermodynamic equilibrium.

The radiostationary state of piperylene (1,3-pentadiene) in benzene is also that obtained by high energy triplet sensitization[33].

As in the previous experiment, loss of total diene content versus internal standard was evident. Comparison of Figures 6 and 7 make it obvious that the initial rate of loss diminished as the radiation time increased.

Figure 7. Isomer composition (mole %) of γ-irradiated benzene solutions of 1 as a function of time.

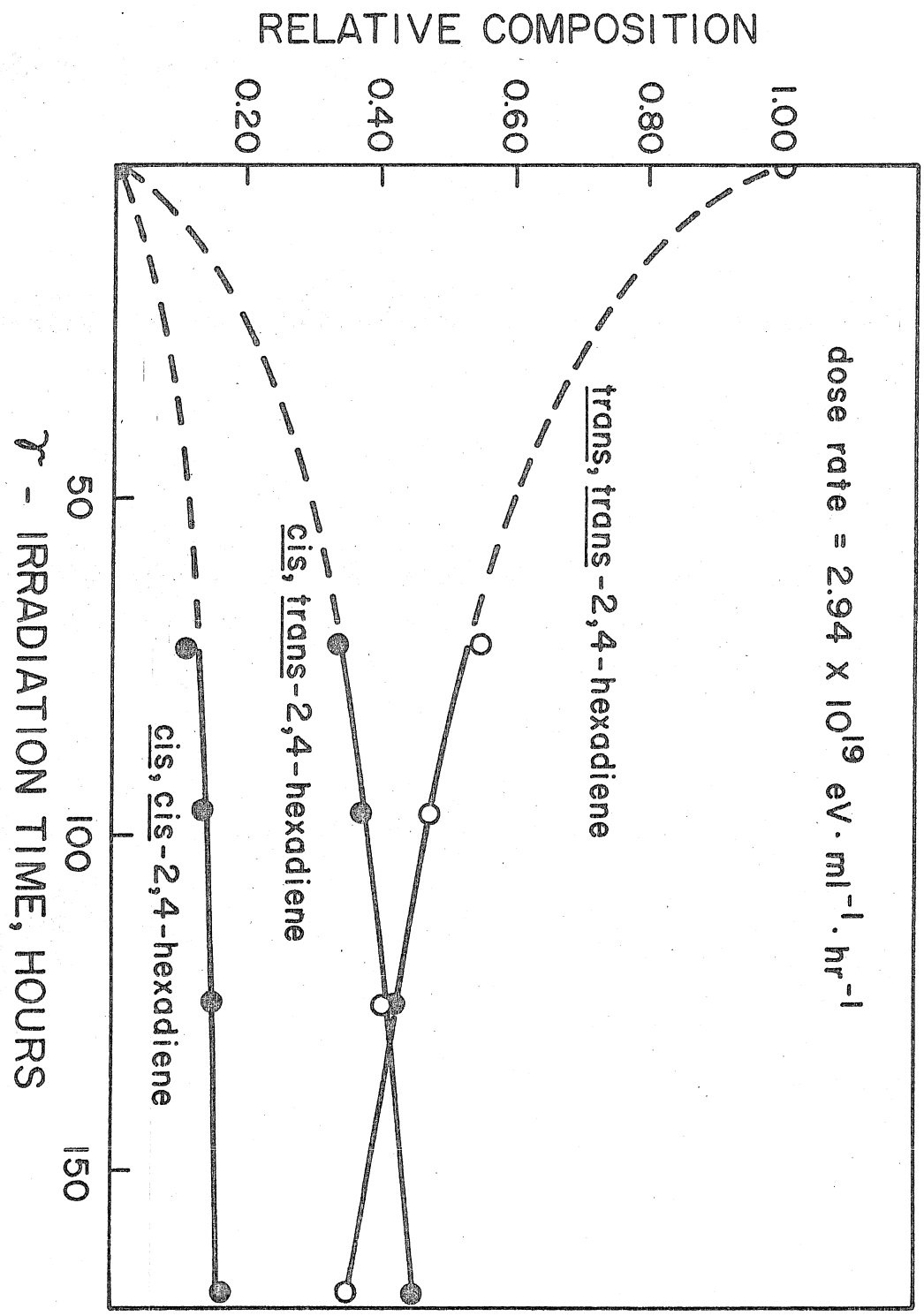
RELATIVE COMPOSITION
0.20
0.40
0.60
0.80
1.00
dose rate = 2.94 x 10^19 eV. ml^-1. hr^-1
trans, trans-2,4-hexadiene
cis, trans-2,4-hexadiene
cis, cis-2,4-hexadiene
50
100
150
γ - IRRADIATION TIME, HOURS

Extrapolation of short time results to long irradiation times produces a much lower diene content than was observed. At 168 hrs. this loss was approximately 33% (Figure 8).

It was not determined if the diene to internal standard ratio were being elevated due to radiolytic destruction of the methylcyclohexane, but this is an unexpected result in view of the stabilizing effect of benzene on the radiation sensitivity of saturated hydrocarbons[36].

Dependence of G(2) and G(3) on Trans, Trans-2,4-Hexadine Concentration

Five ampoules containing benzene and varying concentrations of trans, trans-2,4-hexadiene were prepared. Four of these tubes were γ-irradiated ($D = 2.92 \times 10^{19}$ eV·ml^{-1} hr^{-1}) for 1.00 hours, while the fifth tube was saved for a zero-time tube. Absolute conversions of 1 to 2 and 3 were determined after irradiation by measuring the fractions of each isomer present relative to the total diene content and multiplying these fractions by the known initial diene concentration. Conversions were corrected for zero-time content of 2. Conversions to isomers ranged from 1.4% (0.100 M diene) to 8% (0.005 M diene). G(3) and G(2) versus (1) are shown in Figure 9.

A second set of tubes was prepared in the same fashion on 12-15-72 and irradiated for 72 minutes. In this case,

Figure 8. Loss of total diene content with increasing γ-irradiation time. Data from figure 6 is also shown.

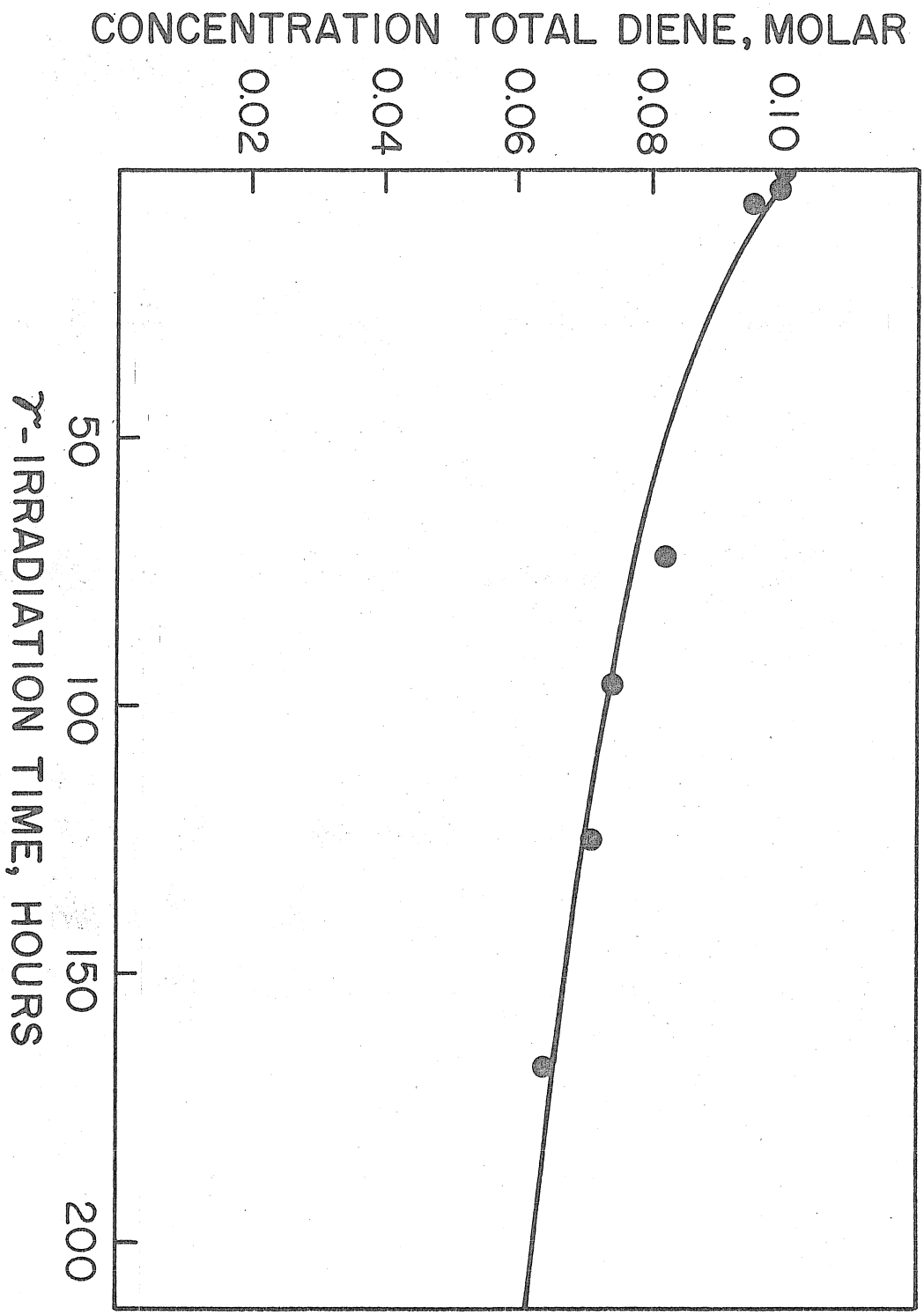
CONCENTRATION TOTAL DIENE, MOLAR
0.02
0.04
0.06
0.08
0.10
γ-IRRADIATION TIME, HOURS
50
100
150
200

however, no zero-time tube was saved to determine starting $\underset{\sim}{2}$ content.

This proved to be a serious error, because unusually large amounts of $\underset{\sim}{2}$ were found in the irradiated tubes. Yields calculated using the average zero-time concentration of $\underset{\sim}{2}$ determined from other experiments with this batch of $\underset{\sim}{1}$, were ~ 2 times the expected values, compared with G($\underset{\sim}{2}$) from experiment IV and the first set of tubes. G($\underset{\sim}{3}$) from this set of tubes was well behaved, however, assuming a normal zero-time content of $\underset{\sim}{3}$ = 0. This demonstrates that there was not a serious dosimetry error.

These facts are consistent with the accidentally catalyzed thermal isomerization of $\underset{\sim}{1}$, occurring before distillation. $\underset{\sim}{2}$ would be expected to be produced much more readily than $\underset{\sim}{3}$ because the equilibrium value[35] of $\underset{\sim}{2}$ is ~ 8 x that of $\underset{\sim}{3}$.

These unusual values of G($\underset{\sim}{2}$) were discarded, but G($\underset{\sim}{3}$) values were included in the data set.

Values of G($\underset{\sim}{2}$) from experiment IV and this experiment were combined and are shown in Figure 9.

The behavior is that expected on the basis of sequence (8)-(15). Isomerization increases with concentration until gradually reaching an asympotic value, showing that the monitored intermediates are totally quenched at high solute concentration.

Figure 9. Initial G values for 2 and 3 production as a function trans, trans-2,4-hexadiene concentration in C_6H_6 .

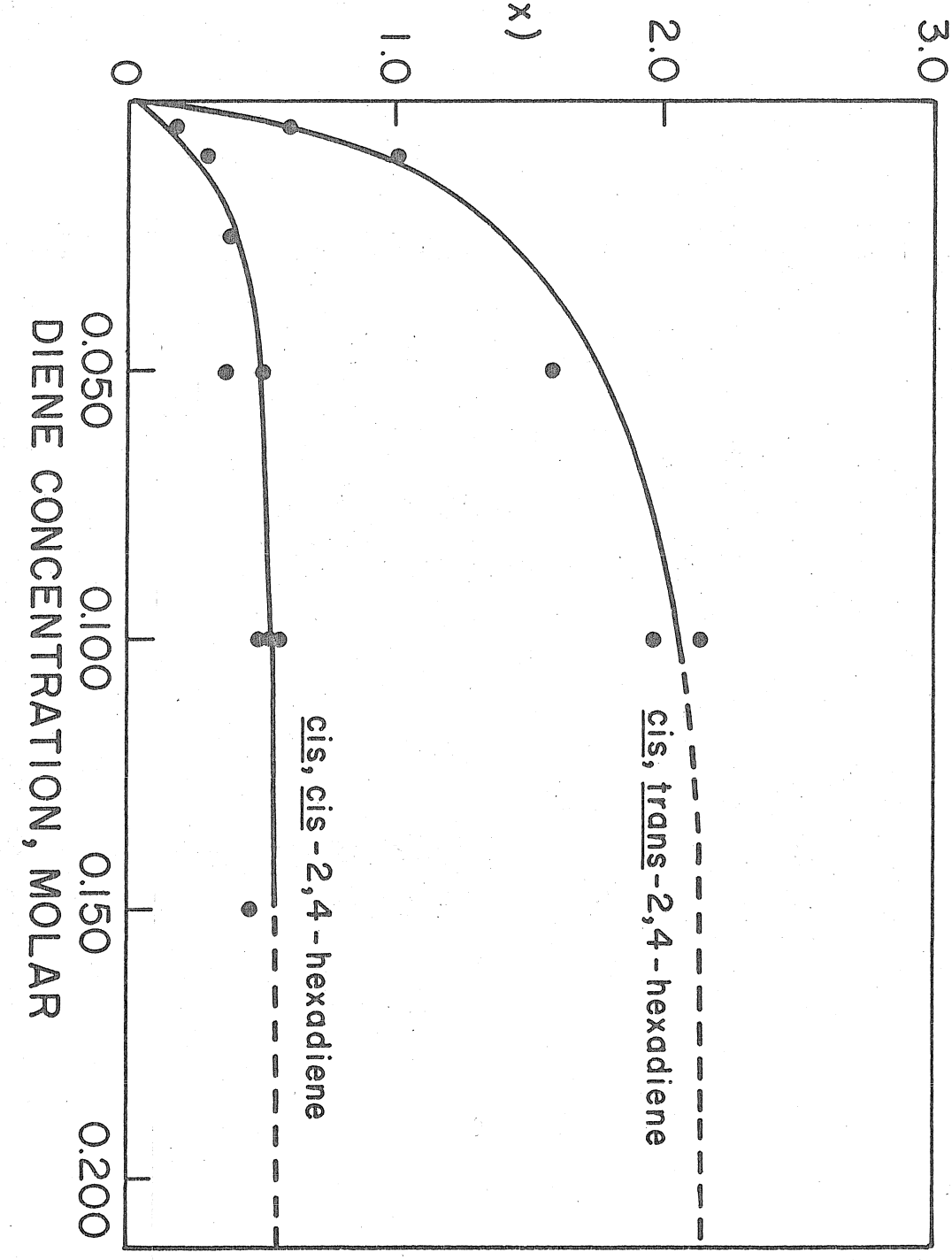
G(x)
3.0
2.0
1.0
0
0.050
0.100
0.150
0.200
DIENE CONCENTRATION, MOLAR
cis, trans-2,4-hexadiene
cis, cis-2,4-hexadiene

DISCUSSION

The results of experiment IV demonstrate that 1 is isomerized when its dilute benzene solutions are γ-irradiated. That this process involves diene excited states is unequivocable, because the composition of the dienic mixture moves steadily away from thermodynamic equilibrium[35] (experiment V).

It is also clear that these excited states are not produced by the direct action of γ-rays on (1). The direct excitation of a component in a γ-irradiated mixture is expected to be proportional to the electron fraction of that component[37].

For solutions of 0.1M or less, the electron fraction of 1 is less than 1%. At a concentration of 0.1M, the average G value for the formation of 2 is 1.97 molecules per 100 eV absorbed by the system. On the basis of the energy absorbed directly by 2, this would correspond to a G value of 1.97/.01 = 197. Since the lowest excited state of the diene requires approximately 2 eV for its production, in the absence of a remarkably efficient excited-state chain mechanism for isomerization, the total energy requirement would be 394 eV. This is energetically impossible. The concentration dependence for diene isomerization shows that a chain mechanism does not operate in this system.

Excitation transfer must, therefore, proceed from solvent-to-solute with the ultimate production of diene excited states. The mechanism could involve direct electronic excitation transfer from benzene to 1, identical to that produced by ultraviolet irradiation.

A second plausible mechanism is suggested by charge scavenging experiments in γ-irradiated cyclohexane. The use of cis- and trans-stilbene as an additive[38,39] in this system leads to a high yield of stilbene excited states. Charge transfer from cyclohexane is evidenced by the appearance of stilbene anions[38]. Excited state yields are quenched by good electron scavengers, so it appears that stilbene excitation follows charge scavenging and eventual neutralization[39].

The situation is different in benzene, however, because ionic recombination times are much shorter[40]. At 0.1M, direct energy transfer from solvent excited states is the predominate mode of stilbene excitation.

An estimate of the importance of the charge transfer mechanism can be gleaned from experiments in which efficient electron scavengers are added to γ-irradiated benzene. One commonly studied, highly reactive electron scavenger is nitrous oxide, N_2O, whose reactions in γ-irradiated benzene are described by Hentz and Sherman[42] as well as Sato et al.[43]

Its electron scavenging efficiency in benzene and cyclohexane is near maximum[42], so that the rate of electron

scavenging by any other solute is probably less than that of N_2O.

The yield of scavenged electrons in γ-irradiated benzene ranges from 0.12 at 0.005 M N_2O, to 0.65 electrons per 100 eV at 0.100 M N_2O. This therefore represents an approximate maximum radiation-chemical yield for solute excited states generated by charge neutralization in benzene, for concentrations less than 0.1 molar. As will be seen later, the yields of diene excited states, both singlet and triplet, substantially exceed these values.

A mechanism involving triplet energy transfer to solute is strongly suggested by the results of experiment V, which demonstrated that the radiostationary state is very close to that expected for high energy triplet photosensitizers. Such transfer is exothermic, and occurs at a diffusion controlled rate. There is abundant evidence that solvent triplet states are generated when benzene is γ-irradiated, so the triplet isomerization of $\underset{\sim}{1}$ is to be expected. This is confirmed by experiment.

The yield of solute triplet states is calculated from the initial rate of production of $\underset{\sim}{3}$ and equation (16). Sequence (8)-(15) predicts the analytical dependence of diene triplet states on quencher concentration (see Appendix III). For those solvent triplet states which are directly produced by high energy radiation, the dependence is:

$$G^{-1}(^3D) = G^{-1}(^3B)\ (1 + \frac{K_{gt}}{K_{yt}}\ [\underset{\sim}{1}]^{-1}) \qquad (24)$$

In this notation, $G(^3B)$ is the radiation-chemical yield of the lowest benzene triplet state produced directly by γ-irradiation. K_{yt} is the rate constant for bimolecular quenching of this state by $\underset{\sim}{1}$, K_{gt} is the rate constant for unimolecular decay of ^3B, and $[\underset{\sim}{1}]$ is the concentration of $\underset{\sim}{1}$.

The reciprocal of the yield of ^3D is plotted versus reciprocal diene concentration in Figure (10). The data correlates well with a linear relationship between the two quantities. A least squares analysis of the data gives a y-intercept of 0.336 ± .050 and a slope of 0.00300 ± 0.00045. The correlation coefficient is 0.921.

These numbers define $G(^3B)$ and K_{gt}/K_{yt} through equation (24). On this basis, $G(^3B) = 2.97 \pm 0.45$ and $K_{gt}/K_{yt} = 8.94 \pm .13 \times 10^{-3}$M. K_{yt} is 1×10^{10} in benzene,[44] so $K_{gt} = 9 \times 10^7\ S^{-1}$.

K_{gt} determined by this method agrees well with evaluations for the benzene triplet decay rate established by stilbene[34] ($16 \times 10^7\ S^{-1}$), cycloheptadienone[34] ($13 \times 10^7\ S^{-1}$), biacetyl[45] ($12 \times 10^7\ S^{-1}$), and 2-butene[46] ($10 \times 10^7\ S^{-1}$), quenching.

Furthermore, $G(^3B) = 2.97$ is consistent with and intermediate to other determinations by nanosecond pulse radiolysis[4] (1.85 ± .3), microsecond pulse radiolysis[45] (1.24), stilbene[34] (4.2) and 1,2-diphenylpropene (4.1) isomerization,[41]

Figure 10. Inverse yield dependence of diene singlet and triplet excited states (calculated from the data of Figure 9, and equations 19 and 16) as a function of inverse $\underset{\sim}{1}$ concentration.

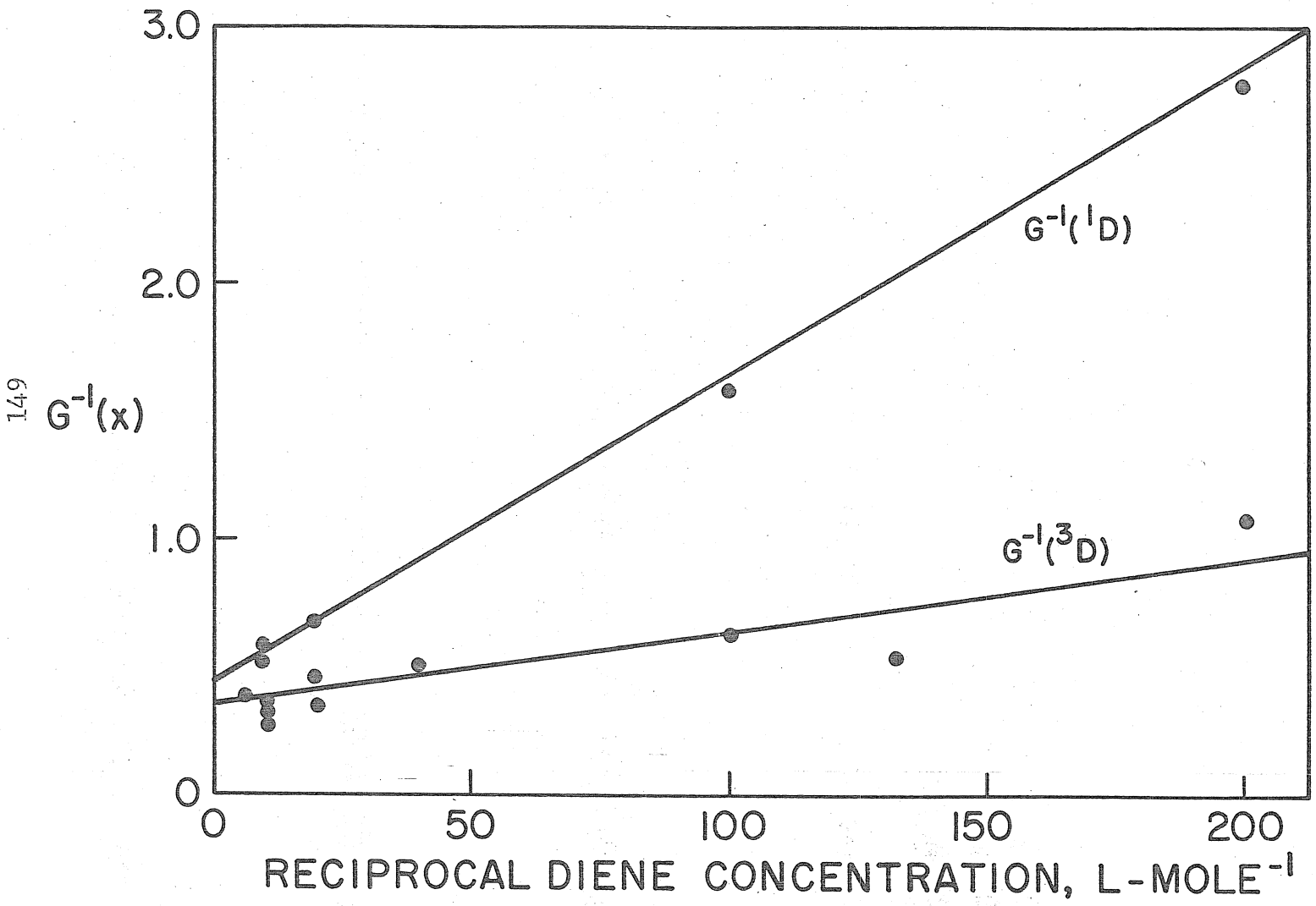
3.0
2.0
1.0
0
$G^{-1}(x)$
$G^{-1}(^1D)$
$G^{-1}(^3D)$
0
50
100
150
200
RECIPROCAL DIENE CONCENTRATION, L-MOLE^{-1}

and finally cycloheptadienone (4.0) rearrangement[34].

As shown in Appendix II, the same analytical form is expected for the yield of diene singlet excited states with changes in quencher concentration.

$$G^{-1}(\underset{\sim}{1}^*) = G^{-1}(^1B)\ (1 + \frac{K_m}{K_{ym}}\ [\underset{\sim}{1}]^{-1}) \qquad (25)$$

A plot of $G^{-1}(\underset{\sim}{1}^*)$, calculated from equation (19), versus inverse diene concentration, is displayed in Figure (10). In this case, the linearity is striking. By least squares analysis, the correlation coefficient is 0.998. The intercept is 0.457 ± .015 and the slope is 0.0123 ± .0004.

As before, these numbers uniquely determine $G(^1B)$, the quenchable yield of benzene excited singlet states, and K_m/K_{ym}, the ratio of the rate constants for unimolecular decay and bimolecular quenching. Under the assumption that the transfer efficiency is unity, this gives $G(^1B)$ = 2.19 ± .06 and K_m/K_{ym} = 0.0268.

It is now necessary to examine the assumption that the transfer efficiency is 1.0, taking the results of experiment III into consideration. Experiment III demonstrates that energy transfer from the lowest excited singlet state of benzene is substantially less than unity. The isomerization experiment was carried out at a concentration of 0.050 molar $\underset{\sim}{1}$, a concentration which experiment I shows to quench 75% of all benzene fluorescence. This fraction of excited states

is no longer available to intersystem cross to give benzene triplets, which efficiently isomerize 1. Since the intersystem crossing efficiency in neat benzene[34,47] is 0.57, this means that 0.57x(1-0.75) or 14% of the original benzene singlets produce triplet excited states.

If the transfer efficiency of the $^1B_{2u}$ state to diene were 1.0, this would result in ratio of diene singlet to triplet excited states of roughly 0.75/0.14 = 5.4. The actual ratio must be much smaller, because the observed ratio 2 and 3 production is 4.1 ± .4. This is reasonably close to the pure triplet ratio 2.71. The ratio of single bond to double bond isomerization demonstrates that the isomerization is still predominately triplet in character. The most economical explanation is that singlet production is inefficient.

A detailed calculation of the transfer efficiency is shown in Appendix III. The result is that the transfer efficiency, p, is 0.11 ± .03 . The treatment is valid if the decay ratio of excited singlet 1 to 2 is identical for direct and sensitized production.

This result must now be used to correct G(^1B), determined by the data in Figure (9). Division by the transfer efficiency for the $^1B_{2u}$ state gives G($^1B_{2u}$) = 19.9.

Several recent, fastidious efforts utilizing pulse radiolysis[45,4] and carefully monitored solute-sensitization experiments[35,41,48] have determined G($^1B^o_{2u}$) = 1.5 ± 0.15 in

convincing fashion. It is therefore necessary to discard the hypothesis that singlet excitation to the diene is delivered by the $^1B_{2u}$ state of benzene.

Two possibilities are excitation transfer from the upper excited singlet states of benzene or by dienic charge scavenging (vida supra). The data show that the yields of diene excited states are roughly three times that expected for a charge transfer mechanism giving exclusive singlet production (choosing N_2O as an optimum electron scavenger).

On a statistical basis for homogeneously distributed charges, ionic recombination should produce singlet and triplet excited states in a ratio fo 1 to 3[4]. Recent work by Penner, Whitten, and Hammond[49] concludes that for neat 1,3-cyclohexadiene, no diene singlet states are formed as a result of charge neutralization, and that the singular production of diene triplet states occurs.

It therefore seems likely that the charge-transfer mechanism cannot accommodate the relatively large amount of observed singlet excitation. The remaining possibility is that an upper benzene singlet state transfers energy to 1.

The main objection to this hypothesis is that such states are extremely short lived ($\sim 10^{-12}$ S).[50] In normal cases it is not possible to intercept them with chemical quenchers before internal conversion.

Benzene and its alkyl derivatives are exceptional cases, however. The rate of internal conversion of the $^1B_{1u}$ state

of benzene[50] is estimated to have a maximum value of 4×10^{10} S^{-1}, corresponding to a lifetime of 2.5×10^{-11} S.

Benzene is also exceptional for its energy-transport properties. The rate of diffusion controlled quenching in benzene is substantially faster than calculated from viscosity measurements and Einstein-Smulokowski diffusion theory[44,51]. Experiment shows that energy migration occurs in addition to simple mass diffusion[51].

This effect is expected to increase markedly for the optically allowed upper excited singlet states of benzene, both by the theories of Birks[52] and Voltz[53]. The exciton diffusion model of Voltz predicts a transfer time between adjacent molecules of 4×10^{-15} S for the exciton state corresponding to the $^1E_{1u}$ state of benzene. The migration rate for the $^1B_{1u}$ state is less by a factor of 10. Voltz[53] calculates a rate constant of 6.5×10^{14} $M^{-1} S^{-1}$ for energy transfer to suitable traps from the upper excited singlet states of toluene.

Energy transfer to solute will be an important process if the transfer rate can compete with internal conversion (10^{12} S^{-1}) of the excited state. Using the above figures with an acceptor concentration of 10^{-2} molar produces a transfer rate of 6.5×10^{12} S^{-1} which exceeds an internal conversion rate of 10^{12} S^{-1}. Trapping is efficient even at moderate-to-low (10^{-1} - 10^{-2}M) acceptor concentrations.

In view of these considerations, it is plausible to expect energy transfer from highly-excited benzene singlet states to 1. Both the $^1E_{1u}$ and $^1B_{1u}$ states are reasonable candidates as donors.

The probability for generating an excited state by secondary electrons produced in a radiation-chemical experiment is predicted by the optical approximation model[54]. The relative ease of production is given by the ratio f_n/E_n, where f_n is the oscillation strength and E_n is the energy of the final state.

On this basis, the relative yields from secondary electron excitation of benzene are $^1B_{2u} = 0.002$, $^1B_{1u} = 0.10$, $^1E_{1u} = 0.69$[54]. These figures have been shown to be correct for gas phase excitation[55,56]. The production of upper singlets is facile compared to $^1B_{2u}$ benzene.

Oster and Kallmann[57] report the interception of high lying singlet states of benzene by $CHCl_3$, on the basis of the observed free radical yields under X-irradiation. $CHCl_3$ does not quench the $^1B_{2u}$ state of benzene. This observation should be re-examined, however, in view of the powerful electron scavenging ability of $CHCl_3$.

Cundall, et al.,[45] explain the low yields of biacetyl excited states in the pulse radiolysis of benzene on the basis of upper excited state transfer to the dissociative states of biacetyl.

Energy transfer from an upper benzene singlet state to

anthracene has been postulated by Cooper and Thomas[4] to account for the high yields of anthracene excited states relative to naphthalene when these molecules were used as excitation acceptors in pulse radiolysis experiments.

Skarstad, Ma, and Lipsky[58] propose the production of higher excited singlet states of benzene which do not efficiently internally convert to explain the results of scintillation studies.

Horrocks[54] reports an interesting study on the relative scintillation efficiencies of 1,2,4-trimethylbenzene, p-xylene, toluene, and benzene as a function of solute concentration. At low solute concentrations, the relative scintillation efficiencies of these four solvents parallel the $^1E_{1u} \rightarrow {}^1B_{2u}$ internal conversion fraction of the solvent. At high solute concentrations (~ 0.1 M) however, each solvent demonstrated the same scintillation intensity. This is consistent with energy transfer before internal conversion of the $^1E_{1u}$ state.

The energy transfer efficiency to diphenyloxazole[59] is found to increase for benzene excitation at 195.0 nm, with an increase in acceptor concentration, providing evidence that upper benzene singlets are transfering energy to DPO.

An acceptance of the mechanism resolves several contradictions for experimental determinations of $G(^1B_{2u})$ appearing in the literature. Hammond et al.[21] determined $G(^1B_{2u}) = 3.4 \pm 0.3$ in an elegant experiment using 0.4 molar biphenyl

as a singlet excitation "relay" agent from benzene to tetramethyloxetanone (TMO).

TMO decomposes under direct irradiation at 313 nm to acetone and dimethylketene (Φ - TMO) = 0.26 ± .01 in benzene, while triplet sensitization produces the same product with lower efficiency (Φ = 0.04 in acetone).

To avoid the complications of energy transfer from both singlet and triplet excited benzene to TMO, biphenyl was added at 0.4 molar to scavenge these states prior to TMO excitation. The relationship between the excited states of biphenyl and TMO is such that only singlet energy transfer to TMO is possible.

From the concentration dependence of TMO disappearance, a yield of 3.4 ± 0.3 is determined for $^1B_{2u}$.

This experiment has been criticized because at the relatively high concentration of biphenyl employed, alternate modes of solute excitation are possible, leading to an anomalously high value for $G(^1B_{2u})$ [34].

Whitten and Zarnegar[48] report an illuminating study of 4-methyl-4-phenyl-2-pentanone (MPP) in benzene. The reaction leads to α-methylstyrene exclusively through an excited singlet state (Φ = 0.020).

A plot of the inverse yield of singlet excited ketone versus reciprocal MPP concentration displays a linear region for (MMP) < 0.020 M and a curved region at (MMP) > 0.020 M which extrapolates at infinite ketone concentration to give

$G(^1B) = 3.3$. This is experimentally equal to the "anomalous" yield of $^1B_{2u}$ reported by Hammond et al.[21].

An extrapolation from the low concentration domain produces another intercept, which gives $G(^1\text{Benzene}) = 1.4$, a value very close to the accepted value for $G(^1B_{2u})$ [34]. Whitten and Zarnegar[48] comment that the increased yield of singlet excitation may be due to energy transfer from an upper singlet state of benzene. From the difference of the two extrapolated concentrations, a value of G = 2 for this state is obtained.

This yield of excess singlet excitation is equivalent to the value established here, G = 2.19 ± .06. Upon correction for the expected small contribution of diene excited states from $^1B_{2u}$ energy transfer, this value becomes 2.03 ± .06.

The observation of a new singlet excitation pathway removes some of the confusion existing in the literature concerning the isomerization of stilbene and 1,2-diphenylpropene as well as trans-stilbene. Solute triplet yields do not reach a limit at 0.1 M but continue to increase slowly with increase in concentration[21,41].

Low concentration extrapolations indicate a total excited state (singlet + triplet) yield of 5.6.

Hentz and Altmiller[41] measure an excited state yield of 7.7 at 1 molar diphenylpropene in benzene, while Hammond et al.,[21] measure 9.9. For the first figure, a difference

of 2.1 is indicated between low and high concentration values, which is very close to the yield of upper singlet excitation determined by this work. It appears that a large fraction of this component can be ascribed to upper state transfer.

CONCLUSION

By a process of elimination, upper excited benzene singlet states have been shown to be excitation donors to trans, trans-2,4-hexadiene in a radiation-chemical experiment. The alternative excitation process, charge transfer from solvent-to-solute, cannot provide sufficient excitation to account for the observed isomerization. Correction for the small amount of solute excitation delivered by the $^1B_{2u}$ state of benzene gives a value of 2.03 ± .09 molecules/100 eV.

The yield of solvent triplet states which do not have the $^1B_{2u}$ state as a precursor was determined to be 2.97 ± 0.45, a value intermediate between pulse radiolysis and solute isomerization studies. The lifetime of the $^3B_{1u}$ state was estimated to be 12×10^{-9} S.

Finally, the energy of the first excited singlet state of trans, trans-2,4-hexadiene was shown to be slightly less energetic (~ 1 Kcal) than that of benzene, 107 Kcal·mole, because of the ability of the quencher to accept singlet excitation. This result is important because of the previous uncertainty regarding the location of this level.

REFERENCES

1. See, for example, J. Kroh and S. Karolczak, Rad. Res. Rev., 1, 411 (1969).
2. J. W. T. Spinks and R. J Woods, "An Introduction to Radiation Chemistry", John Wiley & Sons, Inc., 1964, p. 365.
3. J. B. Birks, "Photophysics of Aromatic Molecules", Wiley Interscience, 1970, p. 580.
4. R. Cooper and J. K. Thomas, J. Chem. Phys., 48, 5097 (1968).
5. T. Gaumann and J. Hoigne, "Aspects of Hydrocarbon Radiolysis", Academic Press, Inc. 1968, p. 117.
6. Ibid., p. 94.
7. Ibid., p. 143.
8. J. Saltiel, Lewis Metts, Mark Wrighton, J. Amer. Chem. Soc., 92, 3227 (1970).
9. R. B. Woodward and R. Hoffman, "The Conservation of Orbital Symmetry", Academic Press, Inc., 1970, p. 43.
10. J. Saltiel, L. Metts, M. Wrighton, J. Amer. Chem. Soc., 91, 5684 (1969).
11. J. Saltiel, A. Rousseau, A. Sykes, J. Amer. Chem. Soc., 94, 5903 (1972).
12. J. Saltiel, David Townsend, and Alan Sykes, J. Amer. Chem. Soc., 95, 5968 (1973).

13. R. N. Compton, R. H. Huebner, P. W. Reinhardt, and L. G. Christophorou, J. Chem. Phys. 48, 901 (1968).

14. See reference 3, p. 283.

15. R. Voltz, Rad. Res. Rev., 1, 301-360 (1968).

16. D. F. Evans, J. Chem. Soc., 1735, (1960).

17. O. A. Mosher, W. Flicker, A. Kuppermann, Chem. Phys. Lett. 19, 332-3 (1973).

18. "Caltech Chemistry and Chemical Engineering Annual Report 1974", California Institute of Technology, October 1974, p. 78.

19. R. Srinivasan, Adv. Photochem. 4, 113 (1968).

20. M. T. Vala, Jr., I. H. Hillier, S. A. Rice, and J. Jortner, J. Chem. Phys. 44, 23 (1966).

21. L. M. Stephenson, D. G. Whitten, and G. S. Hammond, "Chemistry of Ionization and Excitation", G.R.A. Johnson and G. Scholes, Ed., Taylor and Francis, London, 1967, p. 35.

22. J. Saltiel, private communication.

23. "Handbook of Chemistry and Physics", CRC Press, 53 ed., 1972, p. C-326.

24. See reference 2, pp. 106-112.

25. R. H. Schuler and A. O. Allen, J. Chem. Phys., 24, 56, (1956).

26. T. L. Penner, Ph.D. Thesis, California Institute of Technology, Pasadena, CA., 1969.

27. N. J. Turro, "Molecular Photochemistry", Turro, W. A. Benjamin, Inc., 1965, pp. 93-95.

28. S. Murov, "Handbook of Photochemistry", Marcel Dekker, Inc., 1973, p. 3.

29. See reference 3, p. 616.

30. See reference 3, p. 613.

31. G. Koltzenburg, and K. Kraft, Tetrahedron Letters 46 389 (1966).

32. K. Kraft and G. Koltzenburg, Tetrahedron Letters, 47, 4357 (1967).

33. R. A. Caldwell, D. G. Whitten, and G. S. Hammond, J. Amer. Chem. Soc., 88, 2659 (1966).

34. R. R. Hentz and L. M. Perkey, J. Phys. Chem., 74, 3047 (1970).

35. C . Doring and H. Hantel, J. Prakt. Chem., Rheihe 4, Band 24 (1964).

36. G. R. Freeman, J. Chem. Phys., 33, 71 (1960).

37. See reference 2, p. 93.

38. F. S. Dainton, C. T. Peng, and G. A. Salmon, J. Phys. Chem., 72 3801 (1968).

39. R. R. Hentz, D. B. Peterson, S. B. Srivastava, H. F. Barzynski, and M. Burton, Ibid, 70 2362 (1966).

40. J. K. Thomas and I. Maui, J. Chem. Phys., 51, 1834 (1969).

41. R. R. Hentz and H. G. Altmiller, J. Phys. Chem., 74 2646 (1970).

42. R. R. Hentz and W. V. Sherman, Ibid., 73, 2676 (1969).

43. S. Sato, K. Hosoya, S. Shishido, and S. Hirokami, Bul. Chem. Soc. Jap., 45, 2308 (1972).

44. A. A. Lamola and N. J. Turro, "Energy Transfer and Organic Chemistry", Interscience Publishers, 1969, p. 34.

45. R. B. Cundall, G. B. Evans, and P. A. Griffiths, J. Phys. Chem., 72, 3871 (1968).

46. R B. Cundall and P. A. Griffiths, Trans. Faraday Soc., 66, 350 (1970).

47. R. B. Cundall and W. Tippet, Trans. Faraday Soc., 66, 350 (1970).

48. B. M. Zarnegar, D. G. Whitten, J. Phys. Chem., 76, 198 (1972).

49. T. Penner, D. G. Whitten, and G. S. Hammond, J. Amer. Chem. Soc., 92, 2861 (1970).

50. See reference 3, p. 187.

51. See reference 3, p. 583.

52. See reference 3, p. 589.

53. R. Voltz, Rad. Res. Rev., 1, 301 (1968).

54. D. L. Horrocks, J. Chem. Phys., 52, 1566 (1970).

55. A. Skerbele and E. N. Lassettre, J. Chem. Phys., 42, 393 (1965).

56. H. B. Klevens and J. R. Platt, Ibid., 470 (1949).

57. G. K. Oster and H. Kallmann, J. Chem. Phys., 64, 28 (1967).

58. P. Skarstad, R. Ma, and S. Lipsky, Mol. Cryst., 4, 3 (1968).

59. U. Laor and A. Weinreb, J. Chem. Phys., 50, 94 (1969).

APPENDIX I

Experiment II. The 2-ethylnaphthalene sensitized isomerization of trans, trans-2,4-hexadiene.

TABLE (2)

[1] = 0.050 M in neat sensitizer. Irradiation at 305 nm through Pyrex^{R}.

Irradiation time, min.	Isomer Content, % 2	3
0	0.918	0
48	1.152	0.0998
96	1.473	0.256
158	1.925	0.381

Least squares analysis gives 2.6 ± .3 as a ratio of the slopes of the production lines for 2 and 3 . Correlation coefficients were greater than 0.99.

Experiment III. The benzene sensitized photoisomerization of 1.

TABLE (3)

[1] = 0.050 M in neat sensitizer. Irradiation at 254 nm through quartz.

Irradiation time, min.	Isomer Content, % 2	3
0	0.918	
35	1.369	0.153
93	2.260	0.312
125	2.763	0.478

Least squares analysis gives 4.1 ± .4 as a ratio of the slopes of the production lines for 2 and 3 . Correlation coefficients were greater than 0.99.

Experiment IV. The γ-irradiation of 0.10 M 1 in benzene.

TABLE (4)

$D_r = 3.0 \times 10^{19}$ eV·ml^{-1}, hr^{-1}

Irradiation time, min.	Change in Concentration [2], M	[3], M
0	0	0
30	4.58×10^{-4}	1.48×10^{-4}
60	1.19×10^{-3}	3.01×10^{-4}
90	1.61×10^{-3}	4.38×10^{-4}
120	2.40×10^{-3}	5.39×10^{-4}
255	4.37×10^{-3}	1.15×10^{-3}
375	5.91×10^{-3}	1.81×10^{-3}

Experiment V. The radiostationary state of 1 in γ-irradiated benzene.

TABLE (5)

$[1]^{\circ} = 0.100\ M$

$D_r = 2.92 \times 10^{19}$ eV. Ml^{-1}. $hr.^{-1}$

Irradiation time, hr.	Isomer Content, % 1	2	3	[1+2+3]
0	99.8	0.2	0	0.100 M
72.0	55.0	33.8	11.2	0.0825
96.5	48.9	37.7	13.4	0.0744
125.0	41.4	43.1	15.5	0.0708
168.0	37.8	45.7	16.5	0.0645

Experiment VI. G(2) and G(3) as a function of [1].

TABLE (6)

$D_a = 2.92 \times 10^{19}$ eV·ml^{-1}

[1], Molar	G(2)	G(3)
0.150	--	0.462
0.100	2.14	0.538
0.100	1.98	0.504
0.100	--	0.565
0.050	1.58	0.386
0.048	--	0.504
0.025	--	0.374
0.010	1.01	0.298
0.0075	--	0.341
0.005	0.615	0.180

APPENDIX II

Calculation of the transfer efficiency, p, for the quenching of the $^1B_{2u}$ state of benzene by $\underset{\sim}{1}$.

The transfer efficiency, p, is defined as the ratio of the number of acceptor excited states produced to the number of donor excited states quenched by the excitation process.

The quenching fraction is calculated from the Stern-Volmer equation determined by Experiment I.

$$\frac{Io}{I} = 1 + 61.5\ [\underset{\sim}{1}] \qquad (1)$$

For an acceptor concentration $\underset{\sim}{1}$ = 0.050 M, this ratio becomes Io/I = 4.075. The reciprocal of this number is equal to the fraction of states that are <u>not</u> quenched by $[\underset{\sim}{1}]$. Therefore,

$$f_s = 1 - (4.075)^{-1} = 0.754$$

is equal to the fraction of states quenched.

Of these states, p results in diene singlet states. Finally, the number of $\underset{\sim}{2}$ molecules formed by decay of diene singlets is

$$N_{\underset{\sim}{2}'} = (0.754)(1 - \alpha)\ p\ N_s \qquad (2)$$

Where N_s is the original number of benzene excited singlet states. Since $(1 - \alpha) = 0.37$, $N_{2'} = 0.278\ p\ N_s$

It is now necessary to calculate the numbers of $\underset{\sim}{2}$ and $\underset{\sim}{3}$ formed by triplet energy transfer. Returning to equation (1), the number of states which intersystem cross to give benzene triplets, is equal to the number of states which are <u>not</u> quenched by $\underset{\sim}{1}$ times the intersystem crossing efficiency of the $^1B_{2u}$ state $(0.58)^1$.

$$N_{3_B} = (0.58)(0.246)\ N_s = 0.143\ N_s \qquad (3)$$

A certain fraction of these states partition between unimolecular decay and energy transfer to $\underset{\sim}{1}$. The quenching fraction will be determined by the rate of quenching and the total rate of decay of ^3B.

$$f_t = \frac{K_{yt}\ [1]}{K_{yt}\ [\underset{\sim}{1}] + K_D} \qquad (4)$$

The unimolecular decay rate of ^3B was determined to be $8.94 \times 10^7\ s^{-1}$. K_{yt} is 1×10^{10}. At 0.050 M $\underset{\sim}{1}$, f_t is 0.855. The number of diene triplet states produced is

$$N_{3_D} = f_t\ (0.143)\ N_s = 0.122\ N_s \qquad (5)$$

The decay of these triplet states to $\underset{\sim}{2}$ and $\underset{\sim}{3}$ is determined by the measured decay ratios for ^3D. Their numbers are

$$N_{\underset{\sim}{3}} = (1 - \beta - \pi)\ N_{3_D} = 0.0226\ N_s \qquad (5)$$

and

$$N_{2''} = \pi\ N_{3_D} = 0.0611\ N_s \qquad (6)$$

The singlet transfer efficiency is calculated by comparing the observed ratio of $\underset{\sim}{2}/\underset{\sim}{3}$ production with the calculated value.

$$\frac{\underset{\sim}{2}}{\underset{\sim}{3}} = \frac{N_{\underset{\sim}{2}'} + N_{2''}}{N_{\underset{\sim}{3}}} = \frac{0.278\ p + 0.0611}{0.0226}$$

The observed ratio of $\underset{\sim}{2}/\underset{\sim}{3}$ was 4.1 ± .4. Solving for p gives:

$$p = 0.11 \pm 0.03$$

The transfer efficiency, as well as the quenching rate of $\underset{\sim}{1}$, demonstrate that transfer from the $^1B_{2u}$ state is not highly exothermic (3-4 Kcal)[2]. Such a process would be expected to occur with p = 1 and $K_Q = 5 \times 10^{10}$ in benzene.

As discussed by Lamola[2] for the case of triplet energy transfer from biacetyl, the behavior here is consistent with

an exothermicity of ~ 1 Kcal. Quenching rates fall by 2 orders of magnitude for isoenergetic energy transfer[2]. The rate observed here is a factor of 20 less than diffusion controlled. Since the singlet energy of benzene is 108 Kcal·mole^{-1}, the above considerations place the lowest excited singlet state of $\underset{\sim}{1}$ at 107 Kcal·mole^{-1}.

REFERENCES

1. R. R. Hentz and L. M. Perkey, J. Phys. Chem., 74, 3047 (1970).
2. A. A. Lamola and N. J. Turro, editors, "Energy Transfer and Organic Photochemistry", Interscience Publishers, 1969, pp. 47-48.

APPENDIX III

Calculation of the yields of acceptor excited states as a function of [1] .

The fraction of quenching for any state undergoing unimolecular decay (k_D) and simultaneous quenching (k_Q) will be equal to the rate of quenching divided by the total rate of decay of the state.

$$F_q = \frac{K_Q\,[Q]}{K_Q\,[Q] + K_D} \qquad (1)$$

The concomitant yield of excited quencher states will be determined by the transfer efficiency of the process as well as the initial yield of states to be quenched. In this case the yields are radiation chemical yields (G).

$$G(Q^*) = p\,G(S^*)\,F_q \qquad (2)$$

Inverting equation (2) and substituting for F_q gives

$$G^{-1}(Q^*) = \frac{G^{-1}(S^*)}{p}\left(1 + \frac{K_D}{K_Q}\,[Q]^{-1}\right) \qquad (3)$$

which is the general form for equations (20) and (21). For exothermic energy transfer, p becomes 1.0.

In the case of simultaneous singlet and triplet quenching of benzene, a potential complication arises in equation (3) when applied to the triplet state yield. At low quencher

concentrations intersystem crossing from the $^1B_{2u}$ state elevates the yield of solvent triplet states, resulting in a downward curvature of equation (3). This would not be a problem at high quencher concentrations because singlet quenching dominates intersystem crossing.

In the present experiment this is not observed. Taking $G(^1B_{2u}) = 1.5$, a calculation the yield of solvent triplets produced by intersystem crossing shows that a 2.7% error is to be expected at 0.10 M [$\underset{\sim}{1}$] and a 17% error at 0.005 M [$\underset{\sim}{1}$].

The experimental error seems to be ± 15% so that the deviation can be absorbed by the experimental uncertainty.

Another compensating effect occurs which minimizes the low concentration departure from (3). One-third of yield of $^1B_{2u}$ arises from the internal conversion of upper excited singlet states in a radiation chemical experiment[1]. In the present case, these upper states are quenched by $\underset{\sim}{1}$, with a correlated decrease in the yields of $^1B_{2u}$ and, hence, $^3B_{1u}$ benzene. The same effect will occur if intersystem crossing occurs from upper excited singlet states.

REFERENCES

1. J. B. Birks, "Photophysics of Aromatic Molecules" Wiley Interscience, 1970, p. 581.

PROPOSITION I

A critical test of the Brockelhurst theory for germinate-ion recombination is proposed.

The electronic excitation of aromatic solutes (A) in γ-irradiated alkane liquids (S) is generally accepted to occur by the following mechanism[1].

$$S \sim\!\!\!\!\rightarrow S^+ + e^- \quad (1)$$

$$S^+ + A \rightarrow A^+ + S \quad (2)$$

$$e^- + A \rightarrow A^- \quad (3)$$

$$A^+ + A^- \rightarrow A^* + A \quad (4)$$

This scheme may be complicated at high acceptor concentrations by electronic energy transfer from solvent, because a great many saturated hydrocarbons have been found to fluoresce upon vacuum UV or X-ray excitation[2-4]. However, the above mechanism is consistent with the direct observation of solute anions and cations whose decrease is concurrent with appearance of solute excited states[1]. Charge scavengers compete with solutes for solvent ions and a reduction in solute excited state yields is found when these compounds are added.[1]

A requirement for step (2) is that the condensed phase ionization potential of the solvent exceeds that of the

solute. Similarly, a necessity for the occurrence of (3) is that the electron affinity of the solute is positive. These conditions are satisfied by many aromatic compounds such as anthracene, biphenyl, and fluorene.

Of primary interest to this proposition is step (4), by which solute radical anions and cations annihilate to produce excited electronic states. This can occur when the recombination energy exceeds the excitation energy of a particular solute excited state.

On a purely statistical basis, this step should produce singlet and triplet excited states in a 1:3 ratio, which is the ratio of the multiplicities of the final states[5]. Energy factors are also important since the lowest triplet state requires less energy for its production than the first excited singlet state. In the instance that recombination energy is sufficient for triplet excitation but deficient for singlet excitation, only triplets will be formed. This is observed in 1,3-cyclohexadiene radiolysis and is attributed to the large S-T splitting[6].

Another case in which this phenomenon is detected is the chemical oxidation of aromatic anions by Wurster's Blue perchlorate[7], and in the electrogenerated chemiluminescence experiments of Bard[8].

In general, the feasability of step (4) can be determined from a study of solute electrochemistry in which one-electron oxidation and reduction potentials are obtained.

Then, in combination with a knowledge of the energy levels of S, the sufficiency or deficiency of a particular excited state can be predicted.

Observed solute excited state yields for sufficient systems are in the range 1 - 0.5 for singlet to triplets, substantially greater than the statistical prediction[5]. Possible enhancement of singlet yields may be due to heretofore unsuspected singlet excitation transfer from short lived solvent excited states[2-4], or, as suggested by Brockelhurst[5], a failure of the initially paired electron spins to become randomized before recombination. Such a situation exists when the ionic recombination time is less than the electronic spin-lattice relaxation time, T_2. This criterion is satisfied here because major recombination occurs within 100 ns after initial ionization, a time which is less than T_2 for most radical anions and cations[5].

This fact forms a primary basis of a new theory by Brockelhurst[5] describing the recombination of radical anion and cation pairs produced by charge scavenging in γ-irradiated alkane solvents (step (4)). Brockelhurst's model is patterned after radical-pair CIDNP theories of Closs[9] and Kaptein[10] and calculates the probability of singlet spin recovery as a function of time after charge separation.

The recombination ratio (singlet/triplet) is expected to be a strong function of the nuclear spin states of the recombining ions. A large deuteration effect is expected,

with a marked increase in S/T. Similarly, a strong magnetic field (> 1 KG) decreases the rate at which the initial spin state of the system decays. The predicted effects are such that if ionic recombination were adjusted by solvent viscosity to occur within 15 ns of initial ionization, a 100% enhancement in the statistical S/T ratio would be observed for perde teroanthracene ions, compared to anthrcene, both in field.

A subsequent letter described the magnetic field-enhanced fluorescence from ionic recombination of fluorene radical ions in squalane at room temperature[11]. An enhancement of 1.5 was produced 150 ns after a 50 ns pulse of 3 meV electrons upon application of a 1 kG magnetic field. A similarly dramatic decrease of acceptor triplet states was not observed, due to the complexity of the system, as expected. The triplet absorbtion was not sensitive to the effect because triplets were produced by intersystem crossing from all previously formed singlet excited states, not just those produced by the ionic mechanism. For this reason an acceptor molecule which intersystem crosses is not a favorable test compound.

In direct contrast, I propose to further critically test Brockelhurst's theory by γ-irradiating 3,5-cycloheptadienone, (1), in a viscous hydrocarbon solvent, in and out of magnetic field. The d_4 and d_8 compounds will be irradiated. To vary the ionic recombination rate, the

solvent viscosity will be varied by temperature change.

As reported by Schuster *et al.*[12] and Hentz and Perkey[13], 1 gives separate and easily distinguishable products upon direct irradiation or triplet sensitization. A critical observation was that direct irradiation produces none of the triplet product.

$$1 \xrightarrow[313\ nm]{h\upsilon} \text{cis-1,3,5-hexatriene} + CO \qquad (5)$$

$$1 \xrightarrow[\text{sensitizer}]{\text{triplet}} \text{bicyclo[3.2.0]hept-6-ene-3-one} \qquad (6)$$

This molecule does not intersystem cross and can be used to count directly singlet and triplet excitations. In contrast to fluorene (vide supra), the triplet yield should be as equally sensitive as the singlet yield toward predicted effects.

Synthesis of CHDO-d4 can be accomplished by acid catalyzed H-D exchange in $CH_3OD - D^+$ solution. The fully deuterated molecule can be obtained in a five step synthesis from cyclohexanone-d6, similar to that for CHDO - h8 [14]. The LAH reduction of tropone gives 3,5-CHDO in high yield[12].

REFERENCES

1. J. K. Thomas, Ann. Rev. Phys. Chem., 21, 17(1970).
2. F. Hirayama, W. Rothman, and S. Lipsky, Chem. Phys. Lett., 5, 296 (1970).
3. W. Rothman, F. Hirayama, and S. Lipsky, J. Chem. Phys., 58 (1973).
4. M. S. Henry and W. P. Helman, J. Chem. Phys., 56, 5734 (1972).
5. B. Brockelhurst, Chem. Phys. Lett., 28 (3), 357 (1974).
6. T. L. Penner, D. G. Whitten, and G. S. Hammond, J. Amer. Chem. Soc. 92, 2861 (1970).
7. A. Weller and K. Zachariasse, J. Chem. Phys., 46(12), 4984 (1967).
8. L. R. Faulkner, A. J. Bard, J. Amer. Chem. Soc., 91, 209 (1969).
9. G. L. Closs and A. D. Trifunac, J. Amer. Chem. Soc., 91, 4554 (1969), and references therein.
10. R. Kaptein, J. Amer. Chem. Soc., 94, 6262 (1972), and preceeding numbers of the publication series.
11. B. Brockelhurst, P. S. Dixon, E. M. Gardy, V. J. Lopata, M. J. Quinn, A. Singh, and F. P. Sargent, Chem. Phys. Lett., 28, 361 (1974).
12. P. I. Schuster, B. Skolnick, and F. H. Lee, J. Amer. Chem. Soc., 90, 1300 (1968).

13. R. R. Hentz and L. M. Perkey, J. Phys. Chem., 74, 3047 (1970).

14. W. E. Parham, R. W. Soeder, J. R. Throckmorton, K. Kuncl, and R. M. Dodson, J. Amer. Chem. Soc., 87, 321 (1965).

PROPOSITION II

Study of intramolecular excitation transfer from a d^6 metal system to a chained, remote organic π system is proposed.

M. S. Wrighton et al.,[1] have observed low temperature emissions from a series of $W(CO)_5L$ compounds, which were assigned as $^3E(e^3b_2^2a_1) \rightarrow {}^1A(e^4b_2^2)$ spin-forbidden luminescence. Synthesis was accomplished by photolysing $W(CO)_6$ at 366 nm in a non-coordinating solvent to produce coordinatively unsaturated $W(CO)_5$ which subsequently reacted with the desired ligand[2]. In this case L was an ether, thioether, ketone or amine, although a wide spectrum of electron-donating ligands are acceptable. Compared to the others, pyridinepentacarboyltungsten(0), 1, was thermally quite stable and could be isolated from solution. Substituted carbonyl complexes were identified by their I.R. spectra in the carbonyl region[3].

Compound 1 was a good emitter, displaying a 2.5×10^{-6} S lifetime at 77°K in methylcyclohexane glass, with an apparent emission maximum at 510 nm[1,4]. From the onset of emission at 475 nm, an energy of ~ 60 Kcal·mole^{-1} can be estimated for the emitting state. If 1 were warmed to room temperature, emission vanished in an Arrhenius fashion,

demonstrating an activation energy of 1.3 Kcal·mole^{-1} for some undefined nonradiative process[5].

$W(CO)_5Py$ demonstrates wavelength dependent substitution photochemistry at room temperature, showing loss of cis carbonyl or pyridine. In 3.66 M 1-pentene (isooctane solvent) the quantum yield of $W(CO)_5$(1-pentene) drops from 0.63 at 436 nm to 0.34 at 254 nm[6]. The quantum yield of cis-$W(CO)_4Py_2$ formation increases from 0.002 to 0.04 over the same wavelength interval in 0.25 M pyridine[6].

I propose to synthesize compounds 2a, 2b, and 2c and, after attaching $W(CO)_5$, examine their emission and other photodynamic properties both at 77°K and room temperature in hope of detecting intramolecular energy between the two chromophores.

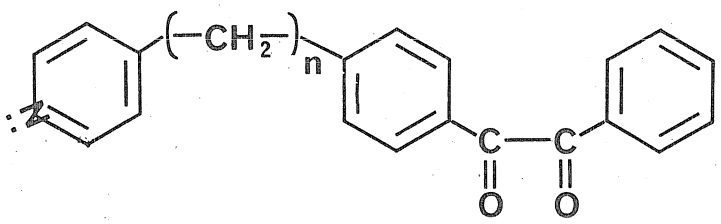

2a, n = 0
2b, n = 2
2c, n = 3

Excitation can be preferentially isolated in the metal centered half of these molecules by exciting at 385 nm, the absorbtion maximum of 1. The extinction ratio of 1 to benzil is roughly 100 at 385 nm[7], ensuring that 99% of incident energy will be captured by the metal moiety.

Because benzil[8] possesses lowest singlet and triplet excited states near 60 and 54 Kcal·mole^{-1}, respectively, rapid intramolecular excitation transfer from the metal portion can be expected in analogy to the energetically similar napthyl-benzophenone system[9,10]. Conceivably, this could occur by several mechanisms including (1) Förster resonance transfer, (2) "trivial" excitation transfer, (3) triplet-singlet resonance transfer and, (4) Dexter exchange (singlet or triplet)[11].

However, the Förster resonance and "trivial" transfer mechanisms are expected to be very unlikely because the spectral overlap integral[11] for the emission of any state produced by absorption in the $\underset{\sim}{1}$- section of the mixed molecule and the absorption spectrum of benzil must be small. For this same reason triplet-singlet resonance exchange, (3), can be neglected. In addition to minimal spectral overlap, $\underset{\sim}{1}$ exhibits a prohibitively short state lifetime for (3) to function[11].

In the case that the three preceeding long-range processes are slow, the short range Dexter mechanism can become important[11]. Both singlet-singlet and triplet-triplet excitation exchanges are possible by this pathway which occurs when interacting chromophores meet at their molecular radii. General compound $\underset{\sim}{2}$ is well suited for Dexter exchange because intimate association of the two chromophores is maintained by the methylene bridge.

It is plausible that both pathways could be functioning in 2 since the spin multiplicity of the ^3E state of 1 is only a formal designation. In fact it must have a considerable admixture of singlet character because of its absorbtion intensity. Hence excitation transfer could result in either triplet or singlet excited benzil.

These two events can be disciminated because benzil and presumably the minimally perturbed benzil of compound 2 demonstrate both fluorescence and phosphorescence upon direct excitation[12]. If only triplet excitation occurs, only benzil phosphorescence will be manifested.

Another novel pathway for singlet excitation of benzil could possibly occur by transfer from an upper excited singlet state of 1, since 1 shows wavelength-dependent photochemistry at room temperature. Apparently chemical reaction can compete with internal conversion, suggesting that this process might be slow in 1.

If in fact excitation transfer is fast within 2, emission in solution might also be detected since benzil shows both 298°K fluorescence and solution phosphorescence[12]. Internal transfer may effectively compete with temperature dependent deactivation of 1, contained in 2. $W(CO)_5Py$ is expected to have a total decay rate of $2 \times 10^8\ s^{-1}$, judged by extrapolating the low temperature Arrhenius behavior to 298°K. Transfer rates between chromophores in 2 are expected to be of this magnitude. In this event, photosubstitution

of 1 will be quenched if the transferring state is also responsible for chemistry.

Ligands 2a,b,c can be synthesized from commercially available 4-phenylpyridine, 4-stilbazole, and 4-(3-phenylpropyl)pyridine. Following catalytic hydrogenation of 4-stilbazole I suggest that all three alkyl-substituted phenyl compounds be formylated by the Gattermann-Koch reaction which proceeds by electrophilic attack of $H\text{-}C^{+}=O$ in $AlCl_3\text{-}Cu_2Cl_2\text{-}HCL$ mixture in the presence of carbon monoxide[13]. A subsequent crossed benzoin condensation could yield the corresponding benzoins which can be easily oxidized to the benzil. The full compounds can be generated by photolysing $W(CO)_6$ in the presence of 2. Presumably both O and N attack could occur but O-bound $W(CO)_5$ is thermally unstable, in contrast to the N-bound isomer.

REFERENCES

1. M. S. Wrighton, G. S. Hammond, and H. B. Gray, J. Amer. Chem. Soc., 93(17), 4336 (1971).
2. E. Koerner von Gustav and F. W. Grevels, Fortschr. Chem. Forsch., 13, 366 (1969).
3. I. Wender and P. Pino, ed., "Organic Synthesis via Metal Carbonyls", Vol. I, Wiley, 1968.
4. M. S. Wrighton, Ph.D. Thesis, California Institute of Technology, Pasadena, Ca. 91109, 1972, p. 158.
5. Ibid., p. 157.
6. Ibid., p. 231.
7. Ibid., p. 184. This ref. gives ϵ (380) $W(CO)_5Py$ = 6904 $M^{-1}cm^{-1}$ at room temperature, which is to be compared to benzil, ϵ=75 $M^{-1}cm^{-1}$ at 375 nm . from H. Jaffe and M. Orchin, "Theory and Applications of Ultraviolet Spectroscopy", John Wiley and sons, N.Y., 1966, p. 298.
8. N. J. Turro, "Molecular Photochemistry", W. A. Benjamin, N.Y., 1965, p. 132.
9. P. A. Leermakers, G. W. Byers, A. A. Lamola, and G. S. Hammond, J. Amer. Chem. Soc,85, 2670 (1963).
10. A. A. Lamola, Ph.D. Thesis, 1965, California Institute of Technology, Pasadena, Ca. 91109.
11. See reference 9, pp. 96-133.

12. H. Bäckström and K. Sandros, Acta. Chem. Scand., 14, 48 (1960).

13. J. Hendrickson, D. Cram, G. S. Hammond, "Organic Chemistry", M^{c}Graw Hill Book Co., San Francisco, 1970, p. 678.

14. M. S. Wrighton, G. S. Hammond, and H. B. Gray, J. Amer. Chem. Soc., 93, 6048 (1971).

PROPOSITION III

The construction of a photoactive electrode is proposed.

The electron transfer reactions of photoexcited Ru $(bipy)_3^{+2}$ to iron(III) as well as other oxidants have been reported[1-5]. In the case of iron(III)[1], diffusion-controlled quenching produces an ion pair, consisting of Fe^{+2} and $Ru(bipy)_3^{+2}$, which can separate efficiently to produce kinetically free species, because both products are positively charged[2,4].

$Ru(bipy)_3^{+2*}$ is a good reductant, possessing a standard potential of -0.81 V. versus S.C.E.[1,3]. In contrast, $Ru(bipy)_3^{+2}$ is a very poor single-electron reductant, with a standard potential of 1.05 V versus S.C.E,[6,7]. As a consequence, many electron transfer reactions of $Ru(bipy)_3^{+2*}$ are stubbornly reversible: reduction of an oxidant by $Ru(bipy)_3^{+2*}$ is followed with back-oxidation by $Ru(bipy)_3^{+3}$. One method of ensuring irreversible reduction of a substrate is to operate at high pH so that solvent reduction of $Ru(bipy)_3^{+3}$ is fast[8]. A second method could be to supply electrons directly to $Ru(bipy)_3^{+3}$ from an external circuit.

To accomplish this act I propose attaching $Ru(bipy)_3^{+2}$ to a carbon electrode by means of amide linkages. 4-amino-2,2′-bipyridine refluxed in the presence of bis(2 , 2′-

bipyridine) bis (dichloro)ruthenium(II) will be produce the amino derivative of $Ru(bipy)_3^{+2}$, 1 .

The carbon electrode surface can be activated by the method of Miller[9]. After heating a graphite rod under oxygen atmosphere the resultant exterior carboxyl groups are treated with thionyl chloride to produce reactive chlorocarbonyls. As a final step, these are to be treated with 1.

Photopotentials can be generated by this system upon transfer of charge to a solution oxidant at the $Ru(bipy)_3^{+2*}$ $-NH_2-$, electrolyte interface, creating a positive hole on the electrode surface. With electron neutralization from the electrode interior, the electrode will assume a more positive value with respect to a reference potential. In solution the efficiency of electron transfer to Fe^{+3} from $Ru(bipy)_3^{+2*}$ is 0.81 ± .16 in 0.5 M $HClO_4$[4]. If this system efficiency can be extrapolated to $Ru(bipy)_3^{+2}$ attached to the electrode surface, it will be very efficient[10].

$Ru(bipy)_3^{+2}$ is quite photostable[5] (in the absence of oxidants) and the $Ru(bipy)^{+3,+2}$ couple is very reversible due to the inert nature of both partners[11].

An imposing problem with any electrode is rapid quenching by energy transfer of electronically excited chromophores close to its surface. This occurs because the electrode possesses an essentially infinite number of electronic states which are energetically capable of coupling with an

external fluctuating dipole. In the present case, quenching of attached, electronically excited $Ru(bipy)_3^{+2*}$ would be rapid. However, electron transfer to a suitable oxidant is also extremely rapid[1]. By working at high oxidant concentrations, it may be possible to overwhelm the suspected process of electrode quenching with electron transfer to solution.

Electrode quenching is not always a problem. By coating platinum electrodes with a diphenylnapthylmethane dye (Victoria Blue B), Anderson *et al.*[10] were able to produce photo-active electrodes without the use of electrolyte reactive species.

REFERENCES

1. C. R. Bock, T. J. Meyer, and D. G. Whitten, J. Amer. Chem. Soc., 96 4710 (1974).
2. C. R. Bock, T. J. Meyer, and D. G Whitten, J. Amer. Chem. Soc., 97 2909 (1975).
3. G. Navon and N. Sutin, Inorg. Chem., 13 2159 (1974).
4. C. Lin and N. Sutin, J. Amer. Chem. Soc. 97 3543 (1975).
5. J. N. Demas and A W. Adamson, J. Amer. Chem. Soc., 95 5159 (1973).
6. A. A. Schilt, Anal. Chem., 35 1599 (1963).
7. G. M. Brown, Ph.D. Dissertation, University of North Carolina, Chapel Hill, N. C., 1974.
8. H. D. Gafney and A. W. Adamson, J. Amer. Chem. Soc., 94, 8238 (1972).
9. B. F. Watkins, J. R. Behling, E. Karit, and L. L. Miller, J. Amer. Chem. Soc. 97 3547 (1975).
10. "Regenerative EMF Cells", American Chemical Society publication 64, American Chemical Society, Washington, D. C., 1967, pp 213-276.
11. J. N. Braddock and T. J. Meyer, J. Amer. Chem. Soc., 95 3158 (1973).

PROPOSITION IV

Natarajan and Endicott[1,2] and Adamson and Gafney[3] have proposed different mechanisms for the $Ru(bipy)_3^{+2}$ photosensitized decomposition of $Co(NH_3)_5Br^{+2}$. Adamson[3] proposes that decomposition to Co(II) follows electron-transfer quenching of $Ru(bipy)_3^{+2}$ to give a labile Co(II) complex which dissociates.

$$Ru(bipy)_3^{+2} + h\upsilon \rightarrow Ru(bipy)_3^{+2*} \quad (1)$$

$$Ru(bipy)_3^{+2*} + Co(NH_3)_5Br^{+2} \rightarrow Ru(bipy)_3^{+3} + Co(NH_3)_5Br^{+1} \quad (2)$$

$$6H_2O + Co(NH_3)_5Br^{+1} \rightarrow Co^{+2}(aq.) + 5NH_3 + Br^- \quad (3)$$

$$Ru(bipy)_3^{+3} \xrightarrow{H_2O} Ru(bipy)_3^{+2} \quad (4)$$

Endicott[1,2] suggests that quenching of $Ru(bipy)_3^{+2}$ is a physical event, which eventually leads to sensitizer oxidation when $Co(NH_3)_5Br^{+2*}$ undergoes internal redox to give bromine atoms.

$$Ru(bipy)_3^{+2*} + Co(NH_3)_5Br^{+2} \rightarrow Co(NH_3)_5Br^{+2*} + Ru(bipy)_3^{+2} \quad (5)$$

$$Co(NH_3)_5Br^{+2*} \xrightarrow{H_2O} Co^{+2}(aq.) + 5NH_3 + Br\cdot \qquad (6)$$

$$Br\cdot + Ru(bipy)_3^{+2} \rightarrow Ru(bipy)_3^{+2} + Br^- \qquad (7)$$

$$Ru(bipy)_3^{+3} \xrightarrow{H_2O} Ru(bipy)_3^{+2} \qquad (8)$$

The quenching behavior of cobaltpentammine halides toward $Ru(bipy)_3^{+2}$ correlates with both their reduction potentials[3] and the expected trend of their lowest triplet states to accept triplet electronic excitation from $Ru(bipy)_3^{+2}$.[4]

I propose a direct, dynamic critical experiment to differentiate between these two sequences. The Adamson sequence predicts that Ru(III) is present immediately after quenching has occurred (i.e., within the lifetime of $Ru(bipy)_3^{+2*}$) while the other sequence predicts an initially small but increasing amount of Ru(III) following quenching.

Previous flash studies[1,2] of this system have been performed on a time scale many times longer than that of $Ru(bipy)_3^{+2*}$ ($\tau = 0.60 \times 10^{-6}$ S) and are therefore inconclusive. I propose to follow the time behavior of the 450 nm absorption band of $Ru(bipy)_3^{+2}$ in the presence of $Co(NH_3)_5Br$ on a nanosecond time scale, immediately after exciting with high intensity 337 nm pulses from a N_2 LASER, equipment which is immediately available[5].

The quenching dynamics of $Ru(bipy)_3^{+2*}$ by $Co(NH_3)_5Br^{+2}$ have been studied by Navon and Sutin[6] as well as Adamson and Gafney[3]. At an ionic strength of 1.5 M $Co(NH_3)_5Br^{+2}$ demonstrates a bimolecular quenching constant of $2.5 \times 10^9\ M^{-1}\ S^{-1}$. Using this value, a concentration of 6.7×10^{-4} M will quench 50% of all $Ru(bipy)_3^{+2}$ excited states and have an optical density of 0.21 [7] at 337 nm.

Employing a 3×10^{-4} M solution of $Ru(bipy)_3^{+2}$ will ensure that less than 10% of the incident light is absorbed by cobalt, avoiding problems of direct photolysis[8].

The 1.00 cm optical density of such a solution is 0.6 at 500 nm (consisting of a 0.015 component due to Co(II) complex absorption). Thus spectral changes will be due mainly to alteration of the ruthenium(II) concentration. $Ru(bipy)_3^{+3}$ does not absorb at this wavelength[9].

Assuming an easily produced initial concentration of 10^{-4} M excited states and quantum yield of 1 $Ru(bipy)_3^{+3}$ per quench[6], an immediate O.D. change of 16% or 0.1 units is predicted by sequence (1)-(4). Such a change is easily measured.

REFERENCES

1. P. Natarajan and J. F. Endicott, J. Phys. Chem., 77 971 (1973).
2. Ibid., p. 1823.
3. H. D. Gafney and A W. Adamson, J. Amer. Chem. Soc., 94, 8238 (1972).
4. M. Wrighton and J. Markham, J. Phys. Chem., 77, 3042 (1973).
5. E. Menger and D. S. Kliger, J. Amer. Chem. Soc., submitted.
6. G. Navon and N. Sutin, Inorg. Chem, 13, 2159 (1974).
7. $Co(NH_3)_5Br^{+2}$ has extinction coefficients of 316 $M^{-1}cm^{-1}$ and 32 $M^{-1}cm^{-1}$ at 337 and 500 nm respectively. This data was calculated from V. Balzani and V. Carasitti, "The Photochemistry of Coordination Compounds", Academic Press, New York, N.Y., 1970, p. 203. $Ru(bipy)_3^{+2}$ has extinction coefficients of 7000 $M^{-1}cm^{-1}$ and 2000 $M^{-1}cm^{-1}$ of 337 and 500 nm (this work).
8. P. Natarajan and J. F. Endicott, J. Amer. Chem. Soc., 95, 2470 (1973).
9. J. N. Demas and A. W Adamson, J. Amer. Chem. Soc., 95, 5159 (1973).

PROPOSITION V

A new utilization of pyrene derivatives as polarity-proximity fluorescence probes for biomembranes is proposed.

Pyrene excited singlet states are quenched by aromatic amines in polar and non-polar solvents[1-6]. With the quencher dimethylaniline (DMA), new, red-shifted emissions are observed in non-polar media, which are assigned to an excited state complex (exciplex) of pyrene (P) and DMA[2].

$$P + h\upsilon \rightarrow P^{1(*)} \quad (1)$$

$$P^{1(*)} + DMA \rightleftarrows (P \cdot DMA)^{1(*)} \quad (2)$$

$$(P \cdot DMA)^{1(*)} \rightarrow P + DMA + h\upsilon' \quad (3)$$

$$P^{1(*)} \rightarrow P + h\upsilon \quad (4)$$

$$(P \cdot DMA)^{1(*)} \rightarrow P^{-} + DMA^{+} \quad (5)$$

The exciplex shows every characteristic expected of a species of large dipole moment. For a series of quenchers the forward rate of reaction (2) is correlated with ease of oxidation of quencher[6]. An increase in solvent ability to stabilize separated charges has a similar result[2].

In polar solvents, the emission maximum of the new emitting species shifts dramatically to lower energies, accompanied by a decrease in emission quantum yield[5]. Pyrene emission energy is relatively unaffected. This decrease is

attributed to enhanced participation of reaction (5), resulting in detectable quantities of ions.

As an illustration, the P-DMA exciplex emission maximum increases from 430 to 518 nm upon changing from hexane (ϵ = 1.89)[7] to pyridine (ϵ = 12.3) while the quantum yield of emission drops rapidly from 0.66 to 0.015 [5]. The marked solvent sensitivity of the pyrene - DMA exciplex system bears a close similarity to 8-anilino-1-naphthalenesulfonate (ANS) which has been used as a polarity discriminating fluorescent probe in biological membrane studies[8]. The ANS fluorescence maximum shifts from 454 to 515 nm upon transition from hexane to water (ϵ = 78.0) while showing a precipitous drop in emission quantum yield from 0.98 to 0.004[8].

This phenomenon is heretofore unexplained[8] although it is interesting to surmise that behavior analogous to pyrene-DMA would be expected from ANS since it consists of a secondary aniline held in close proximity to an aromatic nucleus. Naphthalene-triethylamine forms an emissive exciplex system which shifts from 405 to 470 nm upon transition from hexane to 1,2-dimethoxyethane[9]. ANS would thus seem to be an intramolecular exciplex by analogy.

Pyrene butyric acid (PBA) has been incorporated into the cationic micelles of cetyltrimethyl ammonium bromide in water, a crude membrane model system[10]. Compared to pyrene and pyrene sulfonic acid its luminescence and quenching behavior locate it at an intermediate position from the

micellar surface. Pyrene is solubilized in the apolar interior while amphiphilic pyrene sulfonic acid is located primarily at the micelle-water interface[10]. This behavior is consistent with an association of the negative derivative side group with the positively charged micelle surface[10].

A similar conclusion was reached for the membrane binding of ANS to bovine red blood cell ghosts[11]. Membrane bound ANS fluorescence was enhanced by the solution addition of membrane-active local anesthetics.

I propose to use pyrene and a series of alkyl side chain pyrene derivatives as proximity and polarity probes in red blood cell erythrocyte ghosts in conjunction with the local anesthetics procaine and tetracaine. Red blood cell membranes have been used as models for excitable nerve membranes. By varying the side chain length of the pyrene derivative I hope to monotonically increase the penetration depth of the chromophore into the apolar membrane interior and thereby determine the anesthetic concentration profile.

Procaine, (1), and tetracaine, (2), are shown below. Both possess an aminophenyl group and in this regard might function similarly to DMA with respect to pyrene exciplex formation. In the event that both are poor exciplex reagents, further methylation may increase their reactivity[2].

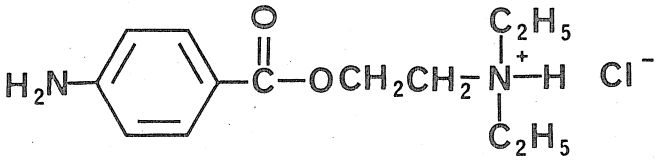

PROCAINE

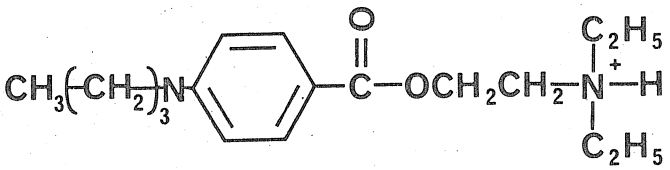

TETRACAINE

Exciplex emission will only be observed from regions of low polarity, while quenching with detectable ion formation is expected in high dielectric constant regions of the cell membrane. Because the quenching is obviously short range, there will be no ambiguity about the relative membrane locations of the two molecules.

I suggest that pyrene sulfonic acid, pyrene butyric acid, and pyrene be initially used as test probes. For deep membrane penetration a longer side chain is desirable. The acid chloride of PBA could be attached to 12-hydroxystearic acid for this purpose[12].

REFERENCES

1. N. Mataga, K. Ezumi, and T. Okada, Mol. Phys., 10, 201, (1965).
2. Ibid., p. 203.
3. N. Mataga, T. Okada, and H. Oohari, Bull. Chem. Soc. Jap., 39, 2562 (1966).
4. Ibid., p. 2563.
5. N. Mataga, T. Okada, and N. Yamamoto, Chem. Phys. Lett., 1, 119 (1967).
6. J. B. Birks, "Photophysics of Aromatic Molecules", Wiley Interscience, N. Y., 1970, pp. 425-433.
7. ϵ is the static dielectric constant of the solvent.
8. A. S. Waggoner and L. Stryer, Proc. Nat. Acad. Sci., 67, 579 (1970).
9. S. P. Van, Ph.D. Thesis, California Institute of Technology, Pasadena, Ca., 1970.
10. M. Grätzel, K. Kalyanasundaram, and J. K. Thomas, J. Amer. Chem. Soc., 96, 7869 (1974).
11. D. D. Koblin, S. A. Kaufmann, and H. H. Wang, Biochem. and Biophys. Res. Comm., 53, 1077 (1973).
12. After the method of reference 8.